Molecular Analysis of *BRAF* and Microsatellite Analysis of Chromosome 14q in Astrocytic Tumors

CHAN Ching Yin

A Thesis Submitted in Partial Fulfillment

of the Requirements for the Degree of

Master of Philosophy

in

Anatomical and Cellular Pathology

The Chinese University of Hong Kong
October 2003

Acknowledgement

I thank God for his great power and love to lead me to this department. Through him, I have been introduced to lots of nice people and have been prospected both intellectually and spiritually.

I met Prof. HK Ng who is always busy but is still willing to help his students. He responds quickly to my enquiries but provides ample time and freedom for me to learn gradually. I express deep gratitude for his care and support. He is both an expert in his career and a good example for his students.

I must also give many thanks to Mr. Jesse Pang for his continuous help and encouragement. He is genuine in nature and express concern sincerely. He always advice in details and is enthusiastic in discussions. From him, I have been kept inspired. Only through him can I enjoy the art of thinking.

For my colleagues and friends, I extremely owe a debt of gratitude for their generous dedication of their valuable time in teaching and helping me. I give my special thank to Dr ZQ Dong for he worked lately in assisting me to take photographs before he left the laboratory for his new life in the US. He is so warm-hearted that he actively offer me various favor every time before I seek his help.

Thanks also go to Mr. David Lo, Mr. Hardy Ko, Miss Joanna Tong and Dr. Michael Chan for their technical support. Other colleagues and friends including Mr. Richard Chan, Mr. Chit Chow, Miss Suk-ling Ma and Angela Lo also provide valuable advices and guidelines for my experiments. I express my sincere thanks to all of them. Others who offered assistance to me would make up an endless list. I would like to express my gratitude to them all.

Lastly, I would like to say 'thank you' to my family. I am extremely grateful towards my Dad for he is always standing by me and my Mum for giving me numerous tangible help, cooking soup and washing clothes... Best wishes to Brother Lionel and Miss. Ester who care me through these days. May God bless every one of you, my dear colleagues, friends and family members.

Abstract

Astrocytic tumors are the most common primary intracranial neoplasm, accounting for 25 – 35% of all primary brain tumors. Despite successful local control by modern surgical techniques, challenges remain with the eradication of infiltrating tumor cells. Even low-grade diffuse astrocytoma has an intrinsic tendency to progress to higher-grade tumors. Molecular understanding of tumor pathogenesis would be important for drawing up more accurate diagnostic criteria, prognosis and development of new treatment strategies.

Recently, activating mutation of *BRAF* was discovered in a wide variety of cancers, with T1796A substitution leading to V599E amino acid change representing 80% of all mutations identified. The first aim of my study is to investigate whether *BRAF* alteration is involved in CNS tumors. I performed direct cycle sequencing on exons 11 and 15 of the *BRAF* gene to evaluate the frequency of *BRAF* mutation in a tumor series comprising of 23 diffuse astrocytomas, 18 AAs, 53 GBMs (including 2 gliosarcomas), 31 oligodendroglial tumors, 23 ependymal tumors, 21 medulloblastomas and 26 meningeal tumors, and 10 cell lines including six from astrocytic tumors, three from medulloblastomas and one from primitive neuroectodermal tumor. I also examined the expression of B-Raf by immunohistochemistry in 25 GBMs, 13 AAs and 9 diffuse astrocytomas. Since *EGFR*, the upstream activator of Raf proteins, is frequently amplified (50%) in primary GBM, *EGFR* gene dosage of astrocytic tumors was investigated for correlation analysis between *EGFR* amplification and *BRAF* alterations.

Heterozygous *BRAF*^{V599E} mutation was revealed in one GBM specimen and 2 GBM cell lines (GBM2603 and GBM6840). Results of sequence electropherograms and karyotyping suggest gain of mutant gene copies in the 2 cell lines. Hence, both sequence alteration and enhanced copy number of mutant *BRAF* allele are involved in the development of GBM. Furthermore, B-Raf expression was detected in approximately 30% of astrocytic tumors but not in normal astrocytes from 10 brain autopsies. Higher expression of B-Raf in astrocytic tumors than in normal astrocytes pointed to possible functional changes in favor of tumorigenesis. Also, B-Raf immunoreactivity was detected in all tumor grades. Abnormal expression of wild-type B-Raf protein in the low-grade diffuse astrocytoma suggests that *BRAF* alteration is an early event in tumorigenesis of astrocytic tumors. Analysis of 30 astrocytic tumors showed mutually exclusively pattern of *EGFR* amplification and B-Raf immunoreactivity. Activation of the wild-type B-Raf proteins might require autocrine signaling. Taken together, my data demonstrated that *BRAF* is altered at the genomic and proteomic level, suggesting that *BRAF* plays an important role in the tumorigenesis of a proportion of astrocytic tumors.

In the second part of my thesis, I carried out deletion mapping of chromosome 14q in astrocytic tumors. Our group has previously performed a genome-wide microsatellite analysis and detected two common regions of deletion (CRDs) on 14q21.2 – q23.12 and 14q32.1 – qter in 50% GBM and 35% AA. These data suggest that chromosome 14q may contain a putative tumor suppressor and its inactivation may contribute to the development of astrocytic tumors. To refine

CRD in 14q21.2 – q23.12 in astrocytic tumors, 18 microsatellite markers were used to analyze the allelic status in 14q of 15 GBMs (including 2 gliosarcomas), 5 AAs and 12 diffuse astrocytoma. Mapping of LOH loci revealed 4 CRDs locating in 14q23.1 – q23.2 (CRD1, D14S592 to D14s1026), 14q24.1 – q24.2 (CRD2, D14S1011 to D14S77), 14q24.3 (CRD3, D14S43 to D14s59) and 14q31.1 – q31.3 (CRD4, D14S1000 to D14S68), spanning 3.3, 4.0, 3.2 and 6.5 Mb, respectively. All of them overlap with those of other tumor types, such as renal cell carcinoma and neuroblastoma. Based on functional implications from other isoforms or alterations in other cancers, *PPP2R5E* and *MLH3* were identified as putative tumor suppressor genes worth further characterization. Nevertheless, the 4 CRDs are still considerably too large for positional cloning of candidate genes. Further refinement of the common regions of deletion is required.

摘要

星形膠質細胞瘤是原發型顱內新生物中最常見的腫瘤，佔所有原發性腦腫瘤的 25 - 35%。雖然現代外科技術已能成功地控制局部的損害，但根除浸潤癌細胞仍是未來面臨的挑戰。即使是低惡性度彌散型星形膠質瘤，也有演變成高惡性度腫瘤的固有趨向。瞭解腫瘤的分子致病機制對於更準確的診斷標準的制定，預後判斷和新治療方法的發展起重要的指引作用。

在近期多種腫瘤 *BRAF* 基因活化突變中，80% 是 T1796A 的換置，導致 V599E 的氨基酸替換。本研究的第一個目標是探討 *BRAF* 在中樞神經系統腫瘤中的變化。研究方法是對 *BRAF* 基因的第 11 和 15 外顯子直接測序並計算 *BRAF* 突變的發生率。樣本包括 23 例彌散型星形膠質瘤、18 例惡性星形膠質瘤(AA)、53 例多形性膠質母細胞瘤(GBM；包括兩例神經膠質肉瘤)、31 例少突神經膠質細胞瘤、23 例室管膜腫瘤、21 例成神經管細胞瘤和 26 例腦膜的腫瘤。10 株腫瘤細胞株包括 6 株原自星形膠質細胞瘤、3 株原自成神經管細胞瘤及 1 株原始神經外胚層的腫瘤細胞株。接著使用免疫組織化學方法檢測 25 例 GBM、13 例 AA 和 9 例彌散型星形膠質瘤的 B-Raf 蛋白表達。因爲表皮生長因子受體 *(EGFR)*在訊息傳遞過程中置於 Raf 的上遊，又常(50%)在原發型 GBM 擴增，因此本研究還檢測了 *EGFR* 在星形膠質細胞瘤中的劑量，用於分析 *EGFR* 擴增與 *BRAF* 變化之間的關係。

測序結果顯示在 1 例 GBM 樣本和 2 株 GBM 細胞株(GBM2603 和 GBM6840) 有 *BRAF*^{V599E} 雜合性突變。基因序列圖和染色體組型分析結果提示 2 株 GBM 細胞株都有突變的 *BRAF* 基因拷貝數的增加。因此，*BRAF* 的序列變化和突變的等位基因拷貝數增加都參與致癌的過程。免疫組織化學方法檢測到大約 30% 的星形膠質細胞瘤的 B-Raf 蛋白表達。同樣方法在 10 例正常腦屍體解剖樣本卻檢測不到。B-Raf 在星形膠質細胞瘤的表達顯著高於正常星形細胞，提示其可能的功能變化有利於腫瘤的發生。而且，在各級腫瘤中都可以檢測到 B-Raf 的陽性免疫組化反應。正常型 B-Raf 蛋白在低惡性度星形膠質瘤的異常表達意味 *BRAF* 的變化是一個早期的現象。分析 30 例星形膠質細胞瘤結果顯示 *EGFR* 擴增和 B-Raf 免疫反應爲相互排斥的模式。正常型 B-Raf 蛋白的啓動可能需要自分泌的訊息。綜上所述，本研究結果顯示 *BRAF* 的變化既在基因水平，也在轉錄水平。*BRAF* 在部份星形膠質細胞瘤的致瘤過程中，可能扮演著關鍵的角色。

本研究第二個目標是從星形膠質細胞瘤的第 14 號染色體長臂中找出更小的缺失區段。本組曾經應用 DNA 微衛星標志進行等位基因組型(LOH)分析，並在 50% 的 GBM 及 35% 的 AA 中發現了兩個共同丟失片段(CRD)，分別爲 14q21.2 - q23.12 及 14q32.1 - qter。這些數據指出第 14 號染色體長臂可能隱藏著腫瘤抑制基因的位點，而這些腫瘤抑制基因的失活可能跟星形膠質細胞瘤的發展有關。爲了在

14q21.2 - q23.12 區域進行更爲精細的 DNA 微衛星檢測，本研究應用了 18 對微衛星標志來分析 13 例 GBM（包括例神經膠質肉瘤）、5 例 AA 和 12 例彌散型星形膠質瘤的等位基因雜合子丟失狀況。雜合子丟失圖顯示了 4 個更精細的 CRD，分別爲 14q23.1 - q23.2 (CRD1， D14S592 - D14S1026)、14q24.1 - q24.2 (CRD2， D14S1011 - D14S77)、14q24.3(CRD3， D14S43 - D14S59) 以及 14q31.1 - q31.3(CRD4，D14S1000 - D14S68)，丟失片段的序列範圍分別爲 3.3、4.0、3.2 及 6.5 Mb。這些丟失片段與其它的腫瘤的共同丟失片段有重疊，例如腎細胞癌、神經母細胞腫瘤。基於其它同種異型的功能或以其他腫瘤爲對照，*PPP2R5E* 和 *MLH3* 爲兩個最有價值進行特性研究的候選腫瘤抑制基因。儘管如此，本研究定位的 4 個 CRD 的片段範圍還有待進一步精細以適應定位克隆之用。

List of abbreviations

AA	anaplastic astrocytoma
ABC	avidin-biotin-peroxidase complex
Akt	v-akt murine thymoma viral oncogene homolog
APC	adenomatous polyposis of the colon
ARF	alternative reading frame
Ask	apoptosis-signal-regulating kinase
ATCC	American Type Culture Collection
B2M	beta2-microglobulin
Bad	BCL2-antagonist of cell death
BCL2	B-cell lymphoma 2
bp	base pair
BRAF	v-raf murine sarcoma viral oncogene homolog B1
BSA	bovine serum albumin
cAMP	adenosine 3',5'-cyclic monophosphate
Cdc	cell division cycle
Cdk	cyclin-dependent kinase
cDNA	complementary DNA
CGH	comparative genomic hybridization
CGP	Cancer Genome Project
CKI	cdk inhibitor
CNS	central nervous system
CR	conservative region
CRD	common region of deletion

List of abbreviations (continued)

CSF	cerebrospinal fluid
Ct	threshold cycle
DAB	diaminobenzidene
dATP	deoxyadenosine 5'-triphosphate
dCTP	deoxycytidine 5'-triphosphate
dGTP	deoxyguanosine 5'-triphosphate
DMBT1	deleted in malignant brain tumors 1
DMSO	dimethyl sulfoxide
DNA	deoxyribonucleic acid
dUTP	deoxyuridine 5'-triphosphate
E. coli	Escherichia coli
E2F	E2 promoter binding factor
EDTA	ethylenediaminetetraacetic acid
EGF	epidermal growth factor
EGFR	epidermal growth factor receptor
EGFRvIII	epidermal growth factor receptor variant type III
eIF	eukaryotic translation initiation factor
Erk	extracellular-signal-regulated kinase
EST	expressed sequence taq
FAM	6-carboxyfluorescein
FBS	fetal bovine serum
FGF	fibroblast growth factor
FISH	fluorescence in situ hybridization
G1	first gap of cell cycle

List of abbreviations (continued)

G2	second gap of cell cycle
GBM	glioblastoma multiforme
GFAP	glial fibrillary acidic protein
Gli	glioma-associated oncogene homolog
G-protein	GTP-binding protein
Grb2	growth factor receptor-bound protein 2
GS	gliosarcoma
Gy	gray
H&E	haematoxylin and eosin
HB-EGF	heparin binding epidermal growth factor-like growth factor
HEPES	N-2-hydroxyethylpiperazine-N'-2-ethanesulfonic acid
HEX	6-carboxyhexafluorescein
HGF	hepatocyte growth factor
HNPCC	hereditary non-polyposis colorectal cancer
H-RAS	v-Ha-ras Harvey rat sarcoma viral oncogene homolog
INK4	inhibitors of CDK4
KIP	kinase inhibitory protein
K-RAS	v-Ki-ras2 Kirsten rat sarcoma 2 viral oncogene homolog
LOH	loss of heterozygosity
M	mitosis
MAPK	mitogen activated protein kinase
MAPKK	mitogen activated protein kinase kinase
MAPKKK	mitogen activated protein kinase kinase kinase
Mb	megabase

List of abbreviations (continued)

MB	medulloblastoma
MDM2	mouse double minute 2 homolog
Mek	MAPK/Erk kinase
MGMT	O^6-methylguanine-DNA methyltransferase
MLH	MutL homolog (E. coli)
Mnk	MAPK-interacting kinase
mRNA	messenger RNA
MSH	MutS homolog (E. coli)
MSI	microsatellite instability
MSQ	mean of starting quantity
MYC	v-myc avian myelocytomatosis viral oncogene homolog
Myt	myelin transcription factor
NEURL	neuralized-like (Drosophila)
NF2	neurofibromatosis 2
N-RAS	neuroblastoma RAS viral (v-ras) oncogene homolog
OCT	optimal cutting temperature
OD	optical density
PBS	phosphate-buffered salline
PCI	phenol/chloroform isoamyl alcohol
PCR	polymerase chain reaction
Pdpk	Phosphoinositide-dependent protein kinase
PI3K	phosphatidylinositol-3-kinase
PNET	primitive neuroectodermal tumor
PP2A	protein phosphatase 2A

List of abbreviations (continued)

PPP2R5E	protein phosphatase 2, regulatory subunit B (B56), epsilon isoform
PTCH	patched homolog
PtdIns-3,4,5-P_3	phosphatidylinositol-3,4,5-triphosphate
PtdIns-3,4-P_2	phosphatidylinositol-3,4-biphosphate
PtdIns-4,5-P_2	phosphatidylinositol-4,5-biphosphate
PtdIns-4-P	phosphatidylinositol-4-phosphate
PTEN	phosphatase and tensin homolog
Raf	v-raf murine sarcoma viral oncogene homolog
Ras	rat sarcoma viral oncogene homolog
RB	retinoblastoma
RBD	ras binding domain
RNA	ribonucleic acid
ROH	retention of heterozygosity
ROX	6-carboxyrhodamine
RPMI	Roswell Park Memorial Institute
RSK	ribosomal S6 kinase
RTK	receptor-tyrosine-kinase
S	DNA synthesis phase of cell cycle
SAS	sarcoma amplified sequence
SD	standard deviation
siRNA	small interfering RNA
Sos	son of sevenless, drosophila homolog
Src	v-src sarcoma (Schmidt-Ruppin A-2) viral oncogene homolog (avian)

List of abbreviations (continued)

SSCP	single strand conformation polymorphism
SUFU	suppressor of fused
TAMRA	tetramethylrhodamine
TBE	tris-boric acid-EDTA
TBS	tris-buffered saline
TGF	transforming growth factor
TP53	tumor protein p53
TP73	tumor protein p73
TSG	tumor suppressor gene
U.S.A.	United States of America
VEGF	vascular endothelial growth factor
WAF	wild-type p53-activated fragment
WHO	World Health Organization

List of tables

Table 1.1.	Major chromosomal abnormalities detected in astrocytic tumors by CGH.	9
Table 1.2.	Major chromosomal abnormalities detected in astrocytic tumors by LOH analysis.	11
Table 1.3.	Frequencies of *BRAF* mutation in human dysplastic and tumor tissues.	42
Table 1.4.	Frequencies of *BRAF* mutation in human cell lines.	44
Table 1.5.	*BRAF* mutations in human tissues and cell lines.	45
Table 3.1.	Clinical information of astrocytic tumors.	65
Table 3.2.	Clinical information of non-astrocytic CNS tumors.	70
Table 3.3.	Cell lines of CNS origin examined in the current study.	76
Table 3.4.	Primers and Taqman probes of *EGFR* and *B2M* for real-time PCR.	94
Table 3.5.	PCR conditions of 18 microsatellite markers used in LOH analysis.	99
Table 3.6.	Amount of PCR products loaded onto denaturing gel.	100
Table 4.1.	B-Raf immunoreactivity of astrocytic tumors.	111
Table 4.2.	Normal range of *EGFR* index (triplicate trials).	123
Table 4.3.	EGFR index (triplicate trials) of astrocytic tumors harboring *EGFR* gain or amplification.	125
Table 5.1.	Reference sequenced genes in CRD1 (between D14S592 and D14S1026).	174
Table 5.2.	Reference sequenced genes in CRD2 (between D14S1011 and D14S77).	175
Table 5.3.	Reference sequenced genes in CRD3 (between D14S43 and D14S59).	177
Table 5.4.	Reference sequenced genes in CRD4 (between D14S1000 and D14S68).	180

List of figures

Figure 1.1.	Frequency of genetic and epigenetic alterations in primary and secondary GBMs.	27
Figure 1.2.	Genetic and epigenetic alterations in primary and secondary GBMs.	28
Figure 1.3.	The cell cycle clock.	31
Figure 1.4.	Distribution of somatic mutations in the B-Raf protein.	41
Figure 4.1	Sequence electropherograms of the GBM case BJ10 and blood sample from the same patient.	103
Figure 4.2	Sequence electropherograms of GBM6840.	104
Figure 4.3	Sequence electropherograms of GBM2603.	106
Figure 4.4	Immunohistochemistry of B-Raf and GFAP in normal and malignant cells.	108
Figure 4.5	Astrocytic tumor cell lines showing positive B-Raf immunoreactivity.	110
Figure 4.6	Different B-Raf immunoreactivities in diffuse astrocytomas.	112
Figure 4.7	Different B-Raf immunoreactivities in AAs.	113
Figure 4.8	Different B-Raf immunoreactivities in GBMs.	114
Figure 4.9	Real-time PCR amplification chart for *EGFR* standards.	118
Figure 4.10	Correlation between threshold cycle and input *EGFR* quantity.	119
Figure 4.11	Real-time PCR amplification chart for *B2M* standards.	120
Figure 4.12	Correlation between threshold cycle and input *B2M* quantity.	121
Figure 4.13	Representative results of microsatellite analysis in the diffuse astrocytoma case WN66.	133
Figure 4.14	Representative results of microsatellite analysis in the diffuse astrocytoma case WC101.	138
Figure 4.15	Representative results of microsatellite analysis in the diffuse astrocytoma case WN12.	140
Figure 4.16	Representative results of microsatellite analysis in the diffuse astrocytoma case NJ125.	142

List of figures (continued)

Figure 4.17 Representative results of microsatellite analysis in the GBM case NJ111. 144

Figure 4.18 Delineation of four CRDs on chromosome arm 14q in astrocytic tumors. 146

Figure 4.19 LOH frequency of individual polymorphic marker. 147

Figure 5.1 Chromosomal regions with high LOH frequency in human cancers. 168

Figure 5.2 Four CRDs in astrocytic tumors and CRDs in other tumors of the same chromosomal region. 172

Contents

Acknowledgement i

Abstract iii

Abstract in Chinese vi

List of abbreviations ix

List of tables xv

List of figures xvi

Contents xviii

1. Introduction 1

1.1. What are astrocytic tumors? *1*

1.1.1. Histological characteristics and classification 2

1.1.2. Epidemiology 2

1.1.3. Treatment and patient survival 4

1.2. Cytogenetics, molecular genetics and epigenetics of astrocytic tumors *6*

1.2.1. Cytogenetics 6

1.2.2. Genetic imbalances 7

1.2.3. Tumor suppressor genes 13

1.2.4. Oncogenes 22

1.2.5. Primary and secondary GBMs 26

1.3. Major pathways involved in astrocytic tumorigenesis *30*

1.3.1. Cell cycle dysregulation and suppression of apoptosis 30

1.3.2. Promotion of proliferation and survival 33

1.4. BRAF mutation in human cancers *38*

1.5. Other CNS tumors included in the current study *52*

2. Aims of study 61

3. Materials and methods 64

3.1. Clinical materials *64*

3.2. Cell lines *75*

3.3. Cell culture *77*

3.4. DNA extraction *78*

3.4.1. Pre-treatment of samples 78

3.4.2. Cell lysis and protein removal 80

3.4.3. Precipitation of DNA 81

3.4.4. Determination of DNA concentration 81

3.5. Mutation analysis of BRAF by cycle sequencing *83*

3.5.1. Amplification of *BRAF* exons 83

3.5.2. Cycle sequencing and automated gel electrophoresis 84

3.6. Immunohistochemistry of B-Raf and GFAP *87*

3.6.1. Pre-treatment of samples 87

3.6.2. Detection of B-Raf and GFAP antigens by ABC method 88

3.6.3. Controls 90

3.7. Quantification of EGFR gene dosage by TaqMan based real-time PCR *91*

3.7.1. Preparation of gene constructs 92

3.7.2. Primers and TaqMan probes 93

3.7.3. Experimental condition and PCR program 95

3.7.4. DNA standards 95

3.7.5. Controls 96

3.7.6. Experimental layout 96

3.8. Microsatellite analysis of chromosome 14q in astrocytic tumors *97*

4. Results 101

4.1. Mutation analysis of BRAF *101*

4.2. Immunohistochemistry of B-Raf protein *107*

4.3. Quantification of EGFR gene dosage *117*

4.4. Correlation between EGFR dosage and BRAF mutation *128*

4.5. Correlation between EGFR dosage and B-Raf expression *129*

4.6. Microsatellite analysis of chromosome 14q in astrocytic tumors *131*

5. Discussions 149

5.1. BRAF mutations as common events in human cancers *149*

5.2. BRAF mutation in CNS tumor specimens *150*

5.2.1. Tumorigenic effect of the V599E substitution 153

5.2.2. V599E B-Raf mutant activation independent of Ras activation 155

5.2.3. Autocrine stimulation of Ras signaling in V599E B-Raf mutant 156

5.3. BRAF expression in astrocytic tumors *159*

5.4. Mutually exclusive pattern between EGFR amplification and BRAF expression *161*

5.4.1. Similar effect of EGFR activation and B-Raf activation 163

5.4.2. Mutual effects between Ras/Raf/Mek/Erk and Akt signaling 164

5.5. Microsatellite analysis of chromosome 14q in human cancers *167*

5.6. Microsatellite analysis of chromosome 14q in astrocytic tumors *170*

5.6.1. Finer mapping of common regions of deletion 170

5.6.2. Genes within the common regions of deletion 173

5.6.3. Overlapping deletion regions in astrocytic and non-CNS tumors 186

6. Further studies 190

6.1. Role of BRAF alterations in astrocytic tumors *190*

6.2. B-Raf expression in astrocytic tumors and correlation with EGFR overexpression *193*

6.3. Microsatellite analysis of 14q in astrocytic tumors *194*

7. Conclusions 195

8. References 198

1. Introduction

1.1. What are astrocytic tumors?

The central nervous system (CNS) comprises mainly of neurons and glial cells. Astrocytes make up a main category of glial cells and are responsible for regulating neuronal growth and survival, guiding cell migration and axon growth during development, promoting synapse formation and modulating synaptic transmission, and orchestrating inflammatory and immune responses during brain infection and injury (Wechsler-Reya and Scott, 2001).

Gliomas comprise of tumor cells resembling glial cells. Similarly, astrocytic tumors are those with histological appearances of astrocytes (Louis *et al.*, 2001; Maher *et al.*, 2001). Diffusely infiltrating astrocytic tumors will be the focus of this study. 'Astrocytic tumors' in the current study referred to the diffusely infiltrating astrocytic tumors of all grades. Non-infiltrating variants, including pilocytic astrocytoma, pleomorphic xanthoastrocytoma, desmoplastic cerebral astrocytoma of infancy and subependymal giant cell astrocytoma, are out of the scope of the present study.

1.1.1. Histological characteristics and classification

Astrocytic tumors are classified by the World Health Organization (WHO) into three grades and can also be practically designated by St. Anne/Mayo's four criteria (Kleihues and Cavennee, 2000). Diffuse astrocytoma is designated into grade II with one criterion, usually nuclear atypia. Anaplastic astrocytoma (AA), characterized by two criteria, usually mitotic activity and nuclear atypia, is designated into grade III. Glioblastoma multiforme (GBM) is designated into grade IV with the presence of endothelial proliferation and/or necrosis, in addition to mitotic activity and nuclear atypia.

As indicated by the term multiforme, GBM is heterogeneous in terms of tumor morphology and behavior (Wechsler-Reya and Scott, 2001). It is subdivided into *de novo* (primary) and secondary ones, based on different progression kinetics (Section 1.1.2).

1.1.2. Epidemiology

The astrocytic tumors are the most common primary intracranial neoplasms. In United States of America (U.S.A.), GBM, AA and diffuse astrocytoma respectively represented 23%, 3.9% and 6% of all primary brain tumors and occurred at 2.96, 0.49 and 0.13 per 100,000 persons during 2000 (Central Brain Tumor Registry of the United States, 2000). In Hong Kong, they represented

15%, 6.5% and 3.6% respectively from 1984 to 1987 (Ng *et al.*, 1988). In Singapore, astrocytic tumors account for a total of 25% of primary brain tumors (Das *et al.*, 2002). In China, gliomas account for 40% of primary CNS tumors (Poon and Ng, 1992). Ethnically, age-adjusted rates for GBM in U.S.A. were 2.5 times higher in whites than in blacks in 1990 – 1994 (Central Brain Tumor Registry of the United States, 2000).

Astrocytic tumors usually manifest in adults with a male predominance based on biopsies of 1914 patients from the Tumor Registry of the University of California and the Institute of Neuropathology of University Hospital, Zurich. Peak incidence of diffuse astrocytoma lies in 30 – 40 years with a male/female ratio of 1.18:1. The male/female ratios become 1.8:1 in AA and 1.5:1 in GBM (Zulch, 1986).

In general, peak incidence of GBM lies in 45 – 70 years. The majority of GBM develop rapidly with a short clinical history and with no clinical or histological evidence of a less malignant precursor lesion. They manifest in a higher age group with a mean at 55 years and are termed *de no* or primary GBM. Other GBM, which develop slower and carry a history of development from lower-grade lesions are called secondary GBM. They manifest in a mean age of 40 years and cannot be distinguished histologically from primary ones (Kleihues and Ohgaki, 1999).

Astrocytic tumors may arise at any site in the CNS, preferentially in the cerebral hemisphere. The frontal and temporal lobes are the most frequently affected locations. Combined fronto-temporal location is particularly typical in GBM. Tumor infiltration often extends into the adjacent cortex, the basal ganglia and the contralateral hemisphere.

1.1.3. Treatment and patient survival

Treatment of diffuse astrocytoma mostly aims at gross total resection for longer relapse-free survival. For deep or diffuse lesions, conventional fractionated radiation via regional fields to a dose of at least 50 Gy usually follows stereotactic biopsy. Post-surgery radiation therapy has been significantly better than those for the surgery-alone, where sex, tumor site, extent of surgery, radiation dose and field, and adjuvant chemotherapy do not influence the prognosis significantly (Shibamoto *et al.*, 1993). A course of observation might be taken with close monitoring of neurological assessment and magnetic resonance imaging. However, most clinicians recommend treatment when confronted with a patient with any of these clinical or imaging features.

The literature on survival of patients with diffuse astrocytoma consists predominantly of retrospective reviews sometimes not well controlled. Criteria for selection of patients to various treatment regimens are not specified. This

leads to controversy in comparison of different treatment strategies. However, the major cause of mortality for a patient with diffuse astrocytoma results form transformation to higher-grade lesions, regardless of the treatment selected. The median survival time of diffuse astrocytoma after surgical intervention is in the range of 6 – 8 years, with marked variation (Walker and Kaye, 2001).

Surgical resection is effective in prolonging survival for selected patients and improving the quality of life for many patients. Without treatment, 95% of patients with GBM die within 3 months. Radiation therapy also increases long-term survival of patients with high-grade glioma, especially those younger than 65 years. Moreover, marginal survival advantage in treatment of AA and GBM has been provided by chemotherapy, along with surgical resection and post-operative radiation therapy. Typical survivals of AA and GBM are extended to 2 – 5 years and 1 – 2 years, respectively (Louis *et al.*, 2001).

Modern microsurgical techniques and excellent post-operative care have been successful in local control of the lesions. Challenges lie on the eradication of cells that have already infiltrated into functioning parenchyma. Molecular biology techniques involving gene therapy that attacks regulation mechanisms of proliferation and abnormal cellular survival are the promising area for modern research.

1.2. Cytogenetics, molecular genetics and epigenetics of astrocytic tumors

The relation of cancer to genetics can be traced back to 1914. Prompted by von Hansemann's observations of aberrant mitoses, Boveri (1914) predicted the presence of oncogenes and tumor suppressor genes (TSGs). The discovery of mutagenic effect of ionizing radiation and other carcinogens then related somatic mutation to cancer. Nowadays, tumor progression is widely regarded as the result of sequential accumulation of genetic abnormalities.

Knudson's 'two-hit' hypothesis had been used initially to describe hereditary tumors caused by somatic mutation of one allele of a TSG in addition to a germline mutation in the other allele. In considering tumor progression as a multi-step process, the theory of mutations in two alleles of TSG has been expanded to include at least loss/deletions and gene silencing by methylation and the combination of them (Knudson, 2001; Tomlinson *et al.*, 2001; Tucker and Friedman, 2002).

1.2.1. Cytogenetics

Among early cytogenetic studies, the majority of diffuse astrocytomas is characterized by a normal karyotype or simple numerical changes, in particular trisomy 7, monosomy 10 and 22, or loss of a gonosome. On the other hand, some AA and most GBM displayed highly complex karyotypes. In addition to frequent

trisomy 7, monosomy 10 and 22, partial deletions on 9p and 17p were also revealed. Other observations include changes in the ploidy range and chromosomal rearrangements involving in particular chromosomes 1 and 9, and double-minute chromosomes associated with amplification of the *epidermal growth factor (EGFR)* gene (Debiec-Rychter *et al.*, 1995; Schrock *et al.*, 1994; Vagner-Capodano, 1991).

The accumulation of chromosomal changes in increasing grades of astrocytic tumors was often seen. However, traditional cytogenetic analysis of brain tumors had been difficult due to difficulties in primary cultures of low-grade tumors, selection bias in cells being analyzed and the complexity of chromosomal abnormalities (Teyssier, 1987 and 1989).

1.2.2. Genetic imbalances

Comparative genomic hybridization (CGH), a modified fluorescence *in situ* hybridization (FISH) technique introduced in 1992, allows the generation of a copy number karyotype of the whole genome (Kallioniemi *et al.*, 1992). Tumor DNA and reference DNA from a normal individual are differentially labeled, mixed together in equal amounts and co-hybridized under conditions of *in situ* suppression hybridization to normal metaphase chromosomes. Chromosomal gains and losses as well as amplifications are mapped along normal metaphase

chromosomes in a single hybridization. Results from different samples can be clearly summarized by plotting the absolute frequency of cases with gains or losses at the respective band against consecutively arranged chromosomes, each from the telomere of short arm to the telomere of long arm.

To summarize all major chromosomal abnormalities detected among different CGH studies, results were extracted from studies of Brunner *et al.* (2000), Mohapatra *et al.* (1998), Nishizaki *et al.* (1998) and Sallinen *et al.* (1997; Table 1.1). The major gains and/or amplifications in GBM lie in chromosomes 1p, 7p, 7q, 12q, 19p and 20q, while losses and/or deletions involve chromosomes 9p, 10 and 13q. Among these chromosomal abnormalities, gain or amplification of chromosome 7 and loss of 9p and 13q are present also in AA, while gain or amplification of 1p, 12q and 20q are detectable in diffuse astrocytoma.

The number of chromosomal aberrations in astrocytic tumors increases with tumor grade (Nishizaki *et al.*, 1998). In search for differential patterns of chromosomal abnormalities among gliomas form CGH results, the correlation between the average number of copy alterations per patient and malignancy for astrocytic tumors were confirmed in 26 reports between 1992 and 2001 (Koschny *et al.*, 2002). The larger number of abnormalities in high-grade tumors supports the view of tumorigenesis being the result of accumulation of genetic alterations.

Table 1.1. Major chromosomal abnormalities detected in astrocytic tumors by comparative genomic hybridization.
Data complied from Brunner *et al*. (2000), Mohapatra *et al*. (1998), Nishizake *et al*. (1998), and Sallinen *et al*. (1997).

Chromosomal abnormalities	Diffuse astrocytoma %	(Total)	Anaplastic astrocytoma %	(Total)	Glioblastoma multiforme (primary) %	(Total)
1p Gain or amplification	23.8	(21)			28.6	(14)
Chromosome 7 gain					68.6	(86)
7p Gain or amplification			25.0	(12)	44.0	(100)
7q Gain or amplification			25.0	(12)	35.7	(14)
9p Loss			16.7	(12)	56.0	(100)
Chromosome 10 loss					61.0	(100)
12q Gain or amplification	28.6	(7)			28.6	(14)
13q Loss			16.7	(12)	45.0	(100)
19p Gain					48.8	(86)
20q Gain or amplification	28.6	(7)			32.1	(28)

The number of chromosomal losses in diffuse astrocytoma with poor prognosis is very similar to those in AA and GBM and cell lines. In Sallinen *et al.*'s study (1997), chromosomal abnormalities ranged from 0 to 4 in diffuse astrocytomas with typical (n = 7) prognosis and 8 to 28 in diffuse astrocytomas with poor (n = 4) prognosis, indicating the association of number of aberrations with poor prognosis in diffuse astrocytoma. Since the number of samples included is rather small, further studies on chromosomal abnormalities in relation to prognosis are required.

Other genome-wide genetic studies, based on relative fragment length polymorphism, were brought about along the development of polymerase chain reaction (PCR) technique. PCR products from polymorphic microsatellite markers on each arm of every human autosome were resolved by electrophoresis and subject to relative quantification (Fults *et al.*, 1990). Although PCR products with different sizes were amplified with different efficiencies, such differences could be normalized by simultaneous analysis of normal DNA from the same patient. Imbalanced amount of tumor alleles after normalization suggests loss of one of the alleles in the tumor, and is described as loss of heterozygosity (LOH). Such whole genome analysis of allelic imbalances is called allelotyping.

A comprehensive allelotyping of nervous system tumors was performed using 129 microsatellite markers throughout the genome (Von Deimling *et al.*, 2000). Although some deletion regions were detected in high-grade but not in lower-grade tumors by CGH, allelotyping revealed LOH in the same regions in all tumors grades, for example LOH in 9p (Table 1.2). Other than confirming the losses in 9p, 10p, 10q, 13q as detected by CGH, the most frequent LOH regions in astrocytic tumors were also located to 17p, 19q and 22q.

Table 1.2. Major chromosomal abnormalities detected in astrocytic tumors by loss of heterozygosity analysis (Von Deimling *et al.*, 2000).

Chromosome	Diffuse astrocytoma ($n = 28$) %	Anaplastic astrocytoma ($n = 33$) %	Glioblastoma multiforme ($n = 90$) %
9p	8	14	36
10p	10	12	67
10q	0	14	75
13q	0	25	27
17p	42	55	28
19q	23	42	30
22q	9	30	24

Allelotyping is more sensitive than CGH, probably due to higher-resolution mapping. However, it cannot replace CGH studies because amplification of one of the alleles or abnormal number of chromosome copies could also lead to allelic imbalances.

Deletions of chromosomes 9p, 10p, 17p, 19q and 22q LOH were detected by CGH and/or allelotyping in all three grades of astrocytic tumors. This suggests the harboring of early tumor-related genes in these chromosomal arms. In contrast, LOH in the long arm of chromosome 10 and 13, and gain or amplification in chromosome 7 were detected in AA and GBM but not in diffuse astrocytoma, suggesting that the chromosomes carry late genes involved in astrocytic tumorigenesis.

Loss in chromosome 10q and gain in chromosome 19q are associated with aggressive clinical behavior in GBM, as revealed by short-term survival, particularly when two are present together. On the contrary, loss of 19q may be a marker of long-term survivors (Burton *et al.*, 2002).

In addition to the above chromosomal imbalances, our group members also detected loss in 14q in 35% (6/17) of diffuse astrocytoma and 50% (10/21) of GBM by high-resolution genome-wide allelotype analysis. Two common regions of deletion (CRDs) were mapped to 14q22.3 – q32.1 (recently updated to 14q21.2 – q32.12 by the human genome project) and 14q32.1 – qter (Hu *et al.*,

2002). Loss in 14q is related to poor prognosis. While one of two diffuse astrocytomas with loss in 14q recurred as GBM at 18 months and led to death at 28 months, the other died at 19 months after diagnosis (Sallinen *et al.*, 1997).

1.2.3. Tumor suppressor genes

Diffusely infiltrating low-grade astrocytomas have an intrinsic tendency for progression to AA and GBM. This change is due to sequential acquisition of genetic abnormalities, which include loss of TSG activities and gain of oncogene activities. On the basis of Knudson's 'two-hit' hypothesis for TSG inactivation, detection of a high LOH frequency in a chromosomal region is considered critical for TSG localization. LOH is used as a tool for finer deletion mapping of aberrant chromosomes after genome-wide analysis for gross aberrations. *Tumor protein p53 (TP53)*, *phosphatase and tensin homolog (PTEN)*, *retinoblastoma (RB)*, $p16^{INK4A}$, $p14^{ARF}$ are the current confirmed TSGs identified in astrocytic tumors.

Tumor protein p53 (TP53)

The *TP53* gene at locus 17p13.1 encodes p53 that acts as the guardian of the genome by mediating either apoptosis or cell cycle arrest in response to DNA damage. Cell death induced through the p53 pathway is executed by the caspase proteinases, by which cleaving of substrates leads to the characteristic apoptotic

phenotype (Schuler and Green, 2001). One of the transcriptional targets of p53 is *p21*^{WAF1} which encodes an inhibitor of the cyclin-dependent kinases (Cdks) in both the G1 and G2/M phases of the cell cycle. The p53-mediated cell cycle arrest is reversible so as to allow DNA to be repaired before inadvertent replication of damaged DNA (Agarwal *et al.*, 1995; Lundberg and Weinberg, 1999). Loss of function in *TP53* is suggested as a cause of genomic instability (Nozaki *et al.*, 1999).

Loss of 17p was detected in high frequency in all three grades of astrocytic tumors. In screening of every *TP53*-coding exon of 25 GBMs, 14 AAs and 6 diffuse astrocytomas for somatic mutation by single strand conformation polymorphism (SSCP), approximately 60% of *TP53* mutation was found among samples with 17p LOH and confirmed by sequencing (Fults *et al.*, 1992). Similar mutation frequency was also obtained in 14 AAs and 8 diffuse astrocytomas by screening only exons 5, 6, 7, and 8, the conserved regions of *TP53* (Von Deimling *et al.*, 2000). Since two-hit of *TP53* was detected in all grades, recessive mechanism of action of p53 is regarded as an early event.

Exogenous p53 suppressed growth of astrocytic tumor cell lines (LNZ308 and T98G) carrying endogenous mutant or null *TP53* alleles (Van Meir *et al.*, 1995). Such decrease in tumor growth could be attributed to either apoptosis or cell cycle arrest, depending on the expression of p21^{WAF1} (Section 1.3.1).

In an attempt to clarify whether the mutation affects sensitivity to therapy and prognosis, the locus of *TP53* mutation in relation to tumor grade was examined. In consideration of the overall *TP53* mutation, significant difference was not found between AA and GBM. However, a significant difference ($P = 0.01$) between the frequencies of mutation was found in exon 8 between AA and GBM (Shiraishi *et al.*, 2002). Therefore, not only do *TP53* mutations contribute to tumorigenesis by genomic instability, it also contribute in progression to malignancy.

While exon 8 of *TP53* is associated with tumor progression, mutations in exon 4 occur in 42% ($n = 12$) of GBM (Li *et al.*, 1998). Whether this mutation is associated with a particular poor prognosis, as in breast carcinoma, await further studies (Powell *et al.*, 2000).

Frequency of *TP53* mutation within primary GBM has been controversial. However, *TP53* mutation is generally less frequent in GBM than AA, suggesting that *TP53* alteration in primary GBM might not be as common as in secondary GBM. Frequency of *TP53* mutation in primary GBM (12%, 2/17) is significantly lower than that in secondary GBM (85%, 11/13; $P = 0.0001$) Fujisawa *et al.*, 2000).

Phosphatase and tensin homolog (PTEN)

The *PTEN* gene is located on chromosome 10q23.3 and encodes a dual-specificity phosphatase that recognizes phosphatidylinositol-3,4,5-triphosphate (PtdIns-3,4,5-P_3) and protein substrates. PTEN acts against phosphatidylinositol-3-kinase (PI3K) by dephosphorylating PtdIns-3,4,5-P_3, which is required for the phosphorylation and activation of v-akt murine thymoma viral oncogene homolog (Akt), a serine/threonine kinase involved in cell growth and survival. PTEN enables G1 arrest by recruiting $p27^{KIP1}$ into the cyclin E-Cdk2 complex and inhibiting Cdk2 kinase activity without affecting cyclin E or $p27^{KIP1}$ expression. PTEN is also implicated in cell migration and spreading depending on its lipid phosphatase activity (Simpson and Parsons, 2001; Tamura *et al.*, 1999; Weng *et al.*, 2001).

GBM cells with mutant PTEN expression contain high endogenous Akt activity and high levels of PtdIns-3,4,5-P_3 and PtdIns-3,4-P_2, the levels of which could be reduced by expression of wild-type PTEN (Haas-Kogan *et al.*, 1998).

Extensive genomic deletions involving chromosome 10 are the most common genetic alteration in GBM. In fine mapping of CRD in chromosome 10 of 198 astrocytic tumors using 53 microsatellite markers, a locus close and distally located to the *PTEN* gene showed pattern of homozygous deletion in four GBMs (Ichimura *et al.*, 1998). LOH around *PTEN* is closely associated with a reduced

overall survival (P = 0.002) but LOH at other gene locus *(DMBT1* and *NEURL)* within 10q23.3 – q26.1 is not ($P > 0.05$; Fan *et al.*, 2002). There might be other candidate genes on 10q, but *PTEN* is considered as a TSG, based on two-hit inactivation and confirmed by functional analysis.

Frequent loss and homozygous deletion in locus surrounding *PTEN*, and mutation at *PTEN* were detected in GBM but not in diffuse astrocytoma and AA (Fan *et al.*, 2002; Smith *et al.*, 2001; Steck *et al.*, 1999). In concordance with the significantly lower frequency of *PTEN* mutation in both AA and diffuse astrocytoma than GBM, *PTEN* mutations were found in 12% (n = 17) of primary GBM but not in secondary GBM (n = 13; Fujisawa *et al.*, 1999 and 2000). In secondary GBM, TSGs other then *PTEN* are likely to be involved because 10q25 – qter (and 19q13.2 – q13.4) deletions without *PTEN* mutation were detected among 5 secondary GBMs.

Patients with AA harboring *PTEN* alteration have statistically significantly worse survival than patients without *PTEN* alteration after adjustment for age, on-study performance score and extent of tumor resection (Smith *et al.*, 2001).

Retinoblastoma (RB)

RB plays a role in cell cycle control by encoding the nucleoprotein (pRb) that acts as the molecular switch in the restriction point of G1/S transition. In late G1,

pRb is phosphorylated by the cyclin D-Cdk 4/6 complexes, so as to release the nuclear proteins and transcription factors (E2F family) for entrance into the S phase. On the contrary, hypophosphorylated form of pRb induces G1 cell cycle arrest (Buchkovich *et al.*, 1989).

LOH at *RB* locus (13q14.1 – q14.2) occurs in 30% of high-grade tumors (2 of 10 AAs and 14 of 44 GBMs), significantly higher than in diffuse astrocytoma (none of 12; $P = 0.025$). Except one case, no LOH could be detected in adjacent loci in cases without LOH at *RB*. However, only 2 inactivating mutations and 2 possible inactivating mutations of *RB* among the *RB*-deleted samples was reported (Henson *et al.*, 1994). The Knudson's two-hit criterion for tumor suppressors is not fulfilled because of the lack of cases harboring both loss and activating mutation of the same gene. However, *RB* transfection of xenografts resulted in loss in neoplastic morphology and G1 phase arrest, supporting the role of *RB* in tumor growth suppression (Fueyo *et al.*, 1998).

LOH on 13q was detected in 12% (2/17) of primary and 38% (5/13) of secondary GBM and typically included the *RB* locus (Nakamura *et al.*, 2000). No mutations were detected in promoter and exon regions of *RB* among 63 astrocytic tumors (32 primary GBMs, 10 secondary GBMs and 21 AAs). However, among the same 63 tumors, aberrant methylation was detected in 16% of the primary

GBMs, 40% of the secondary GBMs and 14% of the AAs (Gonzalez-Gomez *et al.*, 2003). Knudson's two-hit criterion is fulfilled by methylation and loss of allele.

Promoter methylation of *RB* was not found in 15 diffuse astrocytomas and 10 AAs. Promoter hypermethylation of *RB* in secondary GBM (43%, $n = 21$) is significantly more frequent than in primary GBM (14%, $n = 35$; $P = 0.0258$). (Nakamura *et al.*, 2001a). Combining the LOH and methylation results, *RB* alterations occur lately during astrocytic tumor progression and its role is more significant in secondary GBM.

p16^{INK4A}

$p16^{INK4A}$ from the INK4 family acts as the inhibitor of Cdk4/6. Theoretically, disruption of $p16^{INK4A}$ together with $p15^{INK4B}$, another member of the INK4 family, would lead to a prominent growth advantage for a tumor cell (Simon *et al.*, 1999). *p16^{INK4A}* is the principal target in the 9p21 loss region. Moreover, hypermethylation of promoter region involving multiple sites in a 5'-CpG island is associated with inactivation of *p15^{INK4B}* (Herman *et al.*, 1996).

The role of *p16^{INK4A}* in astrocytic tumorigenesis was confirmed by its correlation with negative immunoreactivity (Park *et al.*, 2000). Also, demethylation of *p16^{INK4A}* by 5-aza-2-deoxycytidine treatment led to re-expression of *p16^{INK4A}* (Costello *et al.*, 1996).

p16^{INK4A} infection of rat GBM cell line RT-2 resulted in 98% reduction in colony formation and 60% reduction in growth. Exogenous overexpression of *p16*^{INK4A} induced hypophosphorylation of Rb. The cells were unable to enter S phase, probably due to the binding of p16^{INK4A} to Cdk4 (Hung *et al.*, 2000).

By differential PCR, frequency of homozygous deletion of *p16*^{INK4A} detected was higher in primary (32%, $n = 34$) than secondary (13%, $n = 16$) GBM. On the contrary, higher promoter hypermethylation was detected in secondary GBM (19%) than primary GBM (3%). Therefore, frequency of *p16* ^{INK4A} alterations is similar in primary and secondary GBM (Nakamura *et al.*, 2001b).

p14^{ARF}

p14^{ARF} shares the same genomic locus with *p16*^{INK4A} although they are structurally unrelated. Binding of p14^{ARF} to a complex of Mdm2 and p53 prevents the Mdm2-mediated degradation of p53. Therefore, p14^{ARF} is a potent tumor suppressor in the presence of wild-type p53 (Simon *et al.*, 1999).

Targeted deletions in the *p14*^{ARF} gene do not result in tumor formation. However, loss of *p14*^{ARF} results in dedifferentiation in response to appropriate oncogenic stimuli. Combined K-Ras and Akt signaling could induce GBM formation from neural progenitor cells but not differentiated astrocytes.

Deficiency of $p14^{ARF}$ cooperated with K-Ras alone in tumor formation from both neural progenitor cells and astrocytes (Uhrbom *et al.*, 2002).

Deletion of $p14^{ARF}$ is associated with co-deletion of $p16^{INK4A}$ and increase in frequency upon progression from low- to high-grade in astrocytic tumors. Interestingly, frequency of $p14^{ARF}$ alterations is higher than that of $p16^{INK4a}$. Nakamura *et al.* (2001b) detected simultaneous homozygous deletion of $p14^{ARF}$ and $p16^{INK4A}$ in 13 GBMs, whereas 9 GBMs showed $p14^{ARF}$ deletion alone. No single case showed $p16^{INK4A}$ deletion alone without $p14^{ARF}$ deletion. Overall, 16 GBMs showed both alterations in $p14^{ARF}$ and $p16^{INK4A}$, and 13 GBMs showed $p14^{ARF}$ alterations alone. Except for one case with $p16^{INK4A}$ methylation alone, there was no GBM with $p16^{INK4A}$ alteration without concurrent $p14^{ARF}$ alteration. Similarly, Labuhn *et al.* (2001) reported higher homozygous deletion and promoter hypermethylation of the $p14^{ARF}$ gene than $p16^{INK4A}$.

Although $p14^{ARF}$ methylation occurs in both GBM subtypes, $p14^{ARF}$ deletion and *TP53* deletion are mutually exclusive, suggesting functional redundancy of the 2 genes in astrocytoma tumorigenesis ($P < 0.01$, $n = 20$; Fulci *et al.*, 2000). Homozygous deletion and promoter hypermethylation of the $p14^{ARF}$ gene occurs in 44% and 31% of 34 primary GBMs, respectively. They also account for 44% and 6% of 16 secondary GBMs, respectively. No overall statistical significant difference ($P = 0.129$) exists between the two GBM subgroups. Among 15

secondary GBMs with homozygous deletion, 33% of the paired diffuse astrocytomas were hypermethylated in promoter of $p14^{ARF}$, with no homozygous deletion detected (Labuhn *et al.*, 2001). This suggests that homozygous deletion of $p14^{ARF}$ is a later event than hypermethylation.

1.2.4. Oncogenes

EGFR and *mouse double minute 2 homolog (MDM2)* are the current confirmed oncogenes identified in astrocytic tumors.

Epidermal growth factor receptor

EGFR was the first amplified gene discovered in human GBM (Libermann *et al.*, 1985). In search for amplification of tumor-related genes located on chromosome 7, *EGFR* was reported as the only gene amplified among 16 astrocytic tumors (6 of 10 GBMs, 2 of 2 AAs, and 4 of 4 diffuse astrocytomas; Torp *et al.*, 1991). Quantitative DNA dot blots revealed *EGFR* amplifications in 6 of 14 GBMs (Hurtt *et al.*, 1992). In another study, the *EGFR* locus (7p12.3 – p12.1) was the most commonly and highly amplified (Liu *et al.*, 1998).

EGFR encodes a receptor-tyrosine-kinase (RTK) with an extracellular ligand binding domain, a transmembrane domain and intracellular tyrosine kinase domain, and additional amino acid sequences that function as regulatory domains

(Lemmon and Schlessinger, 1994). Ligand binding induces receptor dimerization, autophosphorylation in a *trans* fashion and elevated tyrosine kinase activity of the RTK. The binding of epidermal growth factor (EGF) leads to simultaneous activation of multiple pathways, including the extensively studied Ras/Raf/Mek/Erk pathway (Jorissen *et al.*, 2003).

EGFR amplification was significantly less common in AA than GBM (P = 0.001, n = 63 and 111; Smith *et al.*, 2001), revealing its role at later stage of malignancy change. Both *EGFR* amplification and EGFR overexpression are more frequent in primary GBM. *EGFR* amplification was found in about 50% (25/49) of primary GBMs but not in secondary ones (0/33; Fujisawa *et al.*, 2000 and Libermann *et al.*, 1985). Virtually all tumors with *EGFR* amplification showed EGFR overexpression (Libermann *et al.*, 1985). About 40% of primary GBM overexpressing EGFR harbor *EGFR* amplification (Harada *et al.*, 2000). EGFR overexpression was detected in about 70% (15/22) of primary GBMs. Among 20 secondary GBMs, only 2 samples showed EGFR overexpression.

Tumorigenicity of *EGFR* was demonstrated by overexpression of normal human EGFR in fibroblast culture (Haley *et al.*, 1989). Anti-sense *EGFR* RNA transfection in human malignant gliomas cell U87MG led to increase of cell population in G1 but decrease in S phase, and reduced transforming potential as determined by soft agar assay (Tian *et al.*, 1998).

More than half of GBMs with amplified *EGFR* genes also show co-amplification of rearranged *EGFR* genes and express of aberrant mRNA species concomitantly (Ekstrand *et al.*, 1991). The most common mutant EGFRvIII contains a deletion of exons 2 – 7, encoding a constitutively autophosphorylated protein which could not be efficiently down-regulated (Fenstermaker and Ciesielski, 2000).

Interestingly, neither addition of EGF nor expression of EGFRvIII affects rate of cell growth in culture. However, tumorigenic capacity was greatly enhanced when cells expressing EGFRvIII were implanted specifically into brain of nude mice. Therefore, EGFRvIII promotes growth by influencing interactions of tumor cells in a way that cannot be assayed *in vitro* (Nishikawa *et al.*, 1994).

Simultaneous *EGFR* overexpression and *TP53* mutation is rare. In Fujisawa *et al.*'s study (2000), only one such case occurred out of 49 GBMs examined. However, Okada *et al.* (2003) accounted the exclusive pattern of *TP53* mutation and *EGFR* amplification to the uses of GBM lysates. In their FISH study, *EGFR* amplification in GBM harboring *TP53* mutation occurred in the cellular level at invading edges of tumor tissue. Therefore, frequency of *EGFR* amplification in secondary GBM might vary due to different sampling location of tumor.

Mouse double minute 2 homolog (MDM2)

Mdm2 mediates p53 degradation via the ubiquitin-proteosome pathway and is itself a target of p53, completing a negative feedback loop (Chen *et al.*, 1999; Leng *et al.*, 2003). Mdm2 also acts as a bridge in formation of pRb-Mdm2-p53 trimeric complex, enabling the modulation of apoptosis by pRb (Yap *et al.*, 1999).

In mapping of amplicons within the 12q13 – q14 in 234 CNS tumors, *MDM2* at 12q14.3 – q15 showed preferential involvement with other two genes (*CDK4* and *SAS*). Although *MDM2* was not the most frequently included gene in the amplicon of 12q, it was detected at the highest levels of amplification when co-amplified. Amplification of *MDM2* without the other amplicons was also reported (Reifenberger *et al.*, 1994). Therefore, *MDM2* is very likely an oncogene on 12q.

Oncogenicity of *MDM2* was later reflected by invasive activity of neonatal rat astrocytes overexpressing Mdm2 (Kondos *et al.*, 1996). *TP53* mutation and LOH on chromosome 17, with one exception were not detected among the astrocytic tumors showing *MDM2* amplification (Reifenberg *et al.*, 1993; Schiebe M *et al.*, 2000). Mdm2 immunoreactivity was also associated with low or negative p53 expression (Biernat *et al.*, 1997; Dietzmann *et al.*, 1996). This reflects the complementary role of *TP53* and *MDM2* alterations in tumorigenesis.

MDM2 amplification was detected in similar frequency in AA and GBM (Reifenberger *et al.*, 1994). Amplification of the gene was detected in 2 of 29 primary GBMs but not in 27 secondary GBMs examined. Immunoreactivity for Mdm2 was found in 52% (n = 29) primary GBMs but only 11% (n = 27) secondary GBMs (P = 0.0015; Biernat *et al.*, 1997). Hence, alterations in *MDM2* are present in both AA and secondary GBM, but are more prominent in primary GBM. Survival estimation revealed a significant correlation of *MDM2* gene amplification or overexpression with shorter survival time (Burton *et al.*, 2002; Schiebe *et al.*, 2000).

On the other hand, a significantly higher frequency of short alternative splice transcripts of *MDM2* in GBM than AA and diffuse astrocytomas (22 of 32 GBMs, 5 of 17 AAs, and none of 12 diffuse astrocytomas; $P < 0.0003$) was detected using a nested reverse transcription-PCR technique (Matsumoto *et al.*, 1998). The presence of Mdm2 splice variants do not have apparent correlation with p53 status, suggesting a different mechanism of tumorigenesis caused by shortened transcripts, which may or may not be related to pRb-Mdm2-p53.

1.2.5. Primary and secondary GBMs

Genetic and epigenetic alterations in primary and secondary GBMs were summarized in Figure 1.1. Despite most genetic abnormalities are present in both

tumor subtypes, they differ greatly in frequencies, favoring the division of primary and secondary GBMs into 2 subgroups. Primary GBM is characterized by *EGFR* and *MDM2* amplification/overexpression, *PTEN* mutations, LOH on entire chromosome 10, while secondary GBM shows frequent *TP53* mutations and LOH on chromosomes 10q and 19q (Figure 1.2; Kleihues and Ohgaki, 1999).

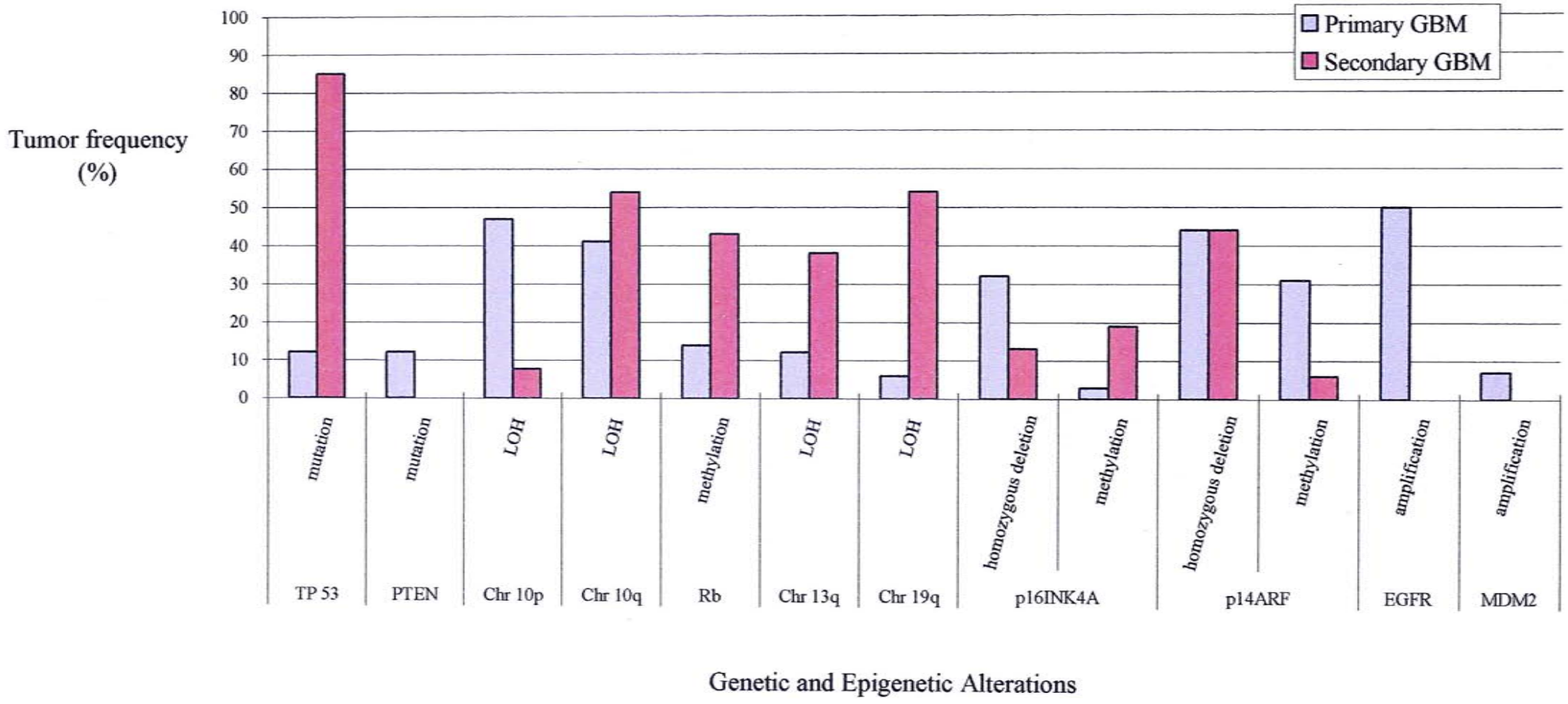

Figure 1.1. Frequency of genetic and epigenetic alterations in primary and secondary GBMs.
Data complied from Biernat *et al.* (1997), Fujisawa *et al.* (1999 and 2000), Labuhn *et al.* (2001), Libermann *et al.* (1985) and Nakamura *et al.* (2000, 2001a and 2001b).

Fig 1.2. Genetic and epigenetic alterations in primary and secondary GBMs.

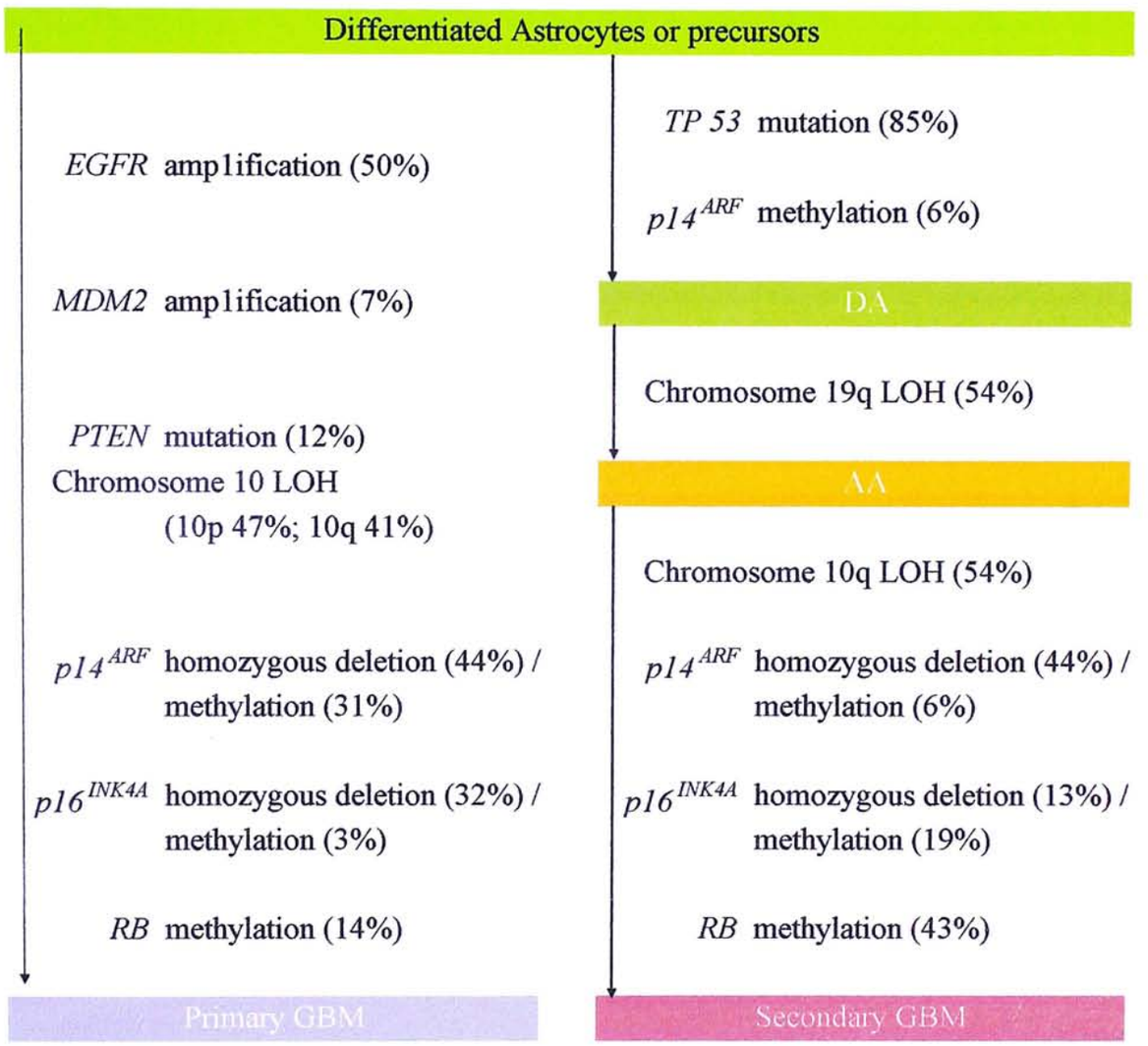

Although alterations in chromosome 10 are involved in both primary and secondary GBM, their patterns of abnormalities are different. Among studies on sub-classification of GBM, LOH analysis on chromosome 10 using 28 informative markers revealed LOH in all markers in the majority (88%, $n = 17$) of primary GBM. In contrast, only partial or complete loss of 10q, with retention of 10p was detected in secondary GBM (Fujisawa *et al.*, 2000).

1.3. Major pathways involved in astrocytic tumorigenesis

Not only could the genetic and epigenetic alterations help in sub-classification of astrocytic tumors into different subtypes, they could also help in explaining the genetic pathogenesis of the tumors. Most of the alterations, if not all, could be incorporated into two major pathways, the cell cycle pathways and the growth factor-regulated signaling pathways. The $p16^{INK4A}$/Cdk4/pRb cell cycle pathway and $p14^{ARF}$/Mdm2/p53 cell cycle arrest pathway play a prominent role in glial transformation. Dysregulation of polypeptide growth factors acting via RTKs, and of intracellular signaling through RTKs plays a critical role in tumor progression.

1.3.1. Cell cycle dysregulation and suppression of apoptosis

The cell cycle clock is regulated by cyclins which assemble with their catalytic partners, the Cdks (Figure 1.3; Lundberg and Weinberg, 1999; Stevens and Fields, 2002). On one hand, the cyclin-Cdk complexes are regulated by cyclin-Cdk-activating kinases and serine/threonine phosphatase. On the other hand, they are negatively regulated by two families of Cdk inhibitors (CKIs), the INK4 family (including $p15^{INK4B}$ and $p16^{INK4A}$) and the Cip/Kip family (including $p21^{WAF1}$ and $p27^{KIP1}$).

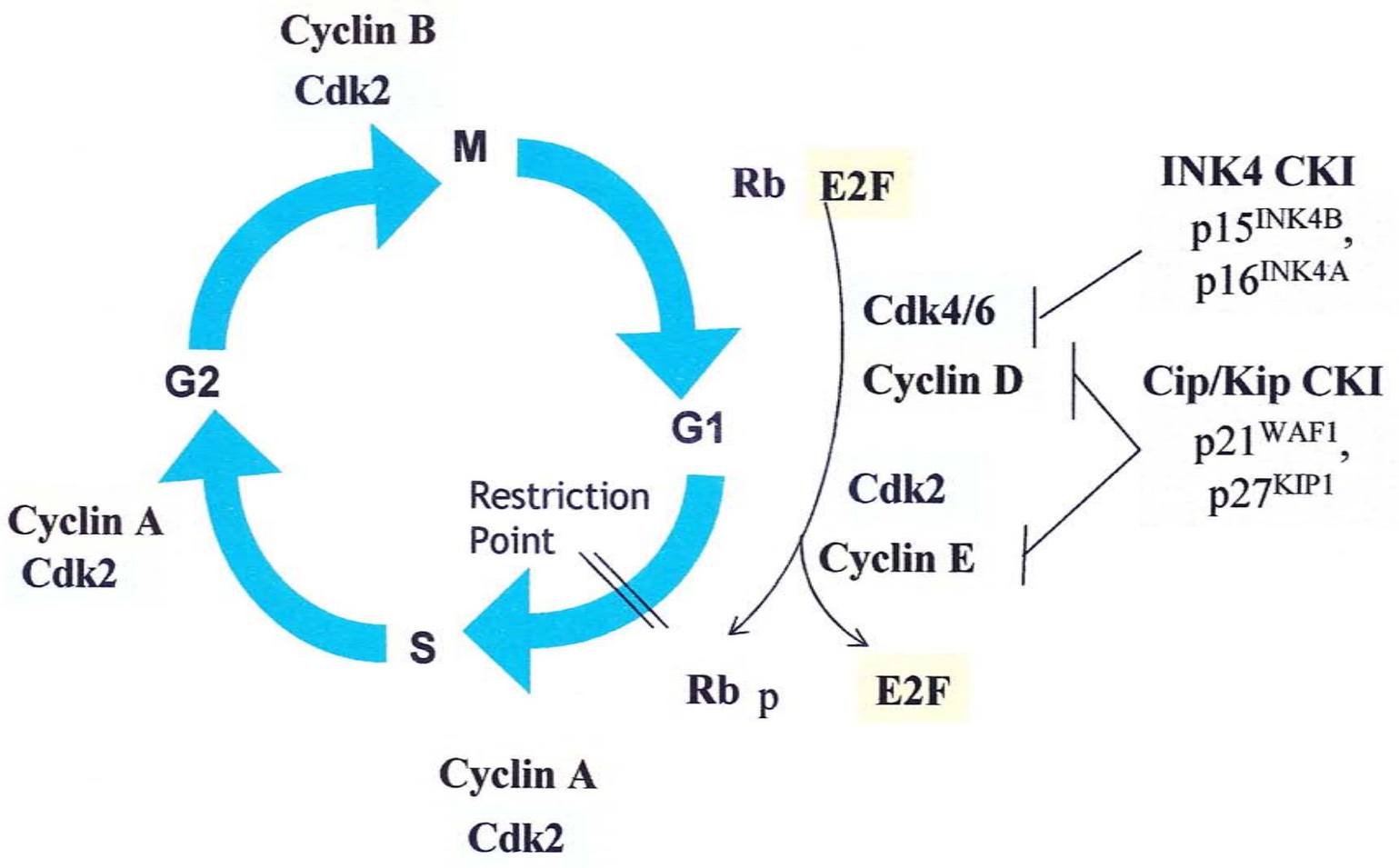

Fig 1.3. The cell cycle clock.
Modified from Lundberg and Weinberg (1999) and Stevens and Fields (2002).

The levels of cyclins vary periodically in tightly regulation of the cell cycle phase, with the D-type cyclins being the first group to be induced in response to mitogenic stimuli. In particular, progression to S phase requires the phosphorylation and hence, inactivation of pRb by cyclinE-Cdk2, allowing the release of E2F family of transcription factors for expression of S phase gene as well as the *cyclin E*. In the presence of mitogenic stimulation, the cells run through a restriction point and complete the cycle. Disruption of any component of the $p16^{INK4A}$/Cdk4/pRb pathway is sufficient to dysregulate the cell cycle.

Analysis of 120 GBMs showed only 7 of the cases without apparent abnormality of $p16^{INK4A}$, *CDK4* or *RB*. Among 195 astrocytic tumors, only 2 of them had alterations in more than one of the three genes (Ichimura *et al.*, 1996). Therefore, dysregulation of the cell cycle is a major event in pathogenesis of GBM and alteration in one of the components is enough to disrupt the running of the cell cycle clock.

p53 plays a role in cell cycle control through the induction of $p21^{WAF1}$ expression. Cell cycle analyses showed glioma cells arrested in the G2 phase before undergoing cell death. Transfer of $p21^{WAF1}$ induced a G2 block but did not induce apoptosis. Co-expression of $p21^{WAF1}$ and p53 prevented gliomas cells from undergoing apoptosis (Gomez-Manzano *et al.*, 1997).

The mechanisms by which p53 mediates apoptosis are unclear. p53-inducible genes may contribute to the induction of both death-receptor and mitochondrial apoptotic pathways (Vousden and Lu, 2002). p53 may also mediate apoptosis by transcriptional induction of redox-related genes. The formation of reactive oxygen species then leads to oxidative degradation of mitochondrial components, culminating in cell death (Polyak *et al.*, 1997). The requirement for activation of parallel apoptotic pathways is postulated (Pietenpol and Stewart, 2002).

1.3.2. Promotion of proliferation and survival

Cellular growth and survival are regulated by two parallel signaling pathways, the mitogen-activated protein kinase (MAPK) cascades and the Akt pathway.

The MAPK cascade

The basic signaling module of the MAPK cascade includes a G-protein working upstream of a core module consisting of three kinases: a MAPK kinase kinase (MAPKKK) that phosphorylates and activates a MAPK kinase (MAPKK), which in turn activates MAPK (Kolch, 2000). To date, six MAPK pathways had been identified. Among them, the Raf/Mek/Erk signaling cascade was the first to be characterized and has been intimately connected with the regulation of cell growth and differentiation. In this cascade, Ras is the G-protein, Raf is the

MAPKKK, Mek (MAPK/Erk kinase) is the MAPKK and Erk (extracellular-signal-regulated kinase) is the MAPK (Hilger, 2002).

In vertebrates, regulation of Raf/Mek/Erk is complex because the Ras family consists of four members (H-Ras, K-Ras4a, K-Ras4b, and N-Ras) whereas the Raf family comprises of C-Raf (Raf-1), A-Raf and B-Raf (Hagemann and Rapp, 1999). Mek and Erk are of 2 isoforms, Mek 1 and Mek 2, and Erk1 and Erk2. Furthermore, B-Raf encodes at least 10 different protein isoforms resulting from complex alternative splicing (Barnier *et al.*, 1995; Eychene *et al.*, 1995).

Alterations in the MAPK cascade in astrocytic tumors

As *EGFR* amplification occurred predominantly in GBM but not in AA and diffuse astrocytoma, overexpression of wild-type or mutant EGFR is widely thought to contribute to the malignant phenotype of GBM. However, the mechanism of how *EGFR* contribute to proliferation and survival is not well understood. The Ras protein, which complex with RTK through Growth factor Receptor-Bound protein 2 (Grb2) and Son of sevenless, drosophila homolog 1 (Sos1), has been considered as the downstream effector which relays signals to the MAPK cascade.

RAS mutation was detected in 30% of all human cancers (Bos, 1989). SSCP screening of codons 12 and 61 of the *H-*, *K-*, and *N-RAS* oncogenes in biopsies

from 18 GBM patients did not yield aberrant band or mutation (Gomori *et al.*, 1999). Nevertheless, blocking Ras activation by expression of the *H-RAS-Asn17* dominant negative mutant or by farnesyl transferase inhibitors decreased *in vitro* proliferation of human astrocytomas cell lines (Guha *et al.*, 1997). Overexpression of *H-RAS* for transformation of astrocytes activated Ras *in vivo* (Ding *et al.*, 2001). Transgenic mouse astrocytoma mirrored both the histopathology and molecular profile of human malignant astrocytomas. Experiments with EGFR kinase inhibitor PD158780 showed the contribution of spontaneously activated EGFR to constitutive phosphorylation of Erk but not members of the Akt pathway in the astrocytic tumor cell line SKMG3 (Thomas *et al.*, 2003).

According to Mandell *et al.* (1998), Erk is highly activated in both low-grade and malignant gliomas. Erk phosphorylates and activates several targets in growth control. Activation of the transcription factor Elk-1 leads to the expression of immediate early genes, including *v-myc avian myelocytomatosis viral oncogene homolog (MYC)* which may regulate cell cycle at multiple points. Increased MYC protein expression may promote G1/S transition by attenuating the expression of the Cdk inhibitor $p27^{KIP1}$. The activation of $p90^{RSK}$ results in histone H3 phosphorylation, increasing accessibility of transcription factor to

DNA. $p90^{RSK}$ activation also inactivates Myt1, a kinase that phosphorylates and inactivates the Cdk1/Cdc2 kinase for G2/M transcription. Activation of carbamoyl phosphate synthetase allows pyrimidine-nucleotide synthesis. Lastly, activation of MAPK-interacting kinase 1 (Mnk1) would in turn activate the eukaryotic translation initiation factor eIF-4E for synthesis of rapid-response genes for growth (Besson and Yong, 2001; Shapiro, 2002). Erk also promotes cell survival and may contribute to tumorigenesis by phosphorylation and inhibition of caspase-9 (Allan *et al.*, 2003).

The Akt pathway and PTEN in astrocytic tumors

Upon activation of membrane receptors by growth factors and survival factors PI3K is recruited to plasma membrane. This results in phosphorylation of membrane lipids PtdIns-4-P and PtdIns-4,5-P_2, and production of the second messengers ptdIns-3,4-P_2 and PtdIns-3,4,5-P_3. The second messengers in turn recruit Akt and Phosphoinositide-dependent protein kinase 1 (Pdpk1) to the membrane and expose the activation loop in Akt. Phosphorylation of Akt at T308 of the activation loop by Pdpk1 turns on the protein kinase activity. Phosphorylation of Akt at C-terminal site causes further activation (Cantley and Neel, 1999).

Akt down-regulates $p27^{KIP1}$ levels and inhibits glycogen synthase kinase 3, which phosphorylates and targets cyclin D for proteolysis (Cantley and Neel, 1999; Di Cristofano and Pandolfi, 2000). It also phosphorylates and retains $p21^{WAF1}$ and $p27^{KIP1}$ in the cytoplasm. Not only promoting cell cycle progression, cytoplasmic $p21^{WAF1}$ also binds to the Apoptosis-signal-regulating kinase (Ask1) to inhibit apoptosis. Furthermore, Akt phosphorylates and compromises the function of BCL2-antagonist of cell death (Bad) and caspase-9, proteins involved in apoptosis (Liang and Slingerland, 2003; Testa and Bellacosa, 2001).

Under serum-free conditions, human GBM cell lines with Akt activation exhibited only weak phosphorylation of MAPK signal pathway, whereas those cell lines lacking constitutive Akt activation demonstrated high levels of phosphorylation (Schlegel *et al.*, 2000). However, in AA and GBM, *PTEN* mutation was known to co-operate with EGFR activation to increase vascular endothelial growth factor (VEGF) mRNA levels by transcriptionally up-regulating the proximal VEGF promotor via the Akt pathway (Pore *et al.*, 2003).

1.4. B-Raf mutation in human cancers

Raf was linked to Ras in 1992 and 1993 (Avruch *et al.*, 1994). However, Raf was related to cancer independent of Ras only recently, through the Cancer Genome Project (CGP) by Davies *et al.* (2002). CGP is a systematic genome-wide screen for mutations in genes that are related to the regulation of cell proliferation, differentiation and death. The authors postulated the involvement of at least one gene mutation in the signaling pathways and succeeded in discovery of *BRAF* mutations in a variety of human cancers.

In general, the family of Raf proteins is involved in regulation of proliferation, differentiation, and apoptosis. They are overlapping in function but are tissue specific and might differ in the regulation of their activation and their ability to connect to downstream signaling pathways (Hagemann and Rapp, 1999). All Raf proteins are cytosolic. C-Raf transcript is expressed ubiquitously in the mouse, with highest expression levels in striated muscle, cerebellum, and fetal brain. A-Raf is preferentially expressed in urogenital tissue. B-Raf shows highest expression levels in neuronal tissues and testis (Naumann *et al.*, 1996). Of the three kinases, A-Raf has the lowest binding affinity towards Ras. Therefore, an alternative activator for A-Raf may exist (Weber *et al.*, 2000). *In vitro*, B-Raf has a higher binding affinity for Mek and displays a higher Mek kinase activity than

C-Raf (Papin *et al.*, 1998). Furthermore, maximal B-Raf activity requires only oncogenic Ras, while A-Raf and C-Raf require synergized activation of Ras and Src (Marais *et al.*, 1997; Mason *et al.*, 1999).

In screening of the coding exons and intron-exon junctions of the *BRAF* gene in 15 cancer cell lines consisting of six breast cancers, one small cell lung cancer, six non-small cell lung cancers, one mesothelioma and one melanoma for sequence variants, three single-base substitutions were detected. Two were in exon 15: T1796A leading to a substitution of valine by glutamic acid at position 599 (V599E) and C1786G leading to L596V. The one in exon 11 was G1403C leading to G468A. All were somatic mutations because none of the three changes were detected in lymphoblastoid cell lines from the same individuals. Further screening of 530 cell lines also revealed *BRAF* mutations in exons 11 and 15. Accordingly, the two exons were screened for mutations in genomic DNA from 378 primary human cancers and short-term cultures. *BRAF* mutations were detected in 67% of primary melanoma, 12% of primary colorectal cancer, 14% of primary ovarian cancer and many other tumor types. Base substitution was also detected in four (DBTRG-05MG, KG-1-C, AM-38 and NMC-G1) of 38 glioma cell lines (Davies *et al.*, 2002).

The three Raf proteins are conserved in three conservative regions (CRs; Mercer and Pritchard, 2003; Figure 1.4). CR1 consists of the Ras binding domain (RBD) and a cysteine-rich domain. CR2 is rich in serine and threonine residues and is thought to be involved in phosphorylation regulation of the Raf proteins. The *BRAF* mutations in various human cancers lie in the third CR. All of the mutated amino acid residues (G463, G465 and G468) in exon 11 lie in the G-loop of ATP binding region and all (F594, G595, L596 and V599) except E585 in exon 15 lie in the activation segment of B-Raf. Out of the mutants, 80% were V599E base substitution (Davies *et al.*, 2002).

After the discovery of *BRAF* as an oncogene, studies on *BRAF* in dysplastic tissues, expanded cancer series and cell lines were performed by different groups. *BRAF* mutations were detected in 46% of papillary thyroid cancer, 21.7% of cholangiocarcinoma, 33.3% of hyperplastic polyp (Table 1.3 and 1.4). Other than the mutation sites just mentioned, large number of other base changes were also detected in exons 11 and 15 of the *BRAF* gene (Figure 1.4; Table 1.5).

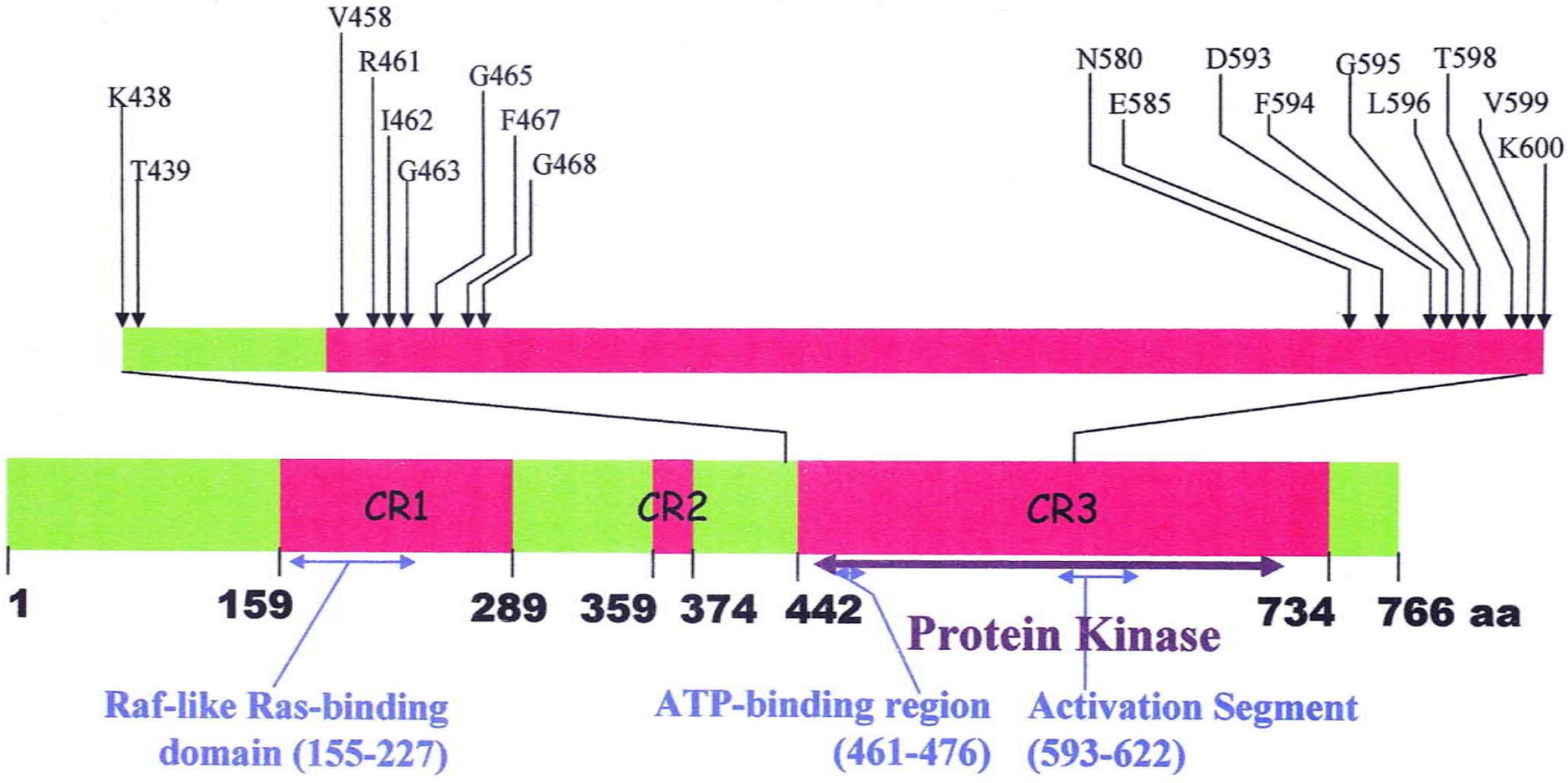

Figure 1.4. Distribution of somatic mutations in the B-Raf protein.

CR, Conservative region; arrows, amino acid residues with mutation detected; aa, amino acid residue.

Data complied from Brose *et al*. (2002), Davies *et al*. (2002), Naoki *et al*. (2002), Pollock *et al*. (2003), Rajagopalan *et al*. (2002), Tannapfel *et al*. (2003) and Yuen *et al*. (2002).

Table 1.3. Frequencies of *BRAF* mutation in human dysplastic and tumor tissues.

Tumor type	Tumor subtype	Number of mutations	Number of cases	(%)	Total number of mutations	Total number of cases	(%)	Reference
Melanoma/Nevi	Compound nevi	16	23	69.6				a
	Congenital nevi	6	7	85.7				a
	Dysplastic nevi	4	5	80.0				a
	Intradermal nevi	37	42	88.1				a
	Primary tumor	16	20	80.0				a and b
	Dermal/subcutaneous metatasis	18	29	62.1				a
	Distant organ metatasis	9	14	64.3				a
	Lymph metastasis	10	12	83.3				a
	Short-term culture	34	50	68.0	150	202	74.3	b and c
Thyroid cancer	Papillary	75	163	46.0				d, e and f
	Non-papillary	1	177	0.6	76	340	22.4	d, e and f
Liver cancer	Cholangiocarcinoma	15	69	21.7				
	Hepatocellular	0	25	0.0	15	94	16.0	g
Colorectal cancer	Familial adenoma	1	63	1.6				h
	Hyperplastic polpy	1	3	33.3				h
	Colorectal carcinoma	4	33	12.1				b
	Sporadic adenoma	3	108	2.8	9	207	4.3	h

(Continued on page 44)

Table 1.3 (continued). Frequencies of *BRAF* mutation in human dysplastic and tumor tissues.

Tumor type	Tumor subtype	Number of mutations	Number of cases	(%)	Total number of mutations	Total number of cases	(%)	Reference
Ovarian cancer	Low malignant	4	60	6.7				i
	Invasive/Malignant	1	47	2.1	5	107	4.7	b and i
								b
Head & neck cancer	Squamous cell carcinoma	6	96	6.3				b and e
	Non-squamous cell carcinoma	0	49	0	6	145	4.1	e
Lung cancer	Adenocarcinoma	8	347	2.3				c, e and j
	Non-adenocarcinoma	3	94	3.2	11	441	2.5	c
Sarcoma					1	182	0.5	b
Bladder cancer					0	27	0	e
Glioma					0	15	0	b
Breast cancer					0	33	0	b
Cervical cancer					0	38	0	e
Prostate cancer					0	40	0	b and e

a, Pollock *et al*. (2003); b, Davies *et al*. (2002); c, Brose *et al*. (2002); d ,Kimura *et a*l. (2003); e, Cohen *et al*. (2003); f, Soares *et al*. (2003); g, Tannapfel *et al*. (2003); h, Yuen *et al*. (2002); i, Gemignani *et al*. (2003); j, Naoki *et al*. (2002).

Table 1.4. Frequencies of *BRAF* mutation in human cell lines.
Data complied from Cohen *et al*. (2003) and Davies *et al*. (2002).

Cell line	No. of Mutations	No. of cases	%
Thyroid cancer	6	9	66.7
Melanoma	20	34	58.8
Colorectal cancer	7	40	17.5
Glioma	4	38	10.5
Sarcoma	5	59	8.5
Ovarian cancer	1	26	3.8
Lung cancer	4	131	3.1
Breast cancer	1	45	2.2
Bladder cancer	0	10	0
Neuroblastoma	0	29	0
Cervical cancer	0	11	0
Gastric carcinoma	0	6	0
Leukaemia & Lymphoma	0	53	0
Pancreatic carcinoma	0	3	0
Prostate cancer	0	3	0
Renal cell carcinoma	0	11	0
Testicular carcinoma	0	7	0
Uterine carcinoma	0	3	0

Table 1.5. *BRAF* mutations in human tumor tissues and cell lines.

Amino acid residue change	Nucleotide change	Cancer	Reference
K438Q	NA	Melanoma short-term culture.	a
K438T	NA	Lung adenocarcinoma.	a
T439P	NA	Lung squamous cell carcinoma.	a
V458L	NA	Lung adenocarcinoma.	a
R461I	G1382T	Colorectal cancer (Sample type unspecified).	b
I462S	T1385G	Colorectal cancer (Sample type unspecified).	b
G463E	G1388A	Colorectal cancer (Sample type unspecified) and ovarian cancer cell line.	b and c
G463V	G1388T	Colorectal cancer cell line.	c
G465A	G1394C	Melanoma short-term culture.	c
G465E	G1394A	Primary melanoma.	c
G465V	G1394T	Lung adenoma and lung cancer cell line.	c and d
F467C	T1400G	Colorectal adenoma.	e
G468A	G1403C G1403T	Lung cancer cell line. Cholangiocarcinoma.	c f
G468E	G1403A	Cholangiocarcinoma and colorectal cancer.	c, e and f
D593G	A1778G	Colorectal adenoma.	e

(Continued on page 47)

Table 1.5 (continued). *BRAF* mutations in human tumor tissues and cell lines.

Amino acid residue change	Nucleotide change	Cancer	Reference
D593V	A1778T	Colorectal adenoma.	e
F594L	T1782G	Cholangiocarcinoma, colorectal carcinoma and familial adenoma.	c, e and f
G595R	G1783C	Colorectal adenoma and colorectal cancer cell line.	c and e
L596R	T1787G	Lung adenoma and ovarian cancer.	c and d
N580S	A1739G	Colorectal adenoma	e
E585K	G1753A	Ovarian cancer	c
L596V	C1786G NA	Cholangiocarcinoma and lung cancer cell line. Lung squamous cell carcinoma.	c and f a
T598I	C1793T	Colorectal adenoma	e
V599D	TG1796-97AT NA	Cholangiocarcinoma, melanoma metatasis and cell line. Melanoma short-term culture.	c, d and f
V599E	T1796A NA	Breast cancer cell line, cholangiocarcinoma, colorectal cancer and cell line, glioma cell Lung squamous cell carcinoma and melanoma short-term culture.	a, b, c, e and g a
V599K	GT1795-96AA	Melanoma metatasis.	g
V599R	GT1795-96AG	Melanoma metatasis.	g
K600E	A1789G NA	Colorectal cancer and Non-papillary thyroid carcinoma. Melanoma short-term culture.	c c

The functional regulation and activation of B-Raf is partly implied by sequence comparison with C-Raf. The inactive C-Raf is phosphorylated in S259 and S621 that bind 14-3-3 proteins retaining C-Raf in an inactive, closed conformation. Upon stimulation, 14-3-3 is displaced from C-Raf by Ras-GTP. C-Raf is then translocated to the plasma membrane, where it is dephosphorylated at S259 by phosphatase such as PP2A (Abraham *et al.*, 2000; Dhillon *et al.*, 2002). Similarly but with a more open conformation, B-Raf is rendered inactive by phosphorylation of S364 and S728 (MacNicol *et al.*, 2000). The phosphorylation of S259 of C-Raf and S364 of B-Raf (at equivalent positions) appears to be negatively regulated by Akt (Guan *et al.*, 2000; Zimmermann and Moelling, 1999).

One crucial event in Ras-induced activation of C-Raf is phosphorylation of S338. The corresponding amino acid residue in B-Raf is the constitutively phosphorylated S445. Phosphorylation of T341 by Src family is also essential for C-Raf activation. In B-Raf, the equivalent position to Y340 and Y341 are D447 and D448. B-Raf activation without tyrosine kinase signals is attributed to the negative charges of the aspartic acid, which may mimic phosphorylated residue (Marais *et al.*, 1997; Mason *et al.*, 1999). T598 and S601 located within the activation segment were identified as additional major phosphorylation sites of B-Raf at the membrane in response to oncogenic Ras (Mercer and Pritchard, 2003).

Biological effects of *BRAF* mutations were characterized by expression of cDNA containing V599E, L596V, G463V and G468A mutations in cell lines. Kinase-activated B-Raf mutants were able to induce transformation because cDNA constructs in NIH3T3 cells increased focus-forming ability of the cells. Not only did the mutants possessed elevated basal kinase activity (V599E, 10.7-fold; L596V, 5.7-fold; G463, 2-fold; G468A, 12.5-fold) in COS cells, they were also capable to stimulate endogenous Erk (Davies *et al.*, 2002).

The V599E is distinct from other B-Raf mutations because none of the 51 tumors series in Davies *et al.*'s study which harbor V599E mutation contained *K-RAS or N-RAS* mutation. Whenever, simultaneous mutation of *BRAF* and *RAS* mutation were detected, it was non-V599E. Proliferation requirement of V599E mutant cells is uncoupled from Ras activation, although *in vitro* data indicated further activation by mutant Ras. The cell lines with V599D, G465V, G463V and L596V mutation remained dependent on Ras function (Davies *et al.*, 2002).

Microsatellite instability (MSI) in sporadic colorectal cancer often results from epigenetic inactivation of the DNA mismatch-repair gene, *MLH1* in association with DNA methylation (Herman *et al.*, 1998). In studies of *BRAF* mutation pattern in colorectal neoplasia, significantly higher frequency of *BRAF* mutation was found in mismatch-repair-deficient tumors than in mismatch-repair-proficient

ones (Rajagopalan *et al.*, 2002; Wang *et al.*, 2003). The correlation of *BRAF* mutation with mismatch-repair deficiency suggests vulnerable structural or sequence elements surrounding *BRAF* codon 599 in repair-deficient background. In Wang *et al.*'s study (2003), about 60 of 293 colorectal cancers harbored V599E mutation. Within 31 samples with both *MLH1* alterations and *BRAF* mutation among 293 colorectal cancers, 30 were hypermethylated in their promotors and the remaining one harbored *MLH1* germline mutation. Therefore, epigenetics account for at least half (31/60) of *BRAF* mutations in colorectal cancer.

The timing of mutations in melanoma tumorigenesis was investigated by screening of *BRAF* mutations in nevi. Mutation of V599E in nevi (82%) is as high as in primary melanoma (80%; Pollock *et al.*, 2003), suggesting a role of *BRAF* mutations in melanoma initiation. Regarding nevi as premalignant precursors of melanoma, the mutational activation of the Ras/Raf/Mek/Erk pathway would be critical in tumorigenesis but alone is insufficient for tumorigensis. Moreover, *BRAF* mutations were detected in only 10% of the earliest stage of rapid-growth-phase melanomas in contrast to a 75% of melanoma in vertical-growth-phase (Dong *et al.*, 2003). Based on the increase in *BRAF* mutation frequency with tumor grade, the author suggested a role of *BRAF* mutation in tumor progression rather than initiation. Whether *BRAF* mutation

provides an advantage in tumor initiation and/or proliferation requires further studies.

The dysregulation of growth regulatory pathways in melanoma could be summarized into four levels: 1) aberrant production of autocrine growth factors that substitute for exogenous growth factors; 2) alterations in response to negative autocrine growth factors; 3) overexpression of *EGFR*; and 4) alterations of cellular protooncogenes involved in signal transduction and growth suppression (Rodeck, 1993). Although the sequential alterations in melanoma could not be applied directly to the astrocytic tumors, the autocrine activation of melanoma cells could provide hints on tumorigenesis of astrocytic tumors, in which *EGFR* overexpression occurs frequently.

Using melanoma cell lines with activating mutations in the kinase domain of *BRAF*, neutralization on fibroblast growth factor (FGF) and hepatocyte growth factor (HGF) dramatically inhibited Erk activation. Thus, constitutively activated Erk is apparently mediated by excessive growth factors through autocrine mechanisms and B-Raf kinase activation in melanoma (Satyamoorthy *et al.*, 2003). Likewise, *BRAF* mutations in other cancers, including astrocytic tumors, may also be related to alterations in members of mitogenic signaling pathway.

1.5. Other CNS tumors included in the current study

Classifications of CNS tumors have been based on theories of histogenesis, grades of dedifferentiation/anaplasia, or a combination of these. However, heterogeneous variants within a tumor type await sub-classification or even reclassification by genetics. Brief information on the GBM variant gliosarcoma and other CNS tumors included in this study are provided as follows:

Gliosarcoma

Gliosarcoma (GS; WHO IV) is a GBM variant characterized by a biphasic tissue pattern with alternating areas displaying glial and mesenchymal differentiation (Kleihues and Cavenee, 2000). It constitutes 2 – 8% of all GBM (Meis *et al.*, 1991; Morantz *et al.*, 1976) and does not differ from the majority of GBM with regard to age, sex, pretreatment Karnofsky performance status, tumor location, size, median survival, and actuarial survival (Meis *et al.*, 1991). Nevertheless, GS is more likely to metastasize (Morantz *et al.*, 1976). In Lutterbach *et al.*'s study (2001), all of eight GS patients treated at their hospital between 1980 and 1999 had local tumor recurrences.

GS shows genetic aberrations similar to those occurring in primary GBM. None of 19 GSs showed amplification or overexpression of *EGFR* (Reis *et al.*,

2000). However, the number of chromosomes involved in imbalances in GS was significantly lower than that in GBM, indicating a higher genomic stability.

CGH study revealed that the gliomatous and sarcomatous components shared 57% of the chromosomal imbalances (Actor *et al.*, 2002). Genetic studies supported a monoclonal origin of the two components that progressed into sub-clones. Gain or amplification of genes on proximal 12q may facilitate the development of the sarcomatous phenotype (Actor *et al.*, 2002; Reis *et al.*, 2000).

Oligodendroglial tumors and mixed tumors

Oligodendroglial tumors constitute about 5% of all primary gliomas. They occur most commonly in the cerebral hemispheres of adults in a mean age of about 40 years. Male/female ratio ranged from 1.1:1 to 2:1. Oligodendroglioma is diffusely infiltrating tumor composed predominant of cells morphologically resembling oligodendrocytes. Depending on the presence or absence of focal or diffuse histological features of malignancy, the tumor is classified into WHO grade II or III (Kleihues and Cavenee, 2000).

The two most frequent genetic alterations in oligodendroglial tumors, is LOH on chromosomes 19q and 1p, both linked significantly to better response to chemotherapy independent of tumor grade (Goussia *et al.*, 2001; Reifenberger and

Louis, 2003). Deletion regions were identified at 1p34 – p35, 1p36.3 and 19q13.3 (Husemann *et al.*, 1999; Rosenberg *et al.*, 1996; Yong *et al.*, 1995).

Promotor hypermethylations were detected in multiple genes, including *O^6-methylguanine-DNA methyltransferase (MGMT)*, *RB*, *estrogen receptor*, *TP73*, *$p16^{INK4A}$*, *death-associated protein kinase*, *$p15^{INK4B}$*, *$p14^{ARF}$* at 60%, 34%, 30%, 16%, 12%, 10%, 7%, and 2%, respectively. Concordant hypermethylation of *$p16^{INK4A}$* and *$p15^{INK4B}$* were significantly associated with anaplastic oligodendroglial tumors. Hypermethylation of *MGMT* in chromosome 10q26 was significantly associated with LOH at 19q and combined LOH of 1p/19q (Dong *et al.*, 2001). Mutation was undetected in *TP73*, but expression of the gene was transcriptionally inactivated by hypermethylation. Therefore, *TP73* may have an epigenetic origin (Dong *et al.*, 2002a).

Indicators of poor response to therapy and short survival included homozygous deletion of *$p16^{INK4A}$*, mutation of *PTEN* and amplification of *EGFR* (Reifenberger and Louis, 2003). In contrast to astrocytic tumors, loss of 17p and mutations in *TP53* were rare (Smith *et al.*, 2000; Ueki *et al.*, 2002).

Oligoastrocytomas (WHO II & III) are mixed glial tumors that show morphologic features of oligodendroglioma and diffuse astrocytotma. According to Dong *et al.* (2002b), origin of oligoastrocytomas can be monoclonal or derived from different precursor. The first subset is characterized by allelic loss on 1p and

19q, and advanced variants with loss also on 9p, 10q, 13q and/or 17p. The second subset showed divergent allelic loss patterns in the two histologic component with mutation and overexpression of *TP53* detectable in the astrocytic components only. In the same year, temporal oligoastrocytomas was found to be different from frontal, parietal and occipital tumors due to their relative low frequency of LOH at 1p and 19q (Mueller *et al.*, 2002).

Ependymal tumors

Ependymal tumors arise from the ependymal lining of the cerebral ventricles and the remnants of the central canal of the spinal cord. Age distribution of patients ranges from less than 1 year to more than 80 years. However, the disease occurs predominantly in children and adolescents. In children, ependymomas are the third most frequent brain tumors and account for 6 – 12% of all paediatric CNS tumors (Lamszus *et al.*, 2001; Goussia *et al.*, 2001). In children, 90% of tumors are intracranial and 10% are intraspinal. In adults, 60% are tumors of spinal cord and only 40% are intracranial (Vagner-Capodano *et al.*, 1999). While ependymoma (WHO grade II) often causes clinical symptoms by blocking CSF pathways, subependymoma (WHO grade I) is often detected incidentally and has a very favorable prognosis (Ebert *et al.*, 1999; Prayson and Suh, 1999).

Cytogenetic and molecular genetic studies have revealed numerous chromosomal abnormalities in ependymomas, with monosomy 22 or structural rearrangements of chromosome 22 being the most frequent abnormality (Vagner-Capodano *et al.*, 1999). By CGH, our group member found loss on chromosomes 22q, 16, 17, 6, 19, 20 and 1p, and detected chromosome gain in 5q, 12q, 7q, 9q and 4q (Zheng *et al.*, 2000). Frequent (at least 50%, 16 ependymomas) was later detected in 6q, 13q, 16p, 16q, 17q, 19q, 20p, 20q and 22q by allelotyping using 384 polymorphic markers. CRD on chromosome 22 was mapped to 22q13.1 – q13.3. Allelic deletion was also detected on 22q11.2 in 25% cases (Tong *et al.*, 2001). LOH in both regions were reproducible in a later study (Huang *et al.*, 2002).

The *neurofibromatosis 2 (NF2)* gene located on chromosome 22q12 was preferentially mutated in spinal ependymomas (Alonso *et al.*, 2002; Ebert *et al.*, 1999; Rubio *et al.*, 1994; Slavc *et al.*, 1995). Loss and mutation of *NF2* fulfilled Knudson's two-hit hypothesis in the same tumors (Ebert *et al.*, 1999; Lamszus *et al.*, 2001). The region 22q13.1 – q13.3 may harbor TSGs other than *NF2* in ependymomas.

Another abnormality in ependymoma is LOH in chromosome 6q. Mutation of *PTEN* and *TP53* gene, mutation or deletion of $p16^{INK4A}$, allelic loss on chromosome 10q and amplification of *MDM2* and *EGFR* are very rare findings

and do not play a major part in the pathogenesis of ependymal tumors (Alonso *et al.*, 2002; Tong *et al.*, 1999).

Medulloblastoma

Medulloblastoma (MB; WHO IV) is the commonest malignant CNS tumor in children, accounting for 20% of childhood brain tumors. Classical MB occurs predominantly in midline cerebellum of children and is characterized by frequent dissemination of CSF at presentation. It is strongly associated with amplification of *MYC*, the possession of which is totally resistant to therapy and has a fatal outcome. In contrast, MB of desmoplastic histology are more frequently in lateral location. They occurred in an almost equal distribution between children (56%) and adults (44%), and have a better outcome (Mazzola and Pollack, 2003; Pramanik *et al.*, 2003; Sarkar *et al.*, 2002).

Mutations in two genes were found to be significant for tumorigenesis of MB. Among 67 MBs, mutation of β-catenin from 3 cases was reported (Zurawel *et al.*, 1998). In a later study, four activating mutations of β-catenin and two mutations of the *adenomatous polyposis of the colon (APC)* gene were detected in 46 sporadic MBs (Huang *et al.*, 2000). APC forms a complex with two other proteins to down-regulate β-catenin, which translocates to the nucleus to activate

the transcription of various genes, including *MYC*. Therefore, the APC/β-catenin pathway is responsible for tumorigenesis of certain MB subtypes.

Approximately 3% of individuals with the Gorlin's syndrome were predisposed to MB (Evans *et al.*, 1991; Lacombe *et al.*, 1990). The autosomal chromosomal abnormality leading to the familial syndrome was mapped to 9q22.3 and was identified as *PTCH* (Hahn *et al*, 1996; Johnson *et al.*, 1996). Afterwards, LOH in flanking region of *PTCH* was defined in sporadic MBs in various studies (Albrecht *et al.*, 1994; Raffel *et al.*, 1997; Schofield *et al.*, 1995). Then mutation of the *PTCH* gene was detected in desmoplastic MBs and fulfilled the two-hit criterion for tumor suppressors (Pietsch *et al.*, 1997; Raffel *et al.*, 1997).

The protein encoded by *PTCH*, patched act as the membrane receptor for sonic hedgehog signals together with smoothened proteins (Marigo *et al.*, 1996; Stone *et al.*, 1996). Binding of hedgehog proteins to patched receptor leads to de-repression of smoothened and activation of glioma-associated oncogene homolog (Gli) transcription factors for downstream targets.

Recently, somatic mutation in the *suppressor of fused (SUFU)* in chromosome 10q and LOH of the wild-type allele were detected in a subset of children carrying MB. SUFU acts as a negative regulator of the Hedgehog signaling pathway through two distinct mechanisms, either sequestration of Gli in the cytoplasm or interaction with Gli directly on DNA (Kogerman *et al.*, 1999). Several of the

SUFU mutations encode truncated proteins that are unable to export Gli transcription factors form nucleus to cytoplasm (Ellison, 2002; Taylor *et al.*, 2002).

One of our group members performed CGH in 12 MBs and compared findings with previous genome-wide studies covering a further of 107 tumors. Summarized results revealed the most frequent deletions on 17p, 10q, 8p, 11p, 11q and 16q (Yin *et al.*, 2002). Despite 17p loss occurs in 30 – 50% of MB, mutations in *TP53* occur in less than 10% of sporadic MB. Therefore, other TSGs are probably involved in chromosome 17p (Ellison, 2002). By deletion mapping, a novel region of homozygous deletion was identified on 8p22 – p23.1 (Yin *et al.*, 2002).

Meningiomas and haemangiopericytomas

Meningiomas (mostly WHO I), in general, are slow-growing benign tumors attached to the dura mater and composed of neoplastic meningothelial cells. They comprise 20% of intracranial neoplasms, manifest typically in adults and show predominance for women, with a female/male ratio of 3:2 or even 2:1 (Chamberlain, 2001; Heinrich *et al.*, 2003; Kleihues and Cavenee, 2000). Haemangiopericytoma of the CNS, almost always attached to the dura, is highly cellular and richly vascularized.

Mutations in the *NF2* gene are detected in up to 60% of sporadic meningiomas but not in haemangiopericytoma (Joseph *et al.*, 1995). Similar to ependymomas, Knudson's two-hit hypothesis was fulfilled in meningiomas (27%, n = 26) by LOH of 22q markers and inactivating mutations in *NF2*. However, the majority of tumors carry allelic loss of 22q but intact *NF2*. This suggests the presence of other tumor suppressors in the long arm of chromosome 22.

Distinction of haemangiopericytoma from meningioma was genetically supported by homozygous deletions of the $p16^{INK4A}$ in about 25% of meningeal haemangiopericytoma but less than 5% in meningioma (Ono *et al.*, 1996; Verheijen *et al.*, 2002; Weber *et al.* 1997).

Other than abnormalities of chromosome 22q, chromosome 14q loss was also common among meningiomas. LOH for one or more markers was detected in 37% (n = 41) of meningioma, including 3 of 3 recurrent ones. CRDs were defined in 14q24.3 – q31 and 14q32.1 – q32.2 (Tse *et al.*, 1997), which overlaps with the region in astrocytic tumor (14q21.2 – q32.12 and 14q32.1 – qter; Hu *et al.*, 2002).

2. Aims of study

Owing to the infiltrating feature of astrocytic tumors, resection boundary is not distinct. Patients who receive tumor resection often have recurrences. While chemo- and radio-therapy could extend survival in some patients, they cause side-effects and lower the quality of life.

Patients with diffuse astrocytoma can survive for as long as ten years but carry latency for high-grade tumor. GBM patients diagnosed after two years are already described as long-term survivors. Therefore, more accurate criteria for diagnosis, prognosis and decision on treatment program require molecular sub-classification of the tumors. Hopes of cure rely on molecular understanding of the disease.

Recently, Davies *et al.* (2002) raised the role of *BRAF* as an oncogene independent of oncogenic *RAS*. *BRAF* mutations were detected in a large variety of primary human cancers including melanoma, colorectal cancer, ovarian cancer and non-small cell lung carcinomas (Brose *et al.*, 2002; Davies *et al.*, 2002). The *BRAF* mutation rate in melanoma ranges from 60 to 90%.

In Davies *et al.*'s study (2002), the base substitution leading to substitution of valine by glutamic acid at position 599 (V599E) in *BRAF* was found in 4 of 38 glioma cell lines. However, no mutation was detected among 15 primary glioma specimens. This could be due to recruitment of inadequate samples. Gliomas include a wide range of neoplasms but diagnosis of primary glioma was

unspecified in their study. Involvement of different types of primary glioma within a small size could further lower the sample size of tumor type. On the other hand, *BRAF* mutation might be absent in certain types of gliomas. Furthermore, the incidence of *BRAF* mutations in non-glial CNS tumors has not been determined. Therefore, the original study is in need of extension to investigate the pattern of *BRAF* mutation in CNS tumors.

Overexpression of EGFR or the truncated form EGFRvIII is common in primary GBM and is able to activate Ras. Since spontaneous activation of EGFR contribute to Erk phophorylation, oncogenic signal from EGFR might be transmitted through *BRAF* to downstream effectors. Also, disruption of either *EGFR* or *BRAF* mutation might be enough to disrupt mitogenic signaling pathway in tumor precursors. Knowledge of whether *BRAF* mutation in astrocytic tumors, if any, occurs mutually exclusively with *EGFR* amplification could provide additional clues on molecular pathogenesis of astrocytic tumors.

Other than focusing on the newly discovered oncogene, mapping of critical regions harboring TSGs in astrocytic tumors is equally important. Total or partial loss of chromosome 14 was detected among 11 of 18 GBM and AA clones by cytogenetic analysis (Debiec-Rychter *et al.*, 1995). In a genome-wide allelotype analysis on diffuse astrocytoma (fibrillary) and GBM, two CRDs were located to 14q21.2 – q32.12 and 14q32.1 – qter (Hu *et al.*, 2002).

Deletions in 14q are frequent in a variety of cancers. The cancers with CRDs between 14q21.2 – q32.12 include renal oncocytomas (Schwerdtle *et al.*, 1997), gastrointestinal stromal tumors (El-Rifai *et al.*, 2000), malignant mesothelioma (Bjorkqvist *et al.*, 1999; de Rienzo *et al.*, 2000), neuroblastoma (Hoshi *et al.*, 2000; Thompson *et al.*, 2001), meningioma (Simon *et al.*, 1995; Tse *et al.*, 1997) and nasopharyngeal carcinoma (Cheng *et al.*, 1997; Mutirangura *et al.*, 1998).

There are 2 major aims in my research study. The first aim is to investigate whether *BRAF* alteration is involved in CNS tumors. To achieve this aim, the following objectives were raised:

1. To investigate the pattern of *BRAF* mutations among CNS tumors.
2. To examine B-Raf immunoreactivity in astrocytic tumors.
3. To determine the correlation between *EGFR* amplification and *BRAF* mutation in astrocytic tumors.
4. To determine the correlation between *EGFR* amplification and B-Raf immunoreactivity in astrocytic tumors.

The second aim of the current study is to refine CRDs on 14q21.2 – q32.12 in astrocytic tumors by microsatellite analysis.

3. Materials and methods

3.1. Clinical materials

A total of 201 CNS tumors comprising of 100 astrocytic tumors (23 diffuse astrocytomas, 18 AAs and 59 GBMs (including 2 GSs), 31 oligodendroglial tumors, 23 ependymal tumors, 21 MBs and 26 meningeal tumors were included in the current study. Diagnosis of tumor specimens was based on WHO criteria (Kleihues and Cavennee, 2000). All tumors and normal tissues examined in this study were collected from hospitals in Mainland China and Hong Kong (Anhui Provincial Hospital, Anhui; Beijing Hospital, Beijing; Hua Shan Hospital, Shanghai; Kwong Wah Hospital, Hong Kong; Prince of Wales Hospital, Hong Kong; Queen Mary Hospital, Hong Kong; Ren Ji Hospital, Shanghai; Sir Run Run Shaw Hospital, Hangzhou; The Second Hospital Nanjing Medical University, Nanjing; Tuen Mun Hospital, Hong Kong; West China Hospital, Sichuan University, Sichuan; Xiang Ya Hospital, Changsha). Clinical information of astrocytic and non-astrocytic CNS tumors examined in this study was shown in Tables 3.1 and 3.2.

Table 3.1. Clinical information of astrocytic tumors.

Case number[a]	Age[b] (Years)	Sex[b]	Location[b]	Diagnosis[c]	Sample type[d]	Mutation Analysis of *BRAF*	Immunohis-tochemistry of B-Raf	Analysis of *EGFR* Gene Dosage	Microsatellite Analysis of Chromosome 14q
PW88S12021	4	F	Cerebellar	DA	FFPE	✔	✔		
PW88S1729	30	F	Temporal	DA	FFPE	✔	✔		
PW88S9118	6	M	Suprasellar	DA	FFPE	✔			
PW89S11692	66	F	Left fronto-temporol	DA	FFPE	✔	✔		
PW91S12886	16	F	Cerebellar	DA	FFPE	✔	✔		
PW91S8807	7	F	Ponto cerebellar	DA	FFPE	✔	✔		
PW93S9870	35	F	Right parietal	DA	FFPE	✔	✔		
PW94S10895	51	M	NA	DA	FFPE	✔			
WN66	44	M	Left parietal	DA	FT	✔			✔
WN70	NA	NA	NA	DA	FT	✔			✔
HS52	43	F	NA	DA (fibrillary)	FT	✔			✔
NJ125	NA	NA	NA	DA (fibrillary)	FT	✔			✔
NJ133	32	M	Right temporal	DA (fibrillary)	FT	✔			✔
NJ138	24	M	Left tempo-parietal	DA (fibrillary)	FT	✔			✔
NJ171	31	F	Left temporal	DA (fibrillary)	FT	✔			✔
NJ172	35	M	Left temporal	DA (fibrillary)	FT	✔			✔
PW94S530	NA	NA	NA	DA (fibrillary)	FFPE	✔	✔		
WC129	52	F	NA	DA (fibrillary)	FT	✔			✔
WN1	62	M	Right parieto-occipital	DA (fibrillary)	FT	✔			✔
WN12	43	M	Left temporal	DA (fibrillary)	FT	✔			✔
PW96S2536	34	F	NA	DA (gemistocytic)	FFPE	✔	✔		
WC101	33	M	NA	DA (gemistocytic)	FT	✔			✔
PW89S11533	42	M	Posteria fossa	DA (recurred)	FFPE	✔	✔		
BJ27	72	M	Left temporal	AA	FT	✔		✔	✔

(continued on P.66)

Table 3.1 (continued). Clinical information of astrocytic tumors.

Case number[a]	Age[b] (Years)	Sex[b]	Location[b]	Diagnosis[c]	Sample type[d]	Mutation Analysis of *BRAF*	Immunohis-tochemistry of B-Raf	Analysis of *EGFR* Gene Dosage	Microsatellite Analysis of Chromosome 14q
NJ5	65	M	NA	AA	FT	✔		✔	✔
PW01S10055	60	F	NA	AA	FT	✔	✔	✔	
PW01S7917	42	M	Cerebral	AA	FT	✔	✔	✔	
PW87S5385	30	F	NA	AA	FFPE	✔	✔	✔	
PW88S6946	9	M	III ventricle	AA	FFPE	✔		✔	
PW91S5070	34	M	Left frontal	AA	FFPE	✔	✔	✔	
PW93S10785	34	F	Frontal	AA	FFPE	✔	✔	✔	
PW94S10180	65	M	NA	AA	FFPE	✔	✔	✔	
PW98S6257	51	M	Basal ganglia	AA	FT	✔			
PW99S6406	13	M	Parietal	AA	FT	✔	✔	✔	
PW99S7202	48	M	Right cerebellar	AA	FT	✔	✔		
PW99S8413	36	M	Frontal and parietal	AA	FFPE	✔	✔		
PW99S8425	76	F	Fronto-parietal	AA	FT	✔	✔	✔	
WC114	64	M	NA	AA	FT	✔	✔	✔	✔
WC127	28	F	NA	AA	FT	✔	✔	✔	✔
WC30	33	F	Frontal and parietal	AA	FT	✔		✔	✔
PW93S13379	41	M	Left temporal parietal	AA (gemistocytic)	FFPE	✔	✔		
AH326	36	M	NA	GBM	FT	✔	✔	✔	✔
BJ10	30	F	Right temporal	GBM	FT	✔	✔	✔	✔
BJ21	49	M	Left temporal	GBM	FT	✔			✔
HS34	37	M	NA	GBM	FT	✔	✔	✔	✔
HZ15	64	M	Left temporal	GBM	FT	✔			✔
NJ111	61	F	Left parietal	GBM	FT	✔			✔
NJ119	56	F	Right fronto-parietal	GBM	FT	✔			✔

(continued on P.67)

Table 3.1 (continued). Clinical information of astrocytic tumors.

Case number[a]	Age[b] (Years)	Sex[b]	Location[b]	Diagnosis[c]	Sample type[d]	Mutation Analysis of *BRAF*	Immunohis-tochemistry of B-Raf	Analysis of *EGFR* Gene Dosage	Microsatellite Analysis of Chromosome 14q
NJ141	31	F	Left frontal	GBM	FT	✔			✔
NJ146	NA	M	Left fronto-parietal	GBM	FT	✔	✔	✔	✔
NJ158	53	M	Left temporal	GBM	FT	✔			✔
NJ167	47	F	Right parietal-temporal	GBM	FT	✔			✔
NJ22	47	F	NA	GBM	FT	✔		✔	
PW00S8896[e]	72	M	Cerebral	GBM	FFPE		✔		
PW93S12795	73	M	Left callosum & frontal	GBM	FFPE	✔	✔		
PW93S6903	33	F	Left thalamic	GBM	FFPE	✔	✔		
PW94S2990	40	M	NA	GBM	FFPE	✔	✔	✔	
PW94S3772	36	F	NA	GBM	FFPE	✔	✔	✔	
PW94S8399	74	M	NA	GBM	FFPE	✔	✔		
PW95S114	65	F	Left parietal	GBM	FFPE	✔	✔	✔	
PW95S14889	65	F	Left temporal	GBM	FFPE	✔	✔		
PW95S6195	76	M	NA	GBM	FFPE	✔	✔		
PW95S6900	61	M	Right frontal	GBM	FFPE	✔	✔		
PW96S13242	67	F	Temporal	GBM	FFPE	✔	✔		
PW96S14991	29	F	Midline cerebellar	GBM	FFPE	✔			
PW96S2900	71	M	NA	GBM	FFPE	✔			
PW96S7044	59	M	NA	GBM	FFPE	✔			
PW96S889	68	M	Temporal	GBM	FFPE	✔	✔	✔	
PW97S10825[f]	38	M	Right temporal	GBM	FFPE	✔			
PW97S13494[e]	59	F	Temporal	GBM	FFPE	✔	✔		
PW97S1671	73	M	Right parietal	GBM	FFPE	✔	✔		
PW97S3333	26	F	Right frontal	GBM	FFPE	✔	✔		

(continued on P.68)

Table 3.1 (continued). Clinical information of astrocytic tumors.

Case number[a]	Age[b] (Years)	Sex[b]	Location[b]	Diagnosis[c]	Sample type[d]	Mutation Analysis of *BRAF*	Immunohis-tochemistry of B-Raf	Analysis of *EGFR* Gene Dosage	Microsatellite Analysis of Chromosome 14q
PW97S4210[f]	39	M	Left frontal	GBM	FFPE	✔			
PW97S5418	42	M	Right parietal	GBM	FFPE	✔	✔		
PW97S946[f]	41	F	Left temporal	GBM	FFPE	✔			
PW98S11908	34	F	Right frontal	GBM	FFPE	✔	✔	✔	
PW98S12160[f]	59	F	NA	GBM	FFPE	✔			
PW98S12293[f]	75	F	Left temporal	GBM	FFPE	✔			
PW98S12546	66	M	Left frontal	GBM	FFPE	✔	✔	✔	
PW98S14608[e]	49	M	Left temporal	GBM	FFPE		✔		
PW98S7934[e]	73	M	Cerebral	GBM	FFPE		✔		
PW99S1464[e]	65	M	Left temporal	GBM	FFPE		✔		
PW99S2800[e]	68	M	Corpus callosal	GBM	FFPE		✔		
SX23	54	M	NA	GBM	FT	✔		✔	
SX24	32	M	NA	GBM	FT	✔		✔	
WC105	45	M	NA	GBM	FT	✔		✔	
WC121	23	F	NA	GBM	FT	✔			✔
WC140	32	M	NA	GBM	FT	✔			
WC143	59	M	NA	GBM	FT	✔			
WC155	38	F	NA	GBM	FT	✔		✔	
WC159	60	F	NA	GBM	FT	✔		✔	
WC163	61	M	NA	GBM	FT	✔			
WC167	59	M	NA	GBM	FT	✔		✔	
WC173	45	F	NA	GBM	FT	✔			
WN58	66	M	Right temporal	GBM	FT	✔	✔	✔	✔
PW99S10107[e]	44	F	Left frontal	GBM (giant cell)	FFPE		✔		

(continued on P.69)

Table 3.1 (continued). Clinical information of astrocytic tumors.

Case number[a]	Age[b] (Years)	Sex[b]	Location[b]	Diagnosis[c]	Sample type[d]	Mutation Analysis of *BRAF*	Immunohis-tochemistry of B-Raf	Analysis of *EGFR* Gene Dosage	Microsatellite Analysis of Chromosome 14q
PW00S10842	48	M	Left frontal	GBM (recurred)	FFPE	✔	✔		
PW93S8821	17	M	Right parasagittal	GBM (recurred)	FFPE	✔	✔		
WC111	62	M	NA	GBM (Gliosarcoma)	FT	✔			✔
WC174	55	M	NA	GBM (Gliosarcoma)	FT	✔			✔

[a] PW, Prince of Wales Hospital, Hong Kong; WC, West China Hospital, Sichuan University, Sichuan; WN, Xiang Ya Hospital, Changsha.

[b] M, male; F, female; NA, not available.

[c] DA, Diffuse astrocytoma; AA, Anaplastic astrocytoma; GBM, Glioblastoma multiforme.

[d] FT, frozen tissue; FFPE, formalin-fixed paraffin-embedded block.

[e] DNA samples with known *EGFR* amplification.

[f] DNA samples without *EGFR* amplification.

Table 3.2. Clinical information of non-astrocytic CNS Tumors.

Case number[a]	Age[b] (Years)	Sex[b]	Location[b]	Diagnosis	Sample type[c]	Mutation Analysis of *BRAF*	Immunohis-tochemistry of B-Raf	Analysis of *EGFR* Gene Dosage	Microsatellite Analysis of Chromosome 14q
AH33	14	F	Left frontal	Oligodendroglioma	FT	✔			
HS26	18	M	NA	Oligodendroglioma	FT	✔			
HS37	56	F	NA	Oligodendroglioma	FT	✔			
HS43	31	M	NA	Oligodendroglioma	FT	✔			
PW84S344	23	M	NA	Oligodendroglioma	FFPE	✔			
PW85S589	47	M	Right frontal	Oligodendroglioma	FFPE	✔			
PW86S8343	46	M	Left frontal	Oligodendroglioma	FFPE	✔			
PW88S7594	33	M	Cerebellar	Oligodendroglioma	FFPE	✔			
PW91S5142	32	M	Corpus callosum	Oligodendroglioma	FFPE	✔			
PW95S9300	43	F	NA	Oligodendroglioma	FFPE	✔			
QM91H604	55	F	NA	Oligodendroglioma	FFPE	✔			
AH15	26	M	Middle cranial fossa	Anaplastic oligodendroglioma	FT	✔			
AH414	48	M	NA	Anaplastic oligodendroglioma	FT	✔			
PW00S17642	49	M	Frontal	Anaplastic oligodendroglioma	FFPE	✔			
PW00S18017	48	F	NA	Anaplastic oligodendroglioma	FFPE	✔			
PW00S3839	57	M	Frontal	Anaplastic oligodendroglioma	FFPE	✔			
PW91S5273	61	F	Bifrontal	Anaplastic oligodendroglioma	FFPE	✔			
PW92S4279	57	M	Right hemisphere	Anaplastic oligodendroglioma	FFPE	✔			
PW01S11259	18	M	Left frontal	Anaplastic oligodendroglioma (recurred)	FFPE	✔			
PW96S9651	38	M	NA	Anaplastic oligodendroglioma (recurred)	FFPE	✔			
TM94B7749	NA	NA	NA	Anaplastic oligodendroglioma (recurred)	FFPE	✔			
AH415	49	M	NA	Oligoastrocytoma	FT	✔			
AH431	36	M	NA	Oligoastrocytoma	FT	✔			
HS18	47	M	NA	Oligoastrocytoma	FT	✔			

(continued on P.71)

Table 3.2 (continued). Clinical information of non-astrocytic CNS Tumors.

Case number[a]	Age[b] (Years)	Sex[b]	Location[b]	Diagnosis	Sample type[c]	Mutation Analysis of *BRAF*	Immunohis-tochemistry of B-Raf	Analysis of *EGFR* Gene Dosage	Microsatellite Analysis of Chromosome 14q
HS20	28	M	NA	Oligoastrocytoma	FT	✔			
PW87S7123	34	M	Frontal	Oligoastrocytoma	FFPE	✔			
PW89S361	7	M	Cerebral	Oligoastrocytoma	FFPE	✔			
SX20	36	F	NA	Oligoastrocytoma	FT	✔			
SX8	40	F	NA	Oligoastrocytoma	FT	✔			
PW00S12281	55	F	Frontal	Oligoastrocytoma (recurred)	FFPE	✔			
PW99S8413	36	M	Fronto-parietal	Anaplastic oligoastrocytoma	FFPE	✔			
AH240	8	NA	NA	Ependymoma	FT	✔			
AH307	28	M	NA	Ependymoma	FT	✔			
AH412	36	M	NA	Ependymoma	FT	✔			
HS54	12	F	NA	Ependymoma	FT	✔			
KW11	11	F	NA	Ependymoma	FFPE	✔			
PW00S3723	48	F	Spinal cord	Ependymoma	FFPE	✔			
PW87S3784	25	M	IV ventricle	Ependymoma	FFPE	✔			
PW90S5731	38	F	IV ventricle	Ependymoma	FFPE	✔			
PW91S10628	31	F	Right frontal	Ependymoma	FFPE	✔			
PW93S10502	22	F	Posterior fossa	Ependymoma	FFPE	✔			
PW93S3975	10	M	Cervical spinal	Ependymoma	FFPE	✔			
PW94A325	NA	NA	NA	Ependymoma	FFPE	✔			
PW95S17381	40	M	Spinal cord	Ependymoma	FFPE	✔			
PW97S4312	41	F	Spinal cord	Ependymoma	FFPE	✔			
PW98S11306	31	M	Spinal cord	Ependymoma	FFPE	✔			
WC156	36	M	NA	Ependymoma	FT	✔			
WC36	14	F	Right parietal	Ependymoma	FT	✔			

(continued on P.72)

Table 3.2 (continued). Clinical information of non-astrocytic CNS Tumors.

Case number[a]	Age[b] (Years)	Sex[b]	Location[b]	Diagnosis	Sample type[c]	Mutation Analysis of *BRAF*	Immunohis-tochemistry of B-Raf	Analysis of *EGFR* Gene Dosage	Microsatellite Analysis of Chromosome 14q
WN19	5	F	IV ventricle	Ependymoma	FT	✔			
WN57	10	M	IV ventricle	Ependymoma	FT	✔			
WN76	12	M	IV ventricle	Ependymoma	FT	✔			
PW99S10155	47	M	Spinal cord	Ependymoma (papillary)	FFPE	✔			
PW90S4613	27	M	Right thalamus	Ependymoma (recurred)	FFPE	✔			
PW97S15348	43	F	Ventricular	Subependymoma	FFPE	✔			
AH22	10	M	Cerebellar	Medulloblastoma	FT	✔			
AH233	5	M	Cerebellar	Medulloblastoma	FT	✔			
AH24	32	M	Cerebellar	Medulloblastoma	FT	✔			
HZ2	12	M	Cerebellar	Medulloblastoma	FT	✔			
NJ101	7	M	Cerebellar	Medulloblastoma	FT	✔			
NJ169	9	M	Cerebellar	Medulloblastoma	FT	✔			
RJ14	6	NA	Cerebellar	Medulloblastoma	FT	✔			
RJ17	3	NA	Cerebellar	Medulloblastoma	FT	✔			
RJ19	8	NA	Cerebellar	Medulloblastoma	FT	✔			
RJ20	9	NA	Cerebellar	Medulloblastoma	FT	✔			
RJ22	3	NA	Cerebellar	Medulloblastoma	FT	✔			
RJ23	8	NA	Cerebellar	Medulloblastoma	FT	✔			
RJ24	2	NA	Cerebellar	Medulloblastoma	FT	✔			
RJ25	12	NA	Spinal	Medulloblastoma	FT	✔			
RJ27	9	NA	Cerebellar	Medulloblastoma	FT	✔			
RJ30	2	NA	Cerebellar	Medulloblastoma	FT	✔			
RJ6	5	NA	Cerebellar	Medulloblastoma	FT	✔			
RJ7	19 months	NA	Cerebellar	Medulloblastoma	FT	✔			

(continued on P.73)

Table 3.2 (continued). Clinical information of non-astrocytic CNS Tumors.

Case number[a]	Age[b] (Years)	Sex[b]	Location[b]	Diagnosis	Sample type[c]	Mutation Analysis of *BRAF*	Immunohis-tochemistry of B-Raf	Analysis of *EGFR* Gene Dosage	Microsatellite Analysis of Chromosome 14q
RJ9	4	NA	VI ventricle	Medulloblastoma	FT	✔			
SX33	2	M	Cerebellar	Medulloblastoma	FT	✔			
WC149	11	M	Cerebellar	Medulloblastoma	FT	✔			
PW94S10584	NA	NA	NA	Meningioma	FFPE	✔			
PW94S10884	40	F	NA	Meningioma	FFPE	✔			
PW94S11808	58	F	NA	Meningioma	FFPE	✔			
PW94S14614	64	M	NA	Meningioma	FFPE	✔			
PW94S3448	26	F	NA	Meningioma	FFPE	✔			
PW94S6119	58	M	NA	Meningioma	FFPE	✔			
PW94S7119	48	F	NA	Meningioma	FFPE	✔			
PW94S7949	79	F	NA	Meningioma	FFPE	✔			
PW94S9196	42	M	NA	Meningioma	FFPE	✔			
PW95S180	44	M	NA	Meningioma	FFPE	✔			
PW95S4286	34	F	Sellar	Meningioma	FFPE	✔			
PW95S7859	67	F	Frontal	Meningioma (fibroblastic)	FFPE	✔			
PW95S11006	34	M	Right frontal	Meningioma (Meningotheliomatous)	FFPE	✔			
PW95S10525	45	F	Suprasellar	Meningioma (recurred)	FFPE	✔			
PW95S5378	54	F	Sellar	Meningioma (transitional)	FFPE	✔			
HZ11	37	M	Parieto-occipital	Atypical meningioma (recurred)	FT	✔			
HS6	47	F	Sella	Anaplastic meningioma	FT	✔			
PW00S1705	71	F	Left temporal	Anaplastic meningioma	FFPE	✔			
PW94S7269	54	M	NA	Anaplastic meningioma	FFPE	✔			
PW98S2008	51	F	Sphenolid wing	Anaplastic meningioma	FFPE	✔			
PW99S3062	64	M	Cerebellopontine angle	Anaplastic meningioma	FFPE	✔			

(continued on P.74)

Table 3.2 (continued). Clinical information of non-astrocytic CNS Tumors.

Case number[a]	Age[b] (Years)	Sex[b]	Location[b]	Diagnosis	Sample type[c]	Mutation Analysis of *BRAF*	Immunohis-tochemistry of B-Raf	Analysis of *EGFR* Gene Dosage	Microsatellite Analysis of Chromosome 14q
PW00S15111	74	F	NA	Anaplastic meningioma (recurred)	FFPE	✔			
PW01S3557	50	M	cerebellopontine angle	Anaplastic meningioma (recurred)	FFPE	✔			
PW01S9499	58	F	Frontal	Anaplastic meningioma (recurred)	FFPE	✔			
PW95S14176	58	F	NA	Anaplastic meningioma (recurred)	FFPE	✔			
PW01S2440	42	M	Frontal	Hemangiopericytoma	FFPE	✔			

a AH, Anhui Provincial Hospital, Anhui; BJ, Beijing Hospital, Beijing ; HS, Hua Shan Hospital, Shanghai; HZ, Sir Run Run Shaw Hospital, Hangzhou; KW, Kwong Wah Hospital, Hong Kong; NJ, The Second Hospital Nanjing Medical University, Nanjing; PW, Prince of Wales Hospital, Hong Kong; QM, Queen Mary Hospital, Hong Kong; RJ, Ren Ji Hospital, Shanghai; TM, Tuen Mun Hospital, Hong Kong; WC, West China Hospital, Sichuan University, Sichuan; WN, Xiang Ya Hospital, Changsha.

[b] M, male; F, female; NA, not available.

[c] FT, frozen tissue; FFPE, formalin-fixed paraffin-embedded tissue.

3.2. Cell lines

Ten cell lines were examined in the current study (Table 3.3). Six of them were derived from astrocytic tumors, including LNZ308, SKMG3, U138, U343, GBM2603 and GBM6840. The latter two lines were established in-house (Di Tomaso *et al.*, 2000). SKMG3 was a gift from Dr. Joon Uhm, Department of Neurology, Mayo Medical School, Minnesota, U.S.A. The MB cell lines D283 Med and Daoy were obtained from American Type Culture Collection (ATCC; Manassas, U.S.A.), while D384 Med was a generous gift from Dr. Darell Bigner, Duke Comprehensive Cancer Centre, North Carolina, U.S.A. The primitive neuroectodermal tumor (PNET) line, PFSK1 was obtained from ATCC.

Table 3.3. Cell lines of CNS tumor origin examined in the current study.

Tumor Type	Cell Line
Astrocytic tumor	GBM2603
	GBM6840
	LNZ308
	SKMG3
	U138
	U343
Medulloblastoma	D283 Med
	D384 Med
	Daoy
Primitive neuroectodermal tumor	PFSK1

The squamous cell carcinoma line A431, also obtained from ATCC was used as control for B-Raf immunohistochemistry (Section 3.6) and quantification of *EGFR* gene dosage (Section 3.7).

3.3. Cell culture

All cell lines, except D384 Med and PFSK1, were maintained in Minimum Essential Medium Eagle with alpha modification (Sigma-Aldrich Company, Missouri, U.S.A.) adjusted to contain 0.22% sodium and supplemented with 10% fetal bovine serum (FBS; HyClone Laboratories, Inc., Logan, Utah, U.S.A.) and 2 mM L-glutamine (GIBCO, Japan). D384 Med was maintained in Richter's Zinc Option Minimum Essential Medium (GIBCO) with 0.22% sodium bicarbonate, 10 mM HEPES and 20% FBS. PFSK1 was maintained in RPMI-1640 medium (Sigma-Aldrich) adjusted to contain 0.15% sodium bicarbonate, 25 mM glucose, 10 mM HEPES, 1 mM sodium pyruvate, 2 mM L-glutamine and 10% FBS. All cell lines were kept at 37°C in a humidified atmosphere containing 5% CO_2.

Cell passage was performed at 80% confluence in T_{75} (75 cm^2) flask (Nunc, Roskilde, Denmark). Cells were washed with PBS to remove trypsin inhibitor present in FBS. Cell detachment was aided by incubation in 1.5 ml of 0.25% trypsin and 1 mM EDTA (GIBCO) at 37°C for 1 – 4 min. Trypsinization was stopped by the addition of 7.5 ml of complete medium. Cells were spun down at 1200 rpm (Heraeus Sepatech model Megafuge 1.0) for 3 min and resuspended in 15 – 20 ml of complete medium. For routine passages, cells were split 3- to 4-fold and re-seeded in flasks.

3.4. DNA extraction

DNA extracted from tumors, cell lines and constitutional blood samples was subject to mutation analysis of the *BRAF* gene, quantification of *EGFR* gene dosage and LOH analysis of chromosome 14q. The extraction methods for these three types of samples were essentially the same, except for sample pre-treatment.

3.4.1. Pre-treatment of samples

Ninety-three CNS tumors resected from patients were immediately snap frozen and stored at –80°C. A series of sections were cut from each tumor using Leica CM1800 cryostat at –18°C. The first section was cut to 4 μm thickness, stained with haematoxylin and eosin (H&E) and examined microscopically for tumor content by at least one pathologist. When the first section showed a minimum of 80% tumor content, 8 – 20 serial sections of 25-μm-thickness would then be cut and collected for DNA extraction. The last tissue section of 4 μm was also stained with H&E and examined microscopically to confirm tumor content. Frozen tissue matrix (OCT) was removed from tissues by repeated washings (usually three times) each with 1 ml of chilled phosphate-buffered saline (PBS), followed by centrifugation at 3000 rpm for 4 min at room temperature using

microcentrifuge (Eppendorf MiniSpin, Hambury, Germany). After the third wash, the tissue pellets were rid of PBS and subject to DNA extraction.

For formalin-fixed paraffin-embedded tissues, H&E-stained sections of available blocks were examined and about 20 consecutive 10-μm-tissue sections from the most representative one were cut and collected into microfuge tubes. Paraffin was removed by vigorous vortexing in 1.2 ml xylene, followed by centrifugation at 13000 rpm for 4 min. To remove xylene, tissue sections were pressed down using pipette. After washing for three times, residual xylene was removed by gentle vortexing in 1.2 ml 100% ethanol, followed by centrifugation at 13000 rpm for 4 min. Tissue pellet was dried using the Speed Vac concentrator (Savant, U.S.A.).

Tumor-matched blood samples, collected in EDTA-coated Vacuette(s) (Ejazuddin), were available in 33 cases and stored at –20°C. After thawing quickly at 37°C, 3 – 6 ml of blood was transferred into 15 ml polypropylene conical tube and the volume was brought up to 12 ml using chilled PBS. Lymphocytes were collected by centrifugation at 3200 rpm for 15 min at 4°C (Eppendorf centrifuge model 5810R). Since heme of red blood cells is known to inhibit PCR, lymphocytes were repeatedly washed in PBS followed by centrifugation until a clear supernatant was attained.

3.4.2. Cell lysis and protein removal

To release DNA from cells, tissue pellet was suspended in 1 ml of lysis buffer (0.1 M sodium chloride, 0.05 M Tris-HCl, pH 7.4, 1 mM EDTA and 0.5% sodium dodecyl sulfate) containing 400 μg/ml proteinase K. Protein digestion was allowed to proceed at 54°C for a minimum of 6 hours. If tissue clumps remained observed after incubation, 20 – 40 μl of 10 mg/ml proteinase K (final concentration 200 – 400 μg/ml) was added to the mixture and protein digestion was allowed to proceed for another minimum of 6 hours at 54°C.

When digestion was completed, as indicated by disappearance of tissue clumps in lysate, equal volumes of phenol/chloroform/isoamyl alcohol (PCI; 25:24:1, v/v/v), equilibrated at pH 8, was added to extract protein. The mixture was shaken by hand for 10 min, chilled at –20°C for 10 min and centrifuged at 13,000 rpm for 20 min. The cooling before centrifugation prevents release of PCI vapor and enables more complete separation of different liquid phases. The upper aqueous layer containing DNA was collected into new tubes for DNA precipitation.

For lymphocytes and cell lines, cells were pelleted by centrifugation at 1200 rpm for 3 min and lysed in 4 ml lysis buffer containing 100 μg/ml proteinase K. Protein digestion was performed at 54°C, followed by PCI treatment, as pre-treatment of tumor tissues described above.

3.4.3. Precipitation of DNA

DNA was salted out from the aqueous solution by addition of 1 /10 volume of 3 M sodium acetate (pH 5.2) and 2 volumes of chilled 100% ethanol. In case no obvious DNA precipitate was observed after thorough mixing of solutions, 1 µl of 1% glycogen was seeded. With or without appearing of precipitates, DNA precipitation was further aided by storing at –20°C overnight. DNA was recovered from salt solution by centrifugation at 13,000 rpm for 10 min. After complete aspiration of liquid traces, DNA was allowed to dry in air for 5 – 10 min. Colorless DNA pellet was suspended in 20 – 100 µl of autoclaved Milli-Q water. Over-drying of DNA as indicated by reappearance of white color was avoided. To ensure even suspension, DNA was incubated at 54°C for 2 hours.

3.4.4. Determination of DNA concentration

One µl of DNA was diluted in appropriate volume of water and its absorbance was measured at 260 nm, 280 nm and 320 nm using the GeneQuant spectrophotometer (Amersham Biosciences). DNA concentration in µg/ml was calculated by:

(absorbance at 260 nm – absorbance at 320 nm) x 50 x10^{-3} x dilution factor.

Purity of DNA was estimated from the ratio of (absorbance at 260 nm – absorbance at 320 nm) to (absorbance at 280 nm – absorbance of 320 nm). Working DNA solution of 0.1 μg/μl was prepared and stored at –20°C until use.

3.5. Mutation analysis of BRAF by cycle sequencing

Exons 11 and 15 with their flanking sequences of the *BRAF* gene were sequenced for somatic base changes using the ABI Prism BigDye Terminator Cycle Sequencing Ready Reaction Kit version 2.0 (Applied Biosystems).

3.5.1. Amplification of *BRAF* exons

PCR was performed in a final volume of 25 μl containing 100 ng of genomic DNA, 0.75 Unit of AmpliTaq Gold DNA Polymerase (Applied Biosystems), 10 mM Tris-HCl (pH 8.3), 50 mM KCl, 2.5 mM $MgCl_2$, 200 μM of 2'-deoxynucleoside 5'-triphosphate, and 400 pM of each primer (Invitrogen, HKSAR, China) using the GeneAmp PCR system 2700 (Applied Biosystems). Primers were synthesized according to Davies *et al.*, 2002.

Sense primer of exon 11: 5'-TCCCTCTCAGGCATAAGGTAA-3'

Anti-sense primer of exon 11: 5'-CGAACAGTGAATATTTCCTTTGAT-3'

Sense primer of exon 15: 5'-TCATAATGCTTGCTCTGATAGGA-3'

Anti-sense primer of exon 15: 5'-GGCCAAAAATTTAATCAGTGGA-3'

PCR conditions included initial denaturation at 94°C for 10 min, followed by 38 cycles of denaturation at 95°C for 30 sec, annealing at 58°C for 30 sec and extension at 72°C for 1 min, and a final extension step at 72°C for 10 min.

To confirm successful amplification, a 5-µl aliquot of each PCR product was subjectd to electrophoresis. After mixing with 1 µl of 6X gel-loading buffer (25% of bromophenol blue, 0.25% of xylene cyanol FF and 40% of sucrose) DNA was loaded onto a 2% agarose gel containing 50 mM ethidium bromide. Electrophoresis was carried out in 1X TBE buffer (0.09 M Tris, 0.89 M boric acid and 2 mM EDTA, final pH 8.0) at 120 V for 15 min. DNA bands were observed under ultra-violet illumination (UVP transillumniator; California, U.S.A.). For each sample that showed successful amplification, the remaining PCR product was purified using the High Pure PCR Product Purification Kit (Roche Diagnostics Limited, Germany) and eluted in 100 µl of elution buffer (5 mM Tris-HCl, pH 8.5). The DNA was then concentrated into a volume of 5 µl using the Speed Vac concentrator.

3.5.2. Cycle sequencing and automated gel electrophoresis

Cycle sequencing was performed in a final volume of 5 µl containing 1 – 2 µl of DNA template, 2 µl of 2.5X Big Dye Terminator reagent mix (Applied

Biosystems) and 160 pM of either forward or reverse primer (Invitrogen). Cycle sequencing commenced with an initial denaturation at 95°C for 2 min, followed by 46 cycles of denaturation at 96°C for 15 sec, annealing at 54°C for 15 sec and extension at 60°C for 3.5 min.

Sequencing product was diluted to 20 µl with Milli-Q water and purified from unincorporated dye terminators using Sephadex G50 Fine (Amersham Biosciences) spin column. To prepare the spin column, well-suspended Sephadex G50 Fine beads were packed into 1.5 ml microspin columns and spun at 3,000 rpm for 1 min. Product was applied to the center of packed column and subject to centrifugation at 3000 rpm for 1 min. Flowthrough was dried in the Speed Vac concentrator. Content was resuspended in 3.6 µl gel-loading buffer (a mixture containing 1 volume of 25 mM EDTA with 50 mg/ml Blue Dextran and 5 volumes of deionized formamide), denatured at 95°C for 2 min and chilled on ice immediately to prevent re-annealing.

To prepare the resolving gel, 25 ml of 4% denaturing polyacrylamide gel solution (3.8% acrylamide, 0.2% bis-acrylamide, 8.9 mM Tris, 8.9 mM boric acid and 0.2 mM EDTA and 6.0 M urea, pH 8.3; filtered through a 0.45 µm filter) was polymerized by addition of 125 µl of 10% ammonium persulfate and 12.5 µl N,N,N',N'-tetramethylelthylenediamine. The gel was allowed to polymerize for

at least one hour. After loading 1.2 μl of sequencing product into each lane of the gel, electrophoresis was carried out in the automated ABI Prism 377 DNA sequencer (Applied Biosystems). Data collected were analyzed using ABI sequencing analysis software version 3.7.

3.6. Immunohistochemistry of B-Raf and GFAP

3.6.1. Pre-treatment of samples

In this and the following sections, washing in TBS refers to three times of washing in Tris-buffered saline (TBS; 50 mM Tris-HCl, pH 7.6 and 56.8 mM NaCl) for 5 min each.

For formalin-fixed paraffin-embedded tissues, sections of 4 μm thickness were thoroughly dried in a vacuum-drying oven at 40°C (WTBBinder) and deparaffinized in three changes of xylene for 5 min each. Hydration was enabled by gradual changes through ethanol in decreasing gradient (100% ethanol twice, 95% ethanol, 70% ethanol and distilled water for 5 min each). Antigen was retrieved from formalin in 1 mM EDTA (pH 8) by microwave treatment (850W for 3.5 min followed by 170W for 10 min). Slides were then cooled in running water and washed with TBS. Endogenous peroxidase activity was blocked by incubation in 0.3% hydrogen peroxide in TBS for 10 min. Slides were then washed in TBS again prior to primary antibody treatment.

Thick sections of frozen tissues were prepared using scrapel under –18°C, fixed in 10% formalin overnight, embedded in paraffin and processed as described above.

For cell lines, 2 to 4 x 10^5 cultured cells were seeded onto each cover-slip and allowed to grow for 1 – 2 days in 6-well plate (IWAKI, Japan) containing 2.5 ml of completed medium per well. Before immunohistochemistry, cells were washed twice with chilled PBS and fixed in chilled methanol for 10 min. Endogenous peroxidase activity was blocked by incubation in 1% hydrogen peroxide in methanol for 25 min. Slides were washed in TBS after 2 brief washes in distilled water for immunohistochemistry.

3.6.2. Detection of B-Raf and GFAP antigen by ABC method

All chemicals mentioned in this section were buffered in TBS.

Tissues and cells were incubated in 5% normal rabbit serum (DAKO, Denmark) for 5 min to block non-specific protein regions for primary antibody. After drainage of extra rabbit serum, the mouse monoclonal anti-B-Raf in 3% BSA (Sigma) at 1:40 dilution was applied to sections. This antibody is specific to amino acids 12 – 156 of human B-Raf (Santa Cruz Biotechnology, California, U.S.A.). As negative control, 3% BSA was used. After overnight incubation at 4°C, slides or cover-slips were washed in TBS, incubated in biotinylated rabbit anti-mouse antibodies (DAKO) in 0.03% BSA (at 1:200 dilution) for 40 min and washed in TBS. Next, they were incubated in streptavidin conjugated horseradish

peroxidase (ZYMED, U.S.A.) in 0.03% BSA (at 1: 400 dilution) for 45 min and washed in TBS. A solution of 2% DAB and 0.03% hydrogen peroxide was applied and color development was observed under the microscope. After a maximum of 20 min or when desired stain intensity was observed (approximately 3 – 8 minutes), DAB was completely removed by thorough washing under tap water for 15 min. Tissues and cells were counterstained by hematoxylin for 7 min, processed through dehydrating alcohol series (70% ethanol, 95% ethanol, and 100% ethanol twice) and three changes of xylene and mounted in PERMOUNT (Fisher Chemical, New Jersey, U.S.A.).

Positive results were scored if the population of immunoreactive cells in a 400X microscopic view was greater than 5%. Tumor cases with immunopositive cell population greater than 5% but equal to or lower than 15% were designated '+'. Those with immunopositive cell population greater than 15% but equal to or lower than 40% were designated '++'. Those with immunopositive cell population greater than 40% were designated '+++'. Otherwise, '-', was recorded.

Procedures for immunohistochemical staining of GFAP were similar to that of B-Raf. Polyclonal rabbit anti-cow GFAP antibody isolated from bovine spinal cord (DAKO, Denmark) at 1:500 dilution was used in place of mouse anti-B-Raf monoclonal antibody. Five % normal swine serum (DAKO) and biotinylated

swine anti-rabbit immunoglobulins (1:200 dilution; DAKO) were used for blocking non-specific protein interactions and as the secondary antibody. Positive results were again recorded for specimen harboring an immunoreactive cell population greater than 5% under a 400X microscopic view.

3.6.3. Controls

A431 cells were used as positive control for cultured cells, as recommended by Santa Cruz Biotechnology. Based on the detection of 97- and 62-kDa B-Raf proteins in neurons by Dugan *et al.* (1999), neurons in formalin-fixed paraffin-embedded normal cerebrum from autopsy were used as positive control for paraffin-embedded specimens.

Undetectable B-Raf expression in astrocytes was also reported by Dugan *et al.* (1999). In addition, B-Raf protein in muscle was barely detectable after immunoprecipitation and Western blotting in Barnier *et al.*'s study. Therefore, astrocytes in cerebrum autopsy were used as a negative control and skeletal muscle was collected to test the specificity of our antibody.

3.7. Quantification of EGFR gene dosage by TaqMan based real-time PCR

'Real-time' here means the detection of PCR product during amplification without purification or gel electrophoresis separation of end-point product. TaqMan probes based on fluorescence resonance energy transfer were used for assay on gene dosage. Each probe includes a fluorescent reporter and a fluorescent quencher molecule at 5' and 3' end, respectively. During extension phase of PCR, the reporter is freed from the quencher by 5' to 3'-exonuclease activity of Taq polymerase. Fluorescence of the reporter molecule increases as products accumulate. Once a measurable change in the total fluorescence of the reaction mixture can be detected, fluorescence rises appreciably above the background. Such a point is noted as the threshold cycle (Ct). Upon and after this point, a linear relationship exists between the log of the starting amount of a template and its threshold cycle. Detection of unknown starting template amount is therefore enabled by plotting the log of different standards of the template against their threshold cycles.

3.7.1. Preparation of gene constructs

To prepare standards for *EGFR*, a full-length *EGFR* cDNA cloned into the pBluescript-SK plasmid was used. This plasmid was obtained from Dr. Webster K. Cavenee, Ludwig Institute for Cancer Research, San Diego, U.S.A. The full-length *EGFR* cDNA gene covers nucleotide 63 – 3950 of the reference sequence NM_005228.

To correct for minor variations due to differences in input DNA template during real-time PCR, quantification of *EGFR* for each sample was accompanied by quantification of the house-keeping gene, *beta2-microglobulin (B2M)*, located at 15q21 – q22.2. The *B2M* gene construct was prepared by cloning a 90-bp fragment corresponding to part of exon 2 of *B2M* into the pCR2.1-TOPO vector (Invitrogen). This fragment covers nucleotide 166 – 255 of the *B2M* reference sequence NM_004048. Briefly, the *B2M* fragment was amplified from genomic DNA of SKMG3, ligated to the pCR2.1-TOPO vector and transformed into *E. coli* TOP10 competent cells (TOPO TA Cloning Kit; Invitrogen) according to manufacturer's recommendation. A bacterial clone containing the pTOPO-*B2M* plasmid was isolated and the authencity of *B2M* insert was confirmed by sequencing.

Plasmid DNA of both *EGFR* and *B2M* was prepared using the Nucleoband AX plasmid purification kit (Macherey-Nagel, Duren, Germany). Plasmid concentration, determined using the PicoGreen ds DNA Quantitation kit (Molecular Probes Inc., Eugene, Oregan, U.S.A.) was expressed as number of copies/μl which was calculated according to the formula:

$$\frac{\text{DNA concentration in } \mu g/\mu l \times 10^{-6}}{\text{Molecular weight of DNA fragment}} \times \text{Avogadro's number.}$$

3.7.2. Primers and TaqMan probes

Primers and TaqMan probes of *EGFR* and *B2M* used in real-time PCR were designed by Primer Express version 1.0 software (Applied Biosystems) and their sequences were listed in Table 3.4. For *B2M*, the same primer set was used in both cloning and real-time PCR. The TaqMan probes were labeled at the 5' end with 6-carboxyfluorescein (FAM) reporter dye and at the 3' end tetramethylrhodamine (TAMRA) quencher dye. All primers and probes were chemically synthesized by Applied Biosystems.

Table 3.4. Primers and Taqman probes of *EGFR* and *B2M* for real-time PCR.

EGFR	Sense primer	5'-GGTCAGTTTTCTCTTGCAGTCGT-3'
	Anti-sense primer	5'-TCACATCTCCATCACTTATCTCCTTG-3'
	Taqman probe	5'-AGCCTGAACATAACATCCTTGGGATTACGC-3'
B2M	Sense primer	5'-TCCATCCGACATTGAAGTTGAC-3'
	Anti-sense primer	5'-GACCAGTCCTTGCTGAAAGACA-3'
	Taqman probe	5'-CTGAAGAATGGAGAGAGATTGAAAAAGTGGAGC-3'

3.7.3. Experimental condition and PCR program

PCR mix was prepared in a final volume of 25 µl by combining 12.5 µl of 100 ng DNA, 500 nM each of forward and reverse primer and 400 nM TaqMan probe with 12.5 µl of 1X Platinum Quantitative PCR SuperMix-UDG mix containing 1.5 unit of Platinum Taq DNA Polymerase, 20 mM Tris-HCl (pH 8.4), 50 mM KCl, 7 mM $MgCl_2$, 200 µM dGTP, 200 µM dATP, 200 µM dCTP, 400 µM dUTP and 1 unit of uracil DNA glycosylase (Invitrogen). A final concentration of 8 mM $MgCl_2$ was used in *B2M* PCR mix. To avoid PCR carry-over contamination, DNA containing dUTP was digested by uracil DNA glycosylase at 50°C for 2 min. Enzyme was then inactivated at 95°C for 2 min (Longo *et al.*, 1990). DNA amplification consisted of 45 cycles of denaturation at 95°C for 30 sec and annealing/extension at 60°C for 1 min.

To further avoid DNA cross-contamination, all PCR manipulations were carried out with Aserosol Barrier Tips (Continental Lab Products, California, U.S.A.) in a laminar flow work station (Clyde-APAC, Australia).

3.7.4. DNA standards

To construct standard curves for *EGFR* and *B2M*, a serial dilution of each plasmid DNA over the range of $10 - 10^7$ copies were amplified and the Ct values obtained were plotted against the input copy number.

3.7.5. Controls

The GBM cell line SKMG3 with endogenous *EGFR* amplification and the squamous cell carcinoma A431 with gain in *EGFR* copies were used as positive control for increased *EGFR* gene copy number, whereas patient blood samples were included as control for normal gene copy number. Milli-Q water was used in place of DNA in negative control.

3.7.6. Experimental layout

In each real-time experiment, 4-point standard curves of *EGFR* and *B2M* were included to correct PCR efficiency of each individual run, making inter-assay comparison more reliable. Positive and normal controls, as well as the standards, were done in duplicate while samples were performed in triplicate.

3.8. Microsatellite analysis of chromosome 14q in astrocytic tumors

Diffuse astrocytomas, AAs and GBMs were screened for LOH at chromosome 14q21.2 – q32.12, covering a genomic region of 48.1 Mb. Eighteen short tracts of single-copy polymorphic DNA sequences were selected from Marshfield genetic map (http://research.marshfieldclinic.org/genetics) and positioned according to the human genome sequence available at University of California at Santa Cruz (http://www.genome.ucsc.edu).

Microsatellite markers with PCR product less than 250 bp were chosen for LOH analysis. Shorter PCR fragments are easier to be amplified, especially for DNA extracted from paraffin blocks, in which DNA is often fragmented. Markers with higher polymorphism based on the Genome Database (http://www.gdb.org) or appeared highly informative in previous studies were chosen. The 18 markers selected spaced at an average genomic interval of 2.8 Mb.

Forward and reverse primers were synthesized by Invitrogen according to sequences available at the Genome Database. All forward primers were labeled at 5' end with fluorochrome FAM, 6-carboxyhexafluorescein (HEX) or 6-carboxyrhodamine (ROX). The use of different fluorochromes allows simultaneous loading of multiple products labeled with various fluorochromes onto a single lane for electrophoresis. PCR conditions were optimized by varying

annealing temperature, extension temperature, $MgCl_2$ concentration, and addition of dimethyl sulfoxide (DMSO). Each PCR was performed in a volume of 20 µl containing 1 µl of 0.1 µg/µl working DNA, 0.5 Unit of AmpliTaq Gold DNA Polymerase, 100 mM Tris-HCl (pH 8.3), 500 mM KCl, 2 mM $MgCl_2$, 200 µM dNTP, and 200 pM of each primer (Invitrogen). DMSO (5% or 8%) was added in some mixes to enhance PCR specificity. PCR conditions included enzyme activation at 95°C for 10 min and 38 cycles of 95°C for 30 sec, 57.5 – 65.9°C for 30 sec and 72°C for 30 sec, as shown in Table 3.5.

Table 3.5. PCR conditions of 18 microsatellite markers used in LOH analysis.

Microsatellite markers	Product size (bp)	Annealing temperature (°C)	Concentration of DMSO (%)
D14S288	189 – 209	65.9	-
D14S1068	211 – 225	61.5	8
D14S978	200 – 258	63.7	-
D14S1057	151 – 169	61.5	-
D14S980	158 – 184	63.7	-
D14S592	222 – 240	61.5	-
D14S997	204 – 220	57.5	-
D14S1026	118 – 150	57.5	-
D14S1011	175 – 191	59.9	-
D14S588	117 – 141	63.7	-
D14S77	203 – 251	59.9	-
D14S43	158 – 190	57.5	-
D14S61	197 – 227	65.9	-
D14S59	99 – 109	59.9	5
D14S1000	107 – 133	59.9	-
D14S1037	183 – 233	65.9	-
D14S68	148 – 172	59.9	-
D14S280	229 – 241	57.5	-

Varying amount (Table 3.6) of PCR products with different fluorophore-labels were concentrated using Speed Vac concentrator for 10 min, added with or without 0.5 µl of GS-HD400 ROX size standard (Applied Biosystems) and loaded onto gel.

Table 3.6. Amount of PCR products loaded onto denaturing gel.

Fluorophore	PCR product (μl)	ROX-labeled 100 bp size marker (μl)
FAM	3	0.5
HEX	4.5	0.5
ROX	5	-

Conditions of gel electrophoresis were basically the same as that described for DNA sequencing (Section 3.4.2). After addition of 4 μl loading dye (1 volume of 25 mM EDTA with 50 mg/ml blue dextran, 5 volumes of deionized formamide), product was denatured at 95°C for 10 min and chilled on ice immediately. One μl denatured DNA was loaded onto 4% denaturing polyacrylamide gel (3.8% acrylamide, 0.2% bis-acrylamide, 8.9 mM Tris, 8.9 mM boric acid and 0.2 mM EDTA and 6.0 M urea, pH 8.3, filtered through a 0.45 μm filter, polymerized by addition of 125 ul of 10% ammonium persulfate and 12.5 μl N,N,N',N'-tetramethylelthylenediamine per 25 ml). Gel electrophoresis was performed again in the automated ABI Prism 377 DNA sequencer. Results were analyzed using ABI GeneScan analysis software version 3.7.

4. Results

4.1. Mutation analysis of BRAF

Exons 11 and 15 of the *BRAF* gene were screened for base changes by direct cycle sequencing in 195 CNS tumors (Tables 3.1 and 3.2). The tumor series comprised of 23 diffuse astrocytomas, 18 AAs, 53 GBMs (including two GSs), 31 oligodendroglial tumors, 23 ependymal tumors, 21 MBs and 26 meningeal tumors, and 10 cell lines including six from astrocytic tumors (GBM2603, GBM6840, LNZ308, SKMG3, U138 and U343), three from MBs (D283 Med, D384 Med and Daoy) and one from PNET (PFSK1).

The primers for exon 11 and exon 15 generated PCR products of 313 and 224 bp, respectively. Since these fragments were relatively short, sequencing was performed in one orientation. Upon detection of base change, sequencing of a newly amplified fragment was performed in both orientations.

Sequencing signals translated to base sequence were aligned with *BRAF* referenced sequence (NT_007914) using the BLAST engine provided by the National Center for Biotechnology Information (http://www.ncbi.nlm.nih.gov/blast/bl2seq/bl2.html). A total of 14 types of amino acid change have been reported in both exons 11 and 15. Out of them, the T1796A

substitution in exon 15 leading to V599E was detected in one GBM case BJ10 and in two GBM cell lines, GBM2603 and GBM6840. Sequence electropherograms of exon 15 of all three cases showed a heterozygous T/A at the 1796 position of *BRAF*. Detection of an A signal in addition to the T signal indicated mutation in at least one allele.

In the GBM case BJ10 (Figure 4.1), signals given by the wild-type allele and that given by the mutant allele were of similar height. These results indicated mutation in one allele of the *BRAF* gene. Somatic mutation in BJ10 was confirmed by no such base substitution in corresponding blood sample of the same patient.

In GBM6840 (Figure 4.2), heterozygous T/A peaks at the 1796 position were also observed. In the sense strand, an A signal was always accompanied by a weaker T signal. The reverse was true in the anti-sense strand. In both sense and anti-sense strands, the peaks resulted from mutant allele were at least two folds of those resulted from the normal allele. It was suspected that multiple copies of chromosome 7 were present in this cell line. Since GBM6840 is an in-house established cell-line, karyotype of the cell line is available. In 79 metaphase spread of chromosomes, the number of chromosome 7 ranged from 2 to 4 copies, giving a mean of 3.1 and standard deviation (SD) of 0.6. Therefore, the higher peak signal of mutant allele could be explained by duplication or multiplication of the mutant chromosome.

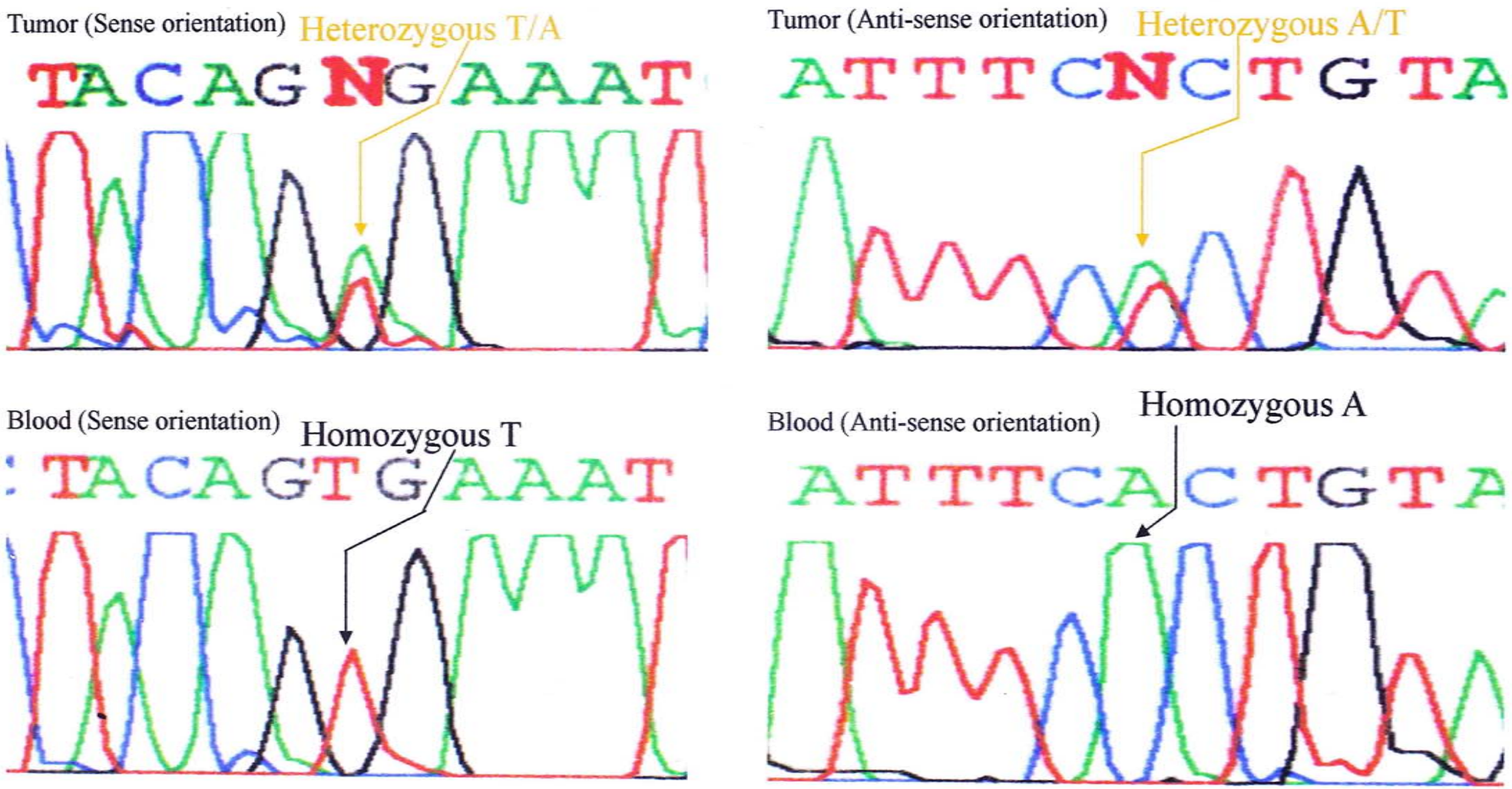

Fig. 4.1. Sequence electropherograms of the GBM case BJ10 and blood sample from the same patient.
Direct sequence analysis revealed heterozygous T/A at base 1796 of the BRAF gene, indicating one allele had been changed from T to A in the tumor sample of BJ10. Such base substitution was not observed in congenital tumor-matched blood.

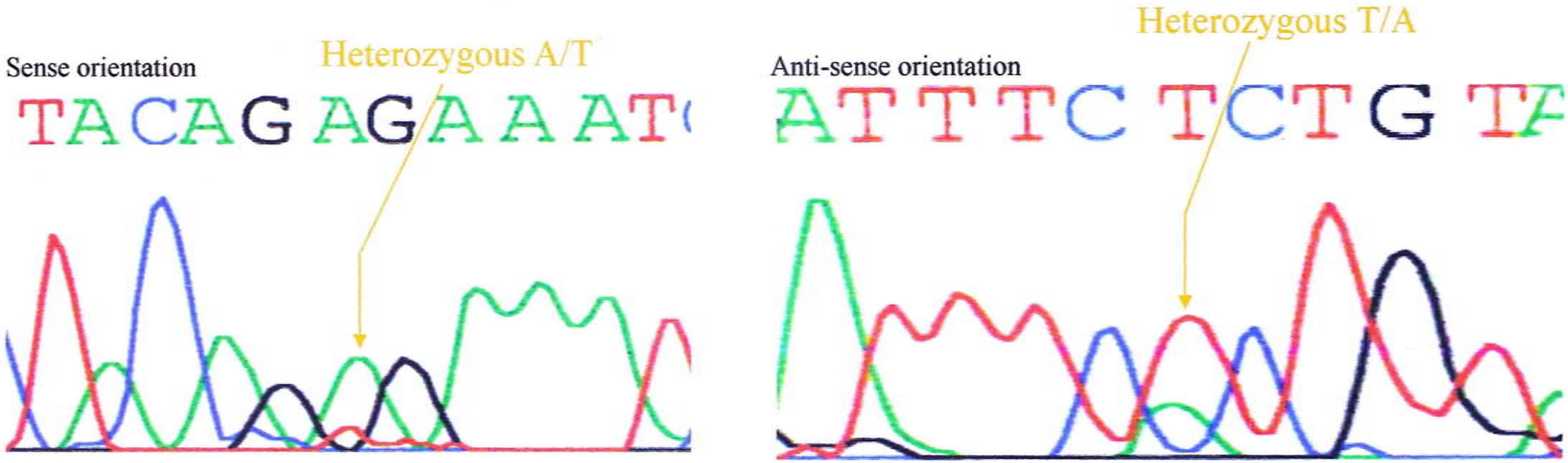

Fig. 4.2. Sequence electropherograms of the GBM6840.

In GBM2603 (Figure 4.3), double peaks at the 1796 position were also observed. In the sense sequence, an A signal was always accompanied by a weak T signal, which was slightly above the background. The present of T signal was reproducible in the anit-sense strand as a weak A signal. This indicated the presence of normal allele instead of random background signal. Karyotype of GBM2603 is also available. Analysis of 49 metaphases showed 3 to 7 copies of chromosome 7, giving a mean of 4.8 ± 0.7 copies. Considering results from karyotyping study, a much higher mutant to normal allele ratio in GBM2603 than GBM6840 indicated the presence of more mutant copies of chromosome 7 in GBM2603 than GBM6840.

All results showing base changes were confirmed by repeating PCR and sequencing of both sense and anti-sense strands. In all other tumors, no base change in the 1796 position of *BRAF* was observed. Direct sequencing revealed no mutation in other positions of exon 15 and in exon 11 of *BRAF* in all samples examined.

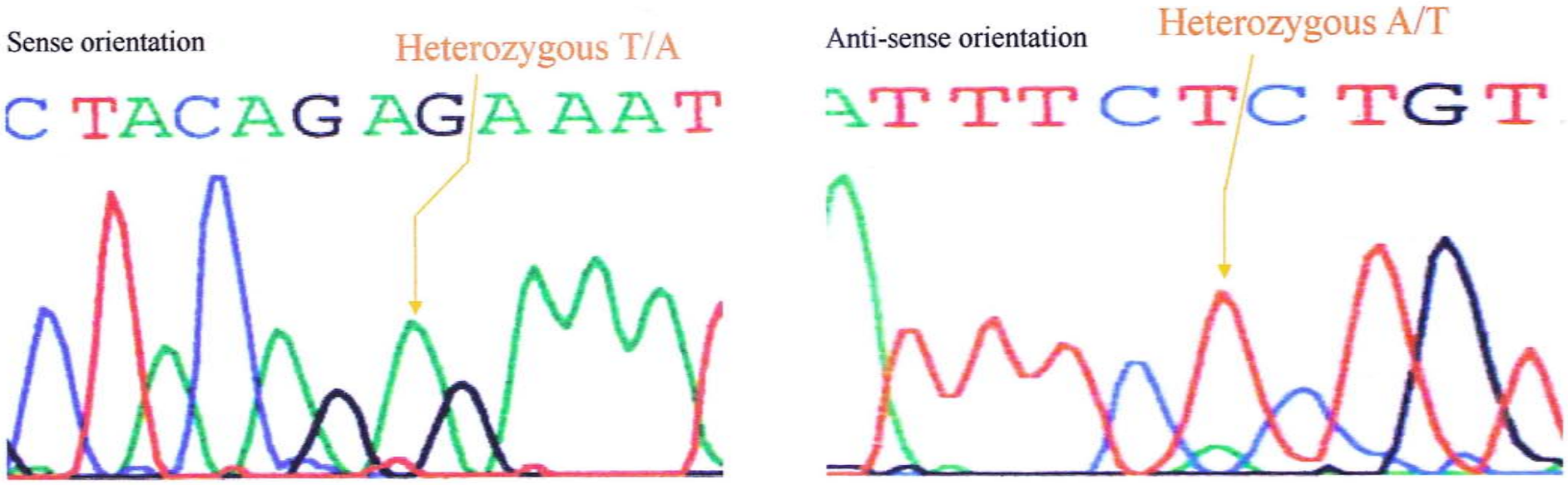

Fig. 4.3. Sequence electropherograms of GBM2603.

4.2. Immunohistochemistry of B-Raf protein

The specificity of the anti-B-Raf antibody was tested by performing immunohistochemistry on the B-Raf expressing cell line A431, and on 10 normal brain and 2 skeletal muscle specimens. In concordance with the information provided by the anti-body supplier, cytoplasm of A431 cells were stained brown and appeared as rings around blue hematoxylin counterstained nuclei. In all brain specimens, brown triangular cytoplasm of neuron cell bodies with protruding axons were shown clearly above the background (Figure 4.4). In contrary, no 'star-shaped' astrocytic cells could be observed in any of the brain specimens. To confirm the presence of astrocytes which were non-reactive to anti-B-Raf antibody, consecutive brain specimens were stain by GFAP. Instead of neurons, brown normal astrocytes were shown up in the GFAP series. Lastly, none of the two muscle specimens showed brown color comparable with those of neuron cells and A431 cells. Therefore, the anti-B-Raf antibody was considered specific in recognition of B-Raf antigen.

Figure 4.4.

Immunohistochemistry of B-Raf and GFAP in normal and malignant cells.

A, neurons (40X) but not astrocytes, showed immunoreactivity to B-Raf in normal brain; B, skeletal muscle (20X) showed negative B-Raf immunoreactivity; C, A431 squamous cell carcinoma (40X) showed positive B-Raf immunreactivity.

To investigate whether B-Raf was abnormally expressed in astrocytic tumors, immunohistochemistry for B-Raf expression was then performed in 25 GBMs, 13 AAs and 9 diffuse astrocytomas from the *BRAF* mutation study, in which tissues were available, and in the six glioma cell lines. B-Raf immunopositivity in tumor tissue was defined by possession of B-Raf immunopositive cells in greater than 5% of the total cell population in at least one 400X microscopic view. While all glioma cell lines were 100% B-Raf immunopositive (Figure 4.5), only 29.8% of astrocytic tumor cases possessed more than 5% of immunopositive cells (Table 4.1).

Positive cases existed in all three grades of astrocytic tumors. Out of 9 diffuse astrocytomas, 4 (44.4%) possessed B-Raf immunoreactivity (Figure 4.6). While two specimens were comprised of 15 – 40% immunopositive tumor cells, the other two were comprised of 5 – 15% and at least 40% immunopositive tumor cells, respectively. Out of 13 AAs, 3 (30.8%) of them were B-Raf immunopositive (Figure 4.7). Two specimens showed 5 – 15% B-Raf immunopositive tumor cells and the remaining one showed 15 – 40%. Lastly, 7 of 25 GBMs (28.0%) showed positive B-Raf immunoreactivity (Figure 4.8). Two specimens were consisted of 5 – 10% B-Raf immunoreactive cells. One specimen showed 15 – 40% B-Raf immunoreactive cells. Four of the GBMs possessed B-Raf immunoreactive cells in at least 40% tumor population.

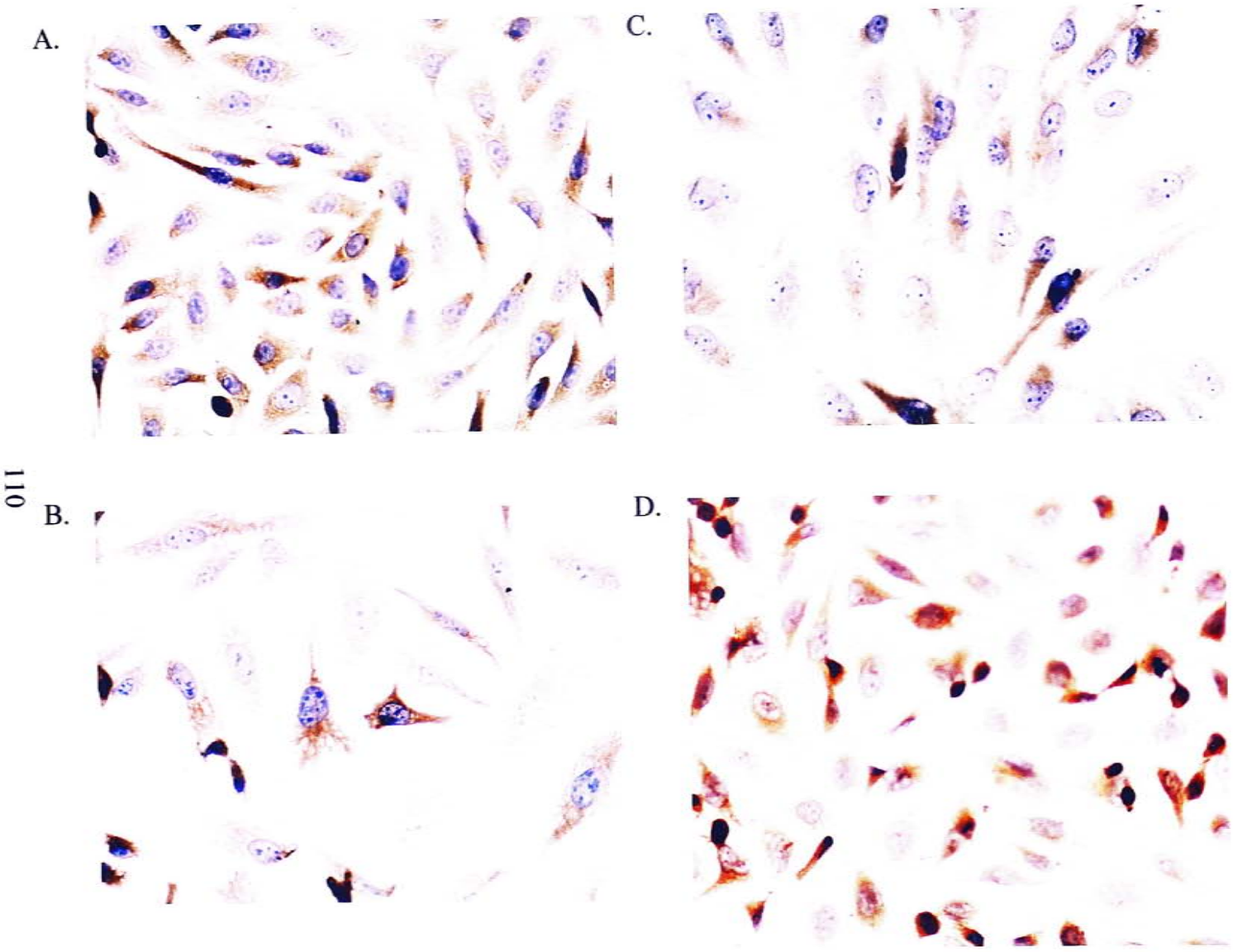

Figure 4.5.
Astrocytic tumor cell lines (40X) showing positive B-Raf immunoreactivity. A, GBM2603 with *BRAF* mutation; B, GBM6840 with *BRAF* mutation; C, SKMG3 harboring *EGFR* amplification; D, LNZ308 with neither *EGFR* amplification nor *BRAF* mutation.

Table 4.1. B-Raf immunoreactivity of astrocytic tumors.

	B-Raf immunoreactivity			
	-	+	++	+++
Diffuse astrocytoma ($n = 9$)	5 (55.6%)	1 (11.1%)	2 (22.2%)	1 (11.1%)
AA ($n = 13$)	10 (76.9%)	2 (15.4%)	1 (7.7%)	0 (0.0%)
GBM ($n = 25$)	18 (72.0%)	2 (8.0%)	1 (4.0%)	4 (16.0%)
All Grades ($n = 47$)	33 (70.2%)	5 (10.6%)	4 (8.5%)	5 (10.6%)

-, immunopositive cells ≤ 5% of total tumor cells within a 400X microscpic view; +, immunopositive cells > 5 and ≤ 15%; ++, immunopositive cells > 15% and ≤ 40%; +++, immunopositive cells > 40%.

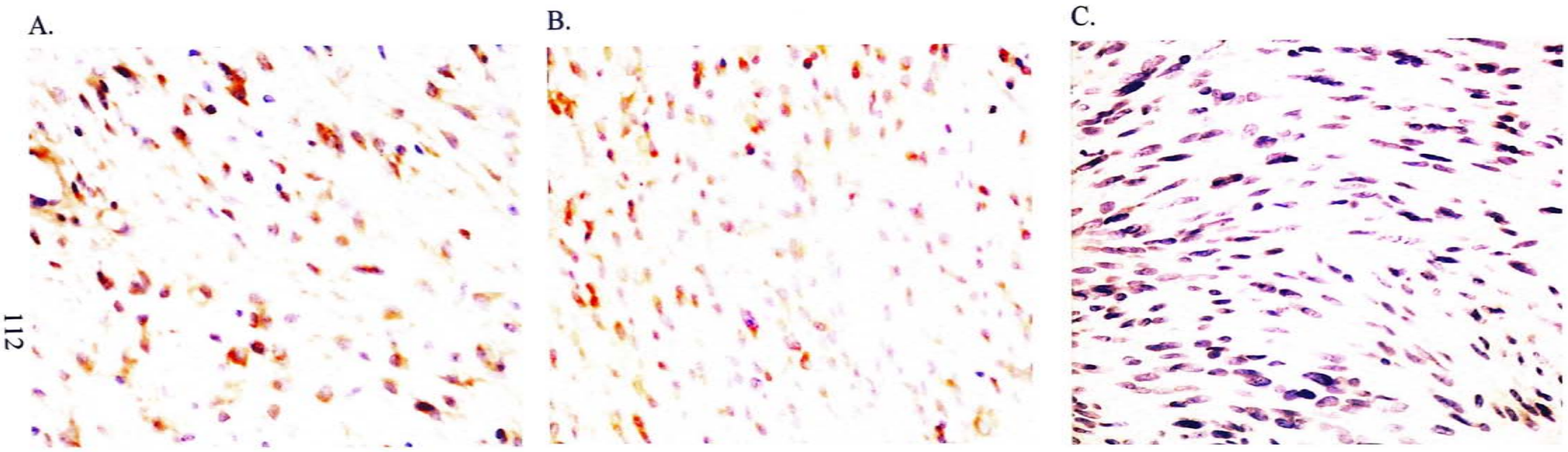

Figure 4.6.

Different B-Raf immunoreactivities in diffuse astrocytomas.

A, PW91S12886, 40X, ++; B, PW94S530, 40X, +; C, PW89S11533, 40X, - (-, immunoreactive cell population less than or equal to 5%; +, immunoreactive cell population more than 5% but less than 15%; ++, immunoreactive cell population from 15% to 40%).

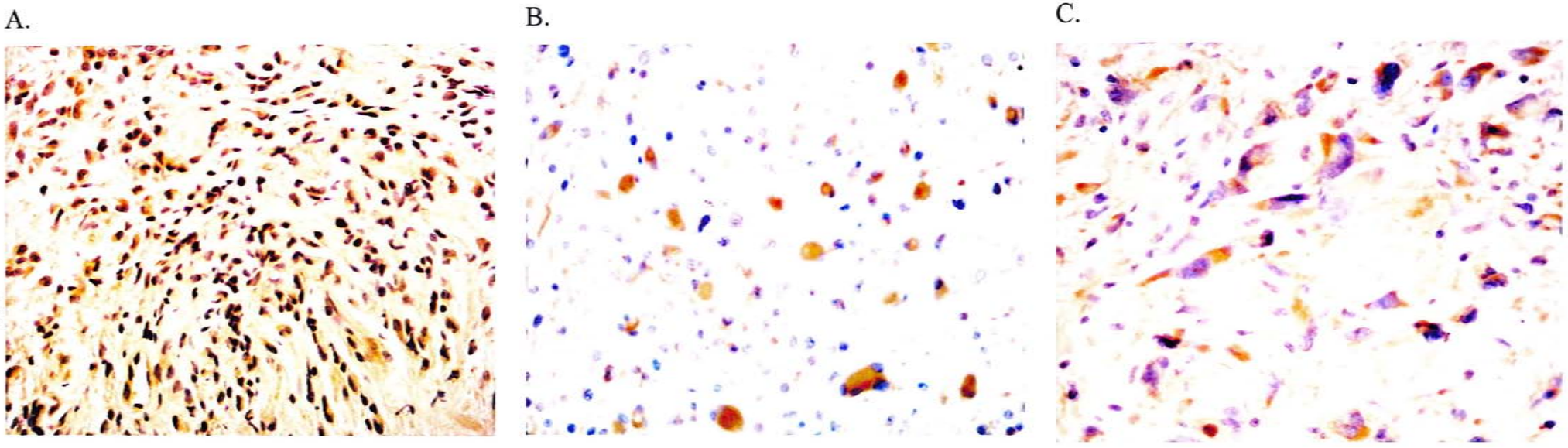

Figure 4.7.

Different B-Raf immunoreactivities in anaplastic astrocytomas.

A, PW99S7202, 40X, +++; B, PW91S5070, 40X, ++; C, PW01S10055, 40X, + (+, immunoreactive cell population more than 5% but less than 15%; ++, immunoreactive cell population from 15% to 40%, +++, immunoreactive cell population more than 40%).

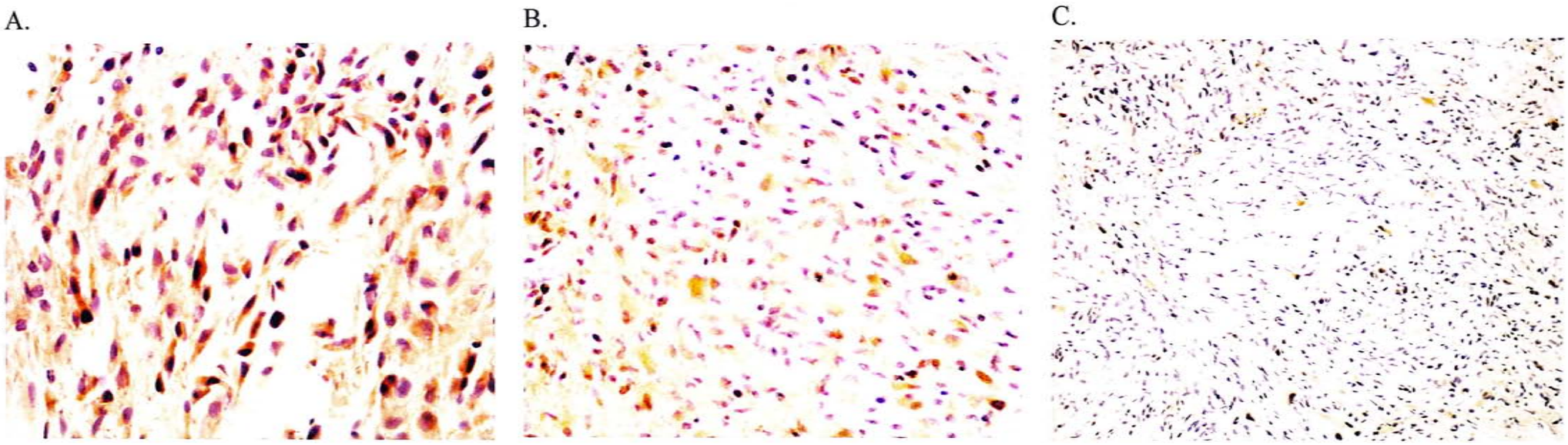

Figure 4.8.

Different B-Raf immunoreactivities in glioblastoma multiformes.

A, BJ10, 40X, +++; B, PW98S11908, 40X, ++, C, PW93S8821, 20X, - (-, immunoreactive cell population less than or equal to 5%; ++, immunoreactive cell population from 15% to 40%, +++, immunoreactive cell population more than 40%).

Using Fisher's exact test, correlation analysis of B-Raf immunoreactivity versus patient age, sex and tumor grade were performed. Patient age ranged from 4 to 76 with a mean at 46.18 and a SD of 19.62. Grouping patients by older/younger than 18 years did not reveal difference in B-Raf immunoreactivity between adults and younger patients ($P = 1.000$). Since the first, second and third quartiles of patient age lay on 34, 42 and 65 years respectively, correlation analyses were repeated after grouping patients by older/younger than 34, 42 and 65 years. However, correlation between B-Raf immunoreactivity and patient age was still not observed ($P = 1.000$, 0.749 and 0.698 respectively). Also, no statistical correlation was detected between B-Raf immunoreactivity and sex ($P = 0.525$). Thus, B-Raf immunoreactivity was not associated to both age and sex.

Tumor cases with positive B-Raf immunoreactivity could be divided by possession of different proportion of immunopositive cells (Table 4.1). No apparent difference in immunopositivity in relation to tumor grade could be observed. Fisher's exact test was performed to investigate whether difference in B-Raf immunoreactivity (- versus at least one +) exist among tumors of different grade. My results did not show any statistical difference in B-Raf immunoreactivity between diffuse astrocytoma and AA ($P = 1.000$), between diffuse astrocytoma and GBM ($P = 1.000$), and between AA and GBM (- verse at least one +, $P = 1.000$). Lastly, AA and GBM

cases were sorted into high-grade group in comparison with low-grade diffuse astrocytoma. Statistical association between tumor grade and B-Raf immunopositivity was still not found using Fisher's exact test ($P = 1.000$). Therefore, B-Raf immunoreactivity of astrocytic tumors was not related to histological grading.

To increase sample size for correlation study in later section (Section 4.4 and 4.5), B-Raf immunohistochemistry was performed for 6 additional GBM cases known to possess *EGFR* amplification in another project of our group but not included in mutation analysis of *BRAF*. All 6 samples showed negative B-Raf immunoreactivity.

4.3. Quantification of EGFR gene dosage

To establish real-time technique in the current study, serial dilutions of 5 *EGFR* standards (from 3 x 10^0 to 3 x 10^5 copies/μl) and 5 *B2M* standards (from 2 x 10^1 to 2 x 10^6 copies/μl) were prepared. The house-keeping *B2M* gene was used to normalize cellular *EGFR* gene copies. Since the literature did not reveal abnormalities in *B2M* within astrocytic tumors, two copies of *B2M* were assumed in every normal or tumor cell. Threshold for gene quantification was calculated by 10 times average SD from as much baseline cycles as possible (Freeman *et al.*, 1999; Giulietti *et al.*, 2001; Heid *et al.*, 1996).

In amplification of *EGFR*, fluorescence signal raised above background beyond cycle 19 (Figure 4.9). Therefore, calculated threshold for *EGFR* gene quantification was 21.45 (10 times average SD from baseline cycles 2 to 19). Threshold cycles decreased linearly with log of input *EGFR* quantity (from 2 x 10^1 to 2 x 10^6 copies, duplicate trials; correlation coefficient = 0.999, Figure 4.10). Similarly, detectable fluorescence signal change was beyond cycle 16 for *B2M* and threshold was taken at 19.82, which was calculated by 10 times average SD from baseline cycles 2 to 16 (Figure 4.11). Threshold cycles also decreased linearly with log of input *B2M* quantity (from 1 x 10^2 to 1 x 10^7 copies, duplicate trials; correlation coefficient = 0.992, Figure 4.12).

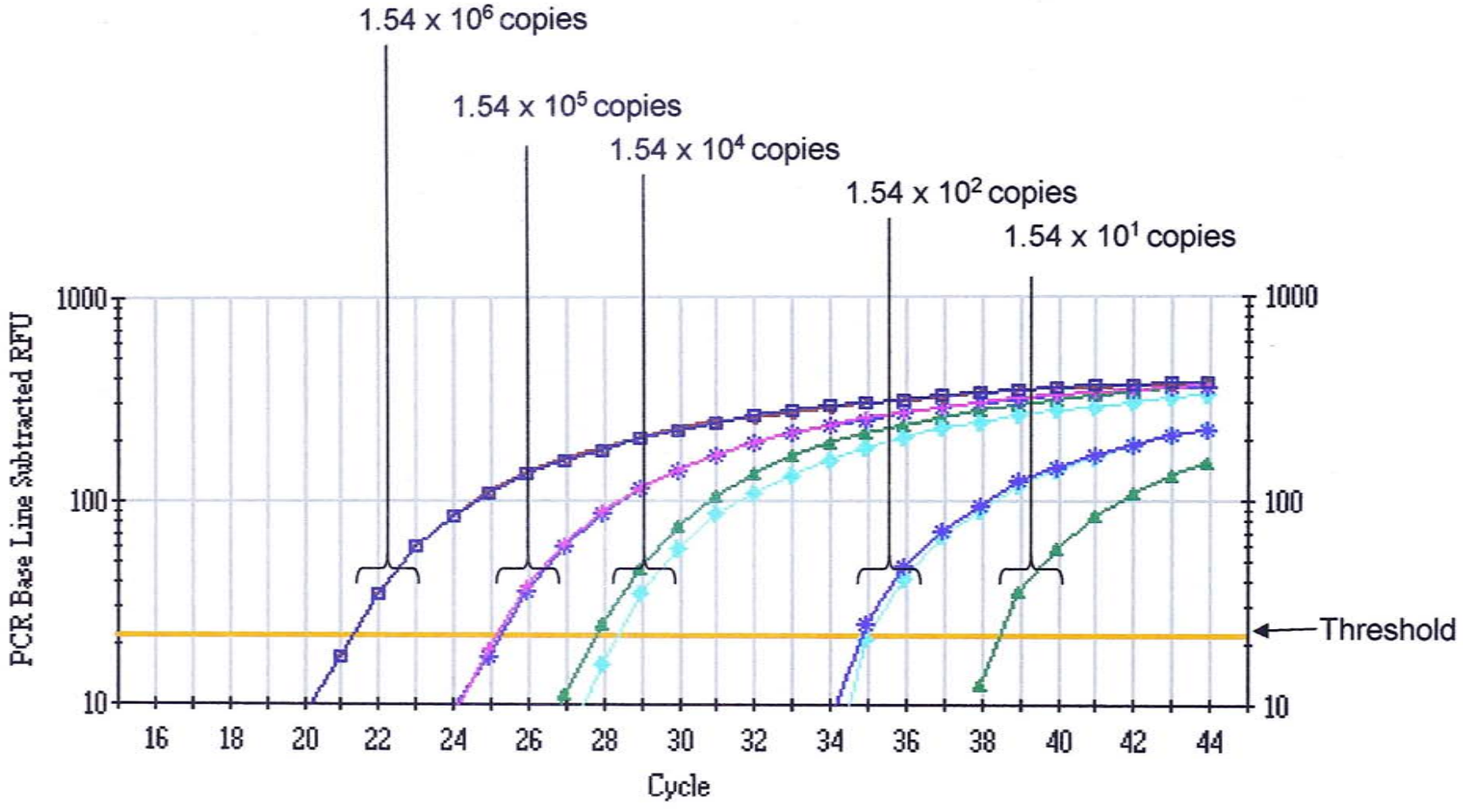

Figure 4.9. Real-time PCR amplification chart for *EGFR* standards.

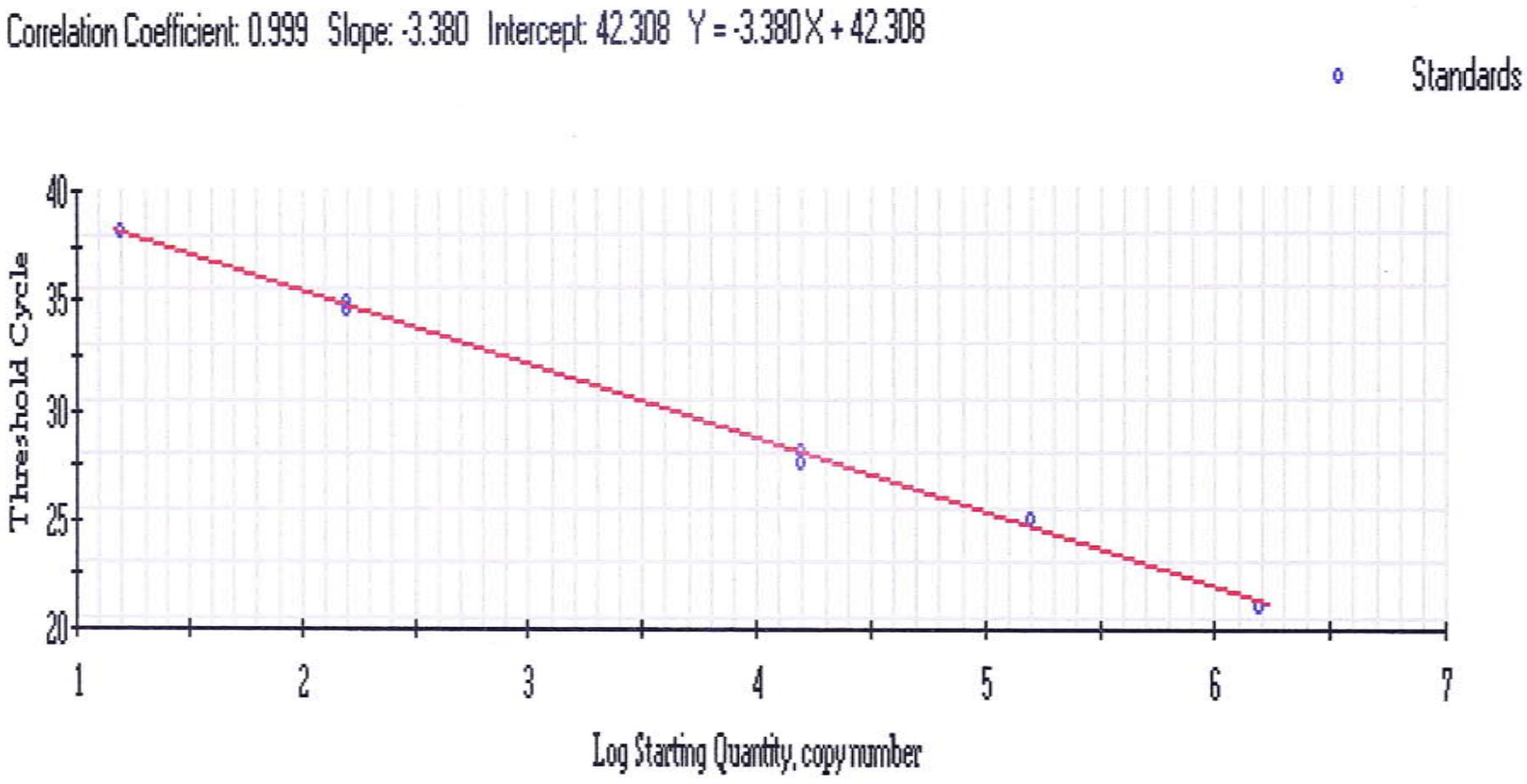

Figure 4.10. Correlation between threshold cycle and input *EGFR* quantity.

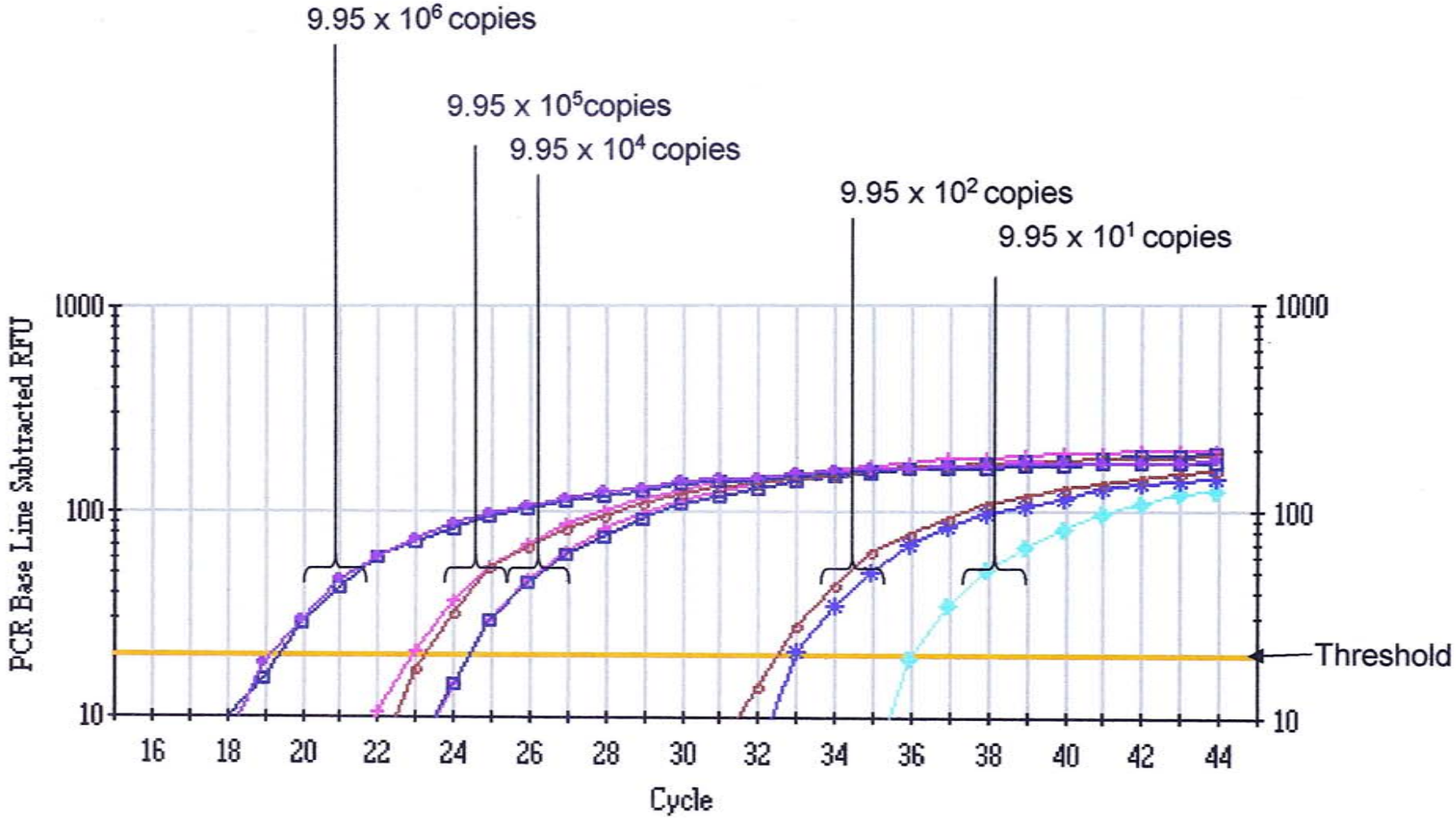

Figure 4.11. Real-time PCR amplification chart for *B2M* standards.

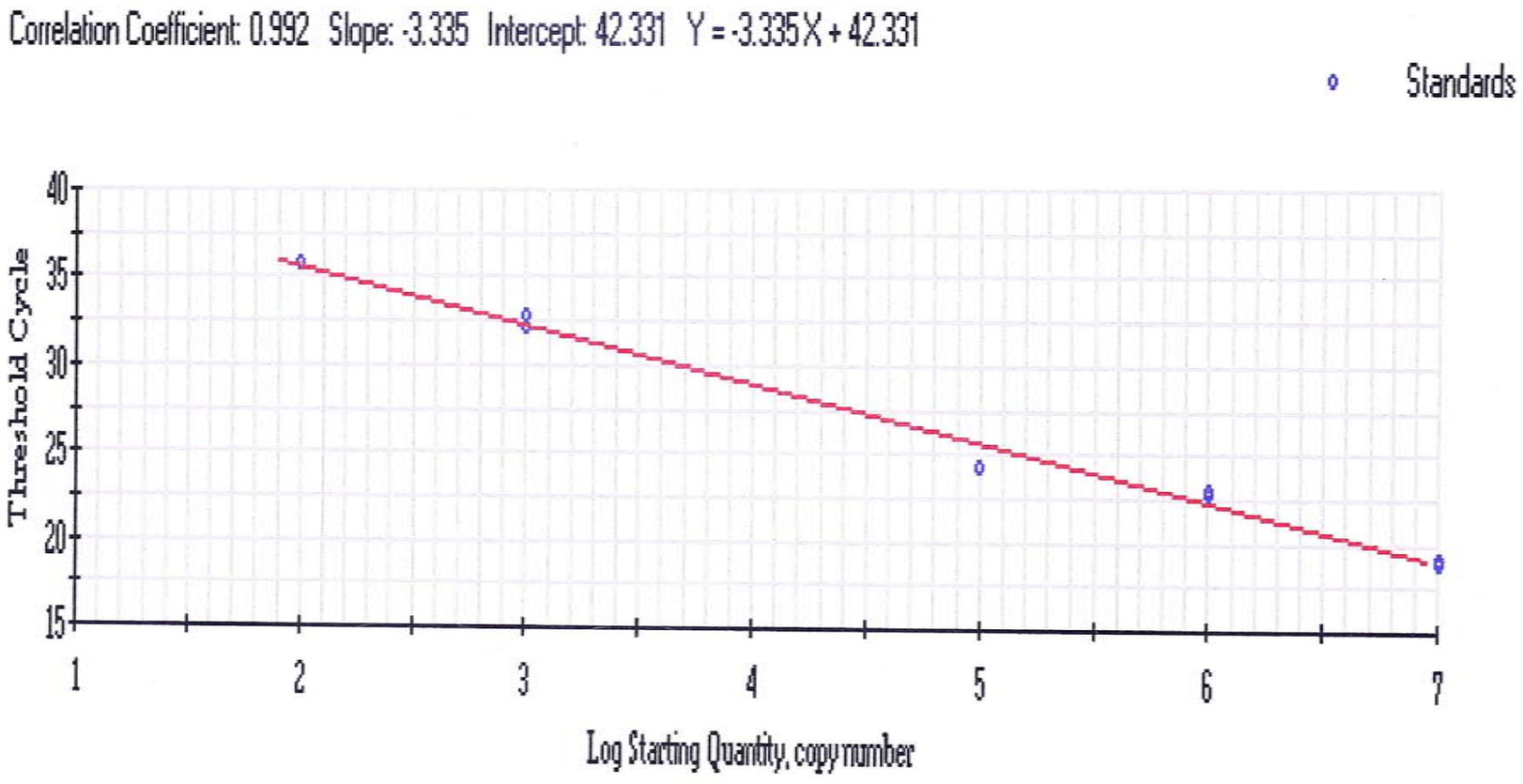

Figure 4.12. Correlation between threshold cycle and input *B2M* quantity.

To validate the real-time assay for *EGFR* quantification, DNA from the two *EGFR* overexpressing cell lines SKMG3 and A431, and 10 patient's blood samples were recruited. A water blank was used as the negative control. From standard curves of the same experiment, starting quantities of *EGFR* and *B2M* of each sample in triplicate trials were defined and averaged to obtain the means of starting quantity (MSQs). Then an *EGFR* index was calculated by MSQ of *EGFR* over MSQ of *B2M*.

In lymphocyte DNA from 10 patients, averaged *EGFR* gene index from three trials ranged from 1.0 to 1.7, averaged at 1.4 with a SD of 0.3. Normal range of *EGFR* index was then defined as 0.9 to 1.9 (mean ± 2 SD, Table 4.2). Samples with *EGFR* index greater than 1.9 but below 5.7 (calculated by 1.9 /2 x 6, indicating the presence of 6 copies) were regarded as gain in *EGFR* gene dosage. *EGFR* gene amplification was considered for those with *EGFR* index greater than 5.7. Averaged *EGFR* index from 3 trials of SKMG3 and A431 were 17.9 and 5.0 respectively, as determined from the 5-point standard curves in the same run. They were much higher above the lower limit (1.9) of normal dosage. Real-time experiments for determination of *EGFR* gene dosage were regarded valid.

Table 4.2. Normal range of *EGFR* index (triplicate trials).

Lymphocyte DNA from patient donor/ Positive control	*EGFR*		*B2M*		
	MSQ	CV (%)	MSQ	CV (%)	*EGFR* Gene Index
HK136	1.51×10^4	2.4	1.26×10^4	7.3	1.0
HK55	3.37×10^5	2.7	3.90×10^5	3.3	0.9
HS51	1.46×10^5	12.4	1.25×10^5	2.5	1.2
NJ10	1.74×10^6	2.6	1.06×10^6	15	1.6
NJ9	7.87×10^4	10.6	5.40×10^4	11.4	1.5
SH11	3.52×10^5	2.1	2.28×10^5	6.5	1.6
SH13	3.83×10^5	4.5	2.76×10^5	7.4	1.4
WC116	1.47×10^5	0.8	8.58×10^4	6.3	1.7
WC12	4.03×10^5	1.7	3.43×10^5	16.9	1.2
WC125	5.77×10^5	5.3	3.71×10^5	12.9	1.6
SKMG3 (control)	1.14×10^6	6.2	6.38×10^6	0.1	17.9
A431 (control)	3.62×10^5	7.4	7.24×10^4	2.8	5.0

MSQ, Mean of starting quantity; CV, confidence value determined by SD / MSQ; *EGFR* Index, MSQ of *EGFR* / MSQ of *B2M*.

EGFR gene status was determined from samples included in *BRAF* mutation screening experiments, in which DNA were available. The series included 18 GBMs and 14 AAs, and 6 glioma cell lines. Triplicate trials were done for each case. Each experiment included four-point standard curves for *EGFR* and *B2M* respectively, SKMG3 as positive control, two normal blood controls and water as negative control.

In the current series, *EGFR* gain was detected in one AA and two GBMs. Averaged *EGFR* index of the AA case WC114 was 3.1. Those of the two GBM cases WC159 and WN58 were 3 and 2.4, respectively. *EGFR* dosage of 6 GBMs included in the *BRAF* mutation screening experiments had been obtained in another study (Table 3.1). Including these samples, *EGFR* gain was detected in 7.1% (1/14) of AA and in 8.3% (2/24) of GBM.

In the present study, *EGFR* amplification was also detected in one AA and 5 GBMs. The AA case WC114 possessed an averaged *EGFR* index of 20.1. *EGFR* index of the GBMs ranged from 10.5 to 56.7 (Table 4.3), with the median being 18.2. One of the 6 GBMs with *EGFR* index quantified in the other study was 29.4. (In that study, *EGFR* index of 10 lymphocyte DNA samples ranged from 0.7 to 1.5, those for SKMG3 and A431 were 17.7 and 4.3, respectively.) Including the 6 additional GBMs, *EGFR* amplification in AA and GBM were 7.1% (1/14) of AA and 25% (6/24) of GBM, respectively.

Table 4.3. *EGFR* index (triplicate trials) of astrocytic tumors harboring *EGFR* gain or amplification.

Astrocytic tumros		First triplicate trials				Second triplicate trials				Averaged *EGFR* Index
		EGFR		*B2M*		*EGFR*		*B2M*		
		MSQ	CV (%)	MSQ	CV (%)	MSQ	CV (%)	MSQ	CV (%)	
GBM	AH326	1.22×10^7	2.6	2.98×10^5	14.2	8.31×10^6	5.0	1.14×10^5	6.6	56.7
	HS34	4.21×10^6	1.6	3.03×10^5	4.8	3.53×10^6	3.9	1.58×10^5	6.5	18.2
	NJ146	4.09×10^6	2.1	2.92×10^5	17.4	2.37×10^6	7.4	1.74×10^4	8.3	13.8
	NJ22	5.37×10^6	2.9	2.10×10^5	1.2	6.40×10^6	7.8	1.52×10^5	3.3	33.9
	PW94S3772	2.36×10^6	0.7	2.32×10^5	2.2	2.39×10^6	9.8	2.23×10^5	10.3	10.5
	PW97S13494[e]	-	-	-	-	-	-	-	-	29.4
	WC159	7.73×10^5	2.3	2.17×10^5	9.0	8.62×10^6	3.8	3.65×10^6	6.7	3.0
	WN58	6.75×10^5	5.0	2.82×10^5	3.7	1.37×10^6	2.4	6.07×10^5	11.5	2.4
AA	WC114	1.51×10^7	3.1	8.69×10^5	8.7	1.60×10^7	3.3	6.78×10^5	7.0	20.1
	WC30	8.57×10^4	19.7	3.36×10^4	5.6	2.20×10^5	3.2	6.32×10^4	9.5	3.1

MSQ, Mean of starting quantity; CV, SD / MSQ; *EGFR* index, MSQ of *EGFR* to MSQ of *B2M*; e, DNA sample with known *EGFR* amplification.

Positive results in the current study were confirmed by another set of triplicate trials. All experiments were valid with respect to *EGFR* gene index of SKMG3 (ranged from 15.3 to 24.3), normal blood control (0.9 to 1.4 and 1.0 to 1.9 respectively) and negative control obtained in the same experiments.

From karyotyping of cell lines GBM2603 and GBM6840, multiple copies of chromosome 7 were observed. However, gain in *EGFR* was not detected by real-time PCR. In GBM6840, the *EGFR* index of 1.1 was attributed to a near triploid pattern in representative metaphases (Di Tomaso *et al.*, 2000). Analysis of 79 cells in metaphase showed the copy number of chromosome 7 varied from 2 to 4 and that of chromosome 15 ranged from 1 to 4. Averaging the ratio of the number of chromosome 7 to the number of chromosome 15 produced a mean at 1.1 with a SD of 0.5.

Similar to GBM6840, gain in *EGFR* in GBM2603 was missed out in real-time PCR. However, ratio of the number of chromosome 7 to the number of chromosome 15 averaged at 2.2 with a SD of 0.9 as revealed by karyotyping and was higher than the *EGFR* index given by real-time PCR (1.6). Different with GBM6840, aneuploidy was not observed in GBM2603. Analysis of 49 metaphases showed 3 to 7 copies of chromosome 7 and 1 to 3 copies of chromosome 15. The deviation between ratio of number of chromosome 7 to number of chromosome 15 and *EGFR* index in

GBM2603 was probably due to the large variation in the number of specific chromosome among cells which was vulnerable to changes during cell passage. Of course, the possibility of gain in chromosome 7 without a parallel gain in *EGFR* dosage could not be ruled out.

4.4. Correlation between EGFR dosage and BRAF mutation

In the current experiment, three GBM cases demonstrated *BRAF* mutation. The tumor sample BJ10 displayed *EGFR* index in the normal range (*EGFR* index = 1.5) whereas the other 2 samples were GBM-derived cell lines, GBM6840 and GBM2603 (*EGFR* indexes = 1.1 and 1.6, respectively). *EGFR* gene amplification and *BRAF* mutation occurred mutually exclusively in the GBM case BJ10. However, among tumor specimens, statistically significant correlation between *BRAF* mutation and gain in *EGFR* was not found (Fisher's exact test, $P = 1.000$). The same was true between *BRAF* mutation and amplification in *EGFR* ($P = 1.000$).

The GBM cell lines were not included in the above correlation analysis between *EGFR* gene dosage and *BRAF* mutation. Firstly, amplified gene sequences are carried primarily on double-minute chromosomes (Sauter *et al.*, 1996) which are always lost on primary culture (Humphrey *et al.*, 1988). Secondly, cells with growth advantage on the culturing environment could be selected out and the cell population might not represent their original tumor specimen. Therefore, *EGFR* status in cell line might not be the same as in the original tumor.

4.5. Correlation between EGFR dosage and B-Raf expression

To increase sample size of tumor harboring *EGFR* amplification, 6 GBM cases known to process *EGFR* amplification from previous project but not included in *BRAF* mutation screening experiments were also included (Table 3.1). All together, 15 astrocytic tumors with normal *EGFR* gene dosage, 3 (10%) with gain of *EGFR* gene dosage and 12 (40%) with *EGFR* amplification were recruited for correlation study between *EGFR* gene dosage and B-Raf immunoreactivity.

Among the 30 astrocytic tumors examined, 23 cases were negative in B-Raf immunoreactivity. *EGFR* amplification was detected in 52.2% of them. On the other hand, all 7 B-Raf immunopositive cases did not harbor *EGFR* amplification. Statistically significant differences in B-Raf immunoreactivity were found between tumors (all grades) with normal *EGFR* gene status and tumors with *EGFR* amplification ($P = 0.047$), and also between tumors with gain in *EGFR* gene and tumors with *EGFR* amplification ($P = 0.029$). Statistical significant differences were also found within GBM samples. That is between GBM tumors with normal *EGFR* gene status and GBM tumors with *EGFR* amplification ($P = 0.029$), and between GBM tumors with gain in *EGFR* gene and GBM tumors with *EGFR* amplification ($P = 0.033$).

Overall, B-Raf immunoreactivity in samples with *EGFR* amplification was significantly different from samples with normal or gain in *EGFR* status as examined by Fisher's exact test ($P = 0.024$). Highly significant association of negative B-Raf immunoreactivity and *EGFR* amplification within GBM was revealed by a P value of 0.008. Astrocytic tumors with *EGFR* amplification did not harbour B-Raf immunoreacitivty.

No statistical significant differences in B-Raf immunoreactivity existed between samples with normal *EGFR* gene status and samples with increased *EGFR* copies (gain or amplification), both in consideration of all samples ($P = 0.235$), in inclusion of AA only ($P = 1.000$) and in employment of GBM only ($P = 0.131$). Significant difference in B-Raf immunopositivity was not detected between tumors with normal *EGFR* gene dosage and tumors with gain in *EGFR* gene both in consideration of all cases ($P = 0.528$) and in GBM only ($P = 1.000$). In other words, astrocytic tumors with normal or gain in *EGFR* dosage could possess B-Raf immunoreactivity, and the probability of possessing B-Raf immunoreactivity did not differ statistically between them. While the 2 GBM cases (WC159 and WN58) harboring gain in *EGFR* gene dosage were positive in B-Raf immunoreactivity, the AA case WC114 with *EGFR* gain was negative in B-Raf immunoreactivity.

4.6. Microsatellite analysis of chromosome 14q in astrocytic tumors

To refine the 14q chromosomal loci that may contain tumor suppressor(s), a total of 12 diffuse astrocytomas, 5 AAs and 13 GBMs (including 2 GSs), and peripheral blood from the same patient were subject to LOH study. Patient ages ranged from 23 to 72, with an average of 45.9 years. The male/female ratio was 1.6 to 1.

Sixteen of 18 microsatellite markers generated informative results in 66% – 90% of cases. Two microsatellite markers of less informative were D14S1068 and D14S59, giving informative results in only 38% and 56% of cases, respectively.

For heterozygous loci, LOH value was defined as allelic ratio of tumor tissue being normalized by allelic ratio of normal tissue and was calculated by (T1/T2)/(N1/N2), where

T1 is the peak height of the tumor allele having the weaker signal peak,

T2 is the peak height of the other tumor allele having the higher signal peak,

N1 is the peak height of the normal allele corresponding to that of T1,

and N2 is the peak height of the normal allele corresponding to that of T2.

Taking the criteria of LOH as losing one of two alleles in more than 50% of tumor population and assuming 20% normal cell contamination, LOH would be indicated by a value of less than 0.6 or greater than 1 /0.6 or 1.67. For example, assuming 100

cells in tumor tissue, lost of allele A, if signal generated from allele B equaled 100 unites, signal resulted from A would be equaled to 20 + 80 x 50% units. Allelic ratio would be given by division of A by B and is equal to 0.6. Therefore, an LOH value of 0.6 or less indicates loss of the allele with lower peak signal in 50% or more of tumor population. An LOH value of 1.67 or more indicates loss of the other allele. The above calculations did not take the difference in PCR efficiency of the two alleles into account. The actual allelic ratio had to be normalized by the allelic ratio of normal DNA from the same patient.

LOH was detected in 9 of 32 astrocytic tumors. They appeared in 4 of 12 diffuse astrocytomas (33%), 2 of 5 AAs (40%), 3 of 13 GBMs (23%). The diffuse astrocytoma case WN66 (Figure 4.13) and WC101 showed LOH in all the informative loci tested, indicating the possibility of losing the whole arm of chromosome 14.

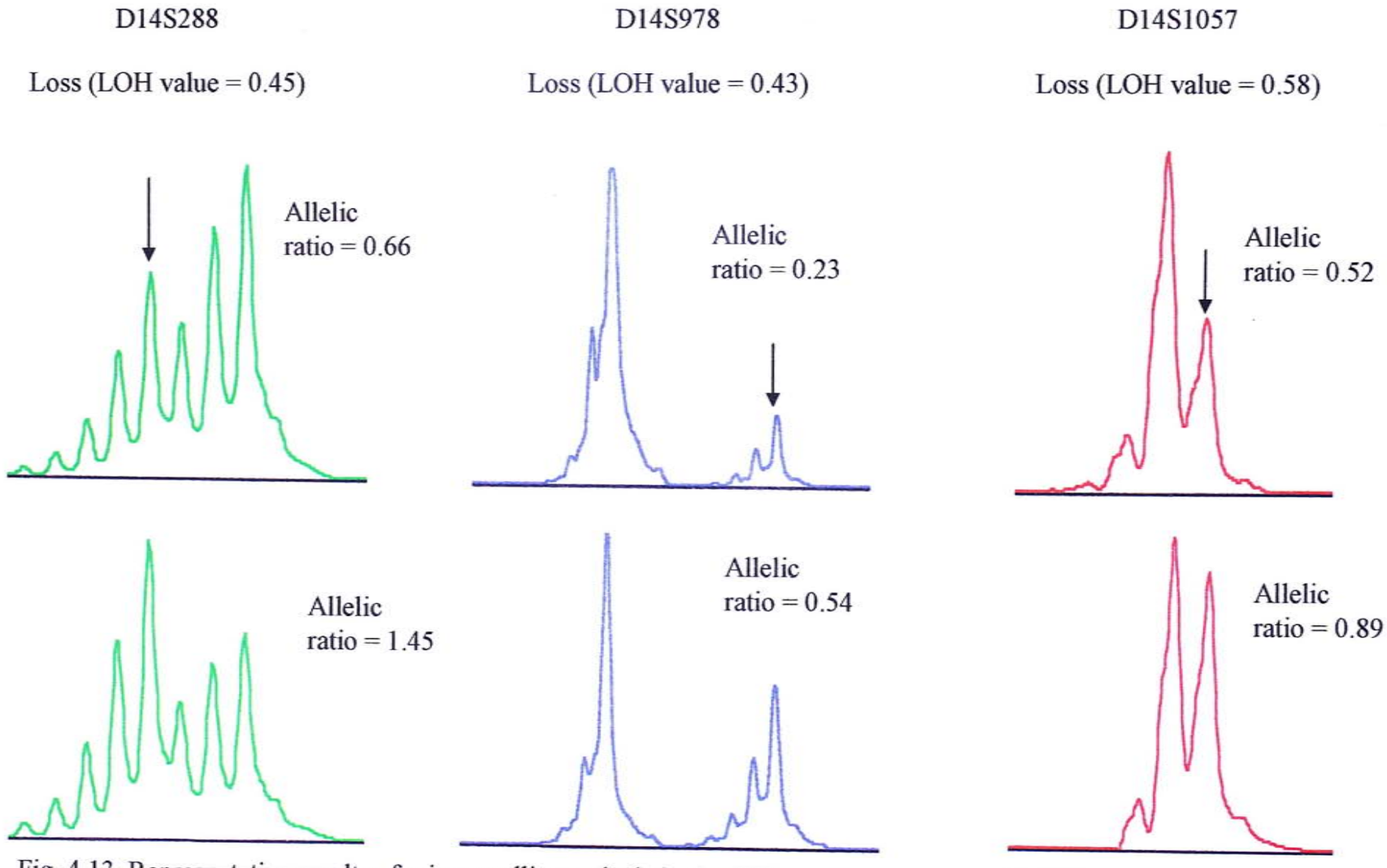

Fig. 4.13. Representative results of microsatellite analysis in the diffuse astrocytoma case WN66.

Upper panel, tumor; lower panel, matched blood; arrows indicate LOH (continued on page 134).

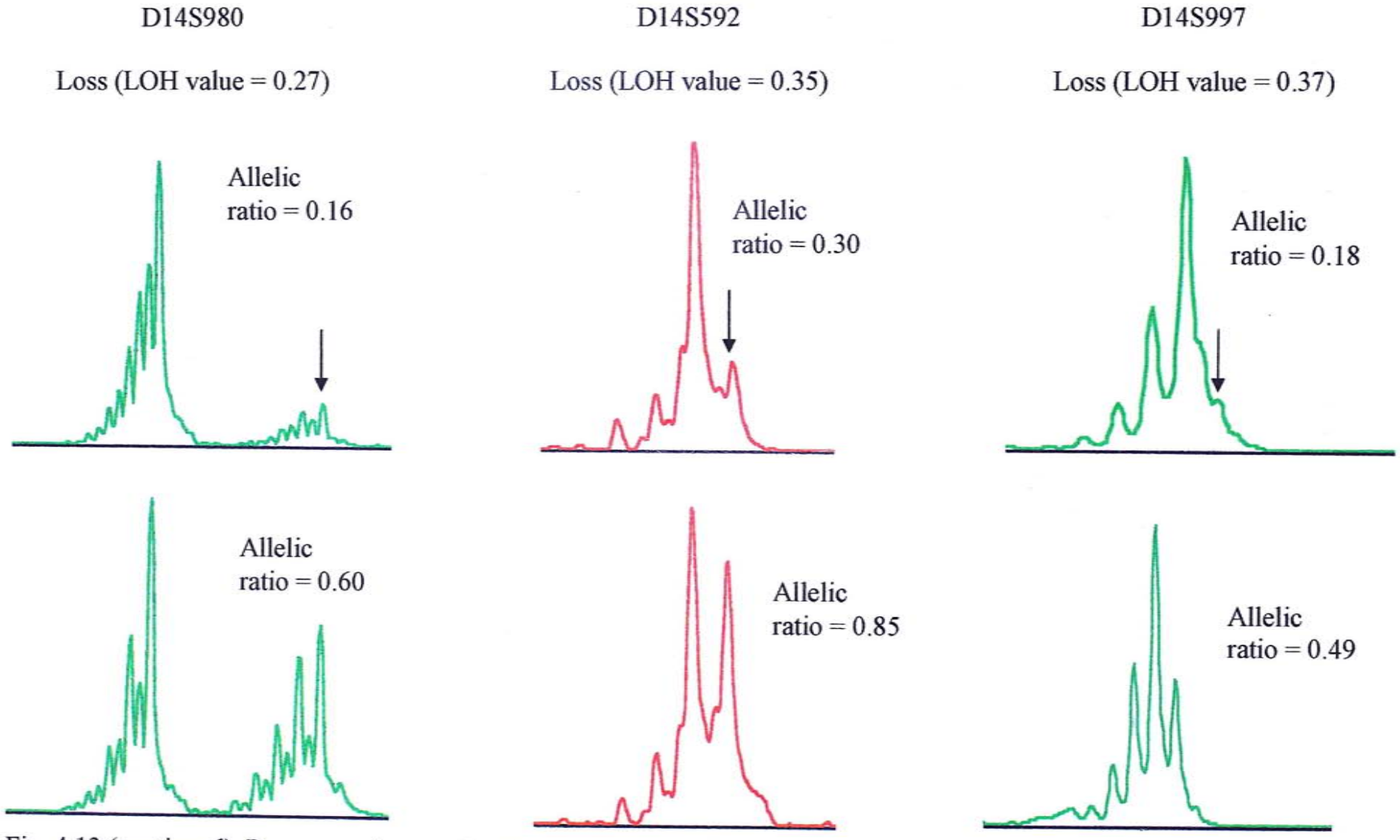

Fig. 4.13 (continued). Representative results of microsatellite analysis in the diffuse astrocytoma case WN66.

Upper panel, tumor, lower panel, matched blood; arrows indicate LOH (continued on page 135).

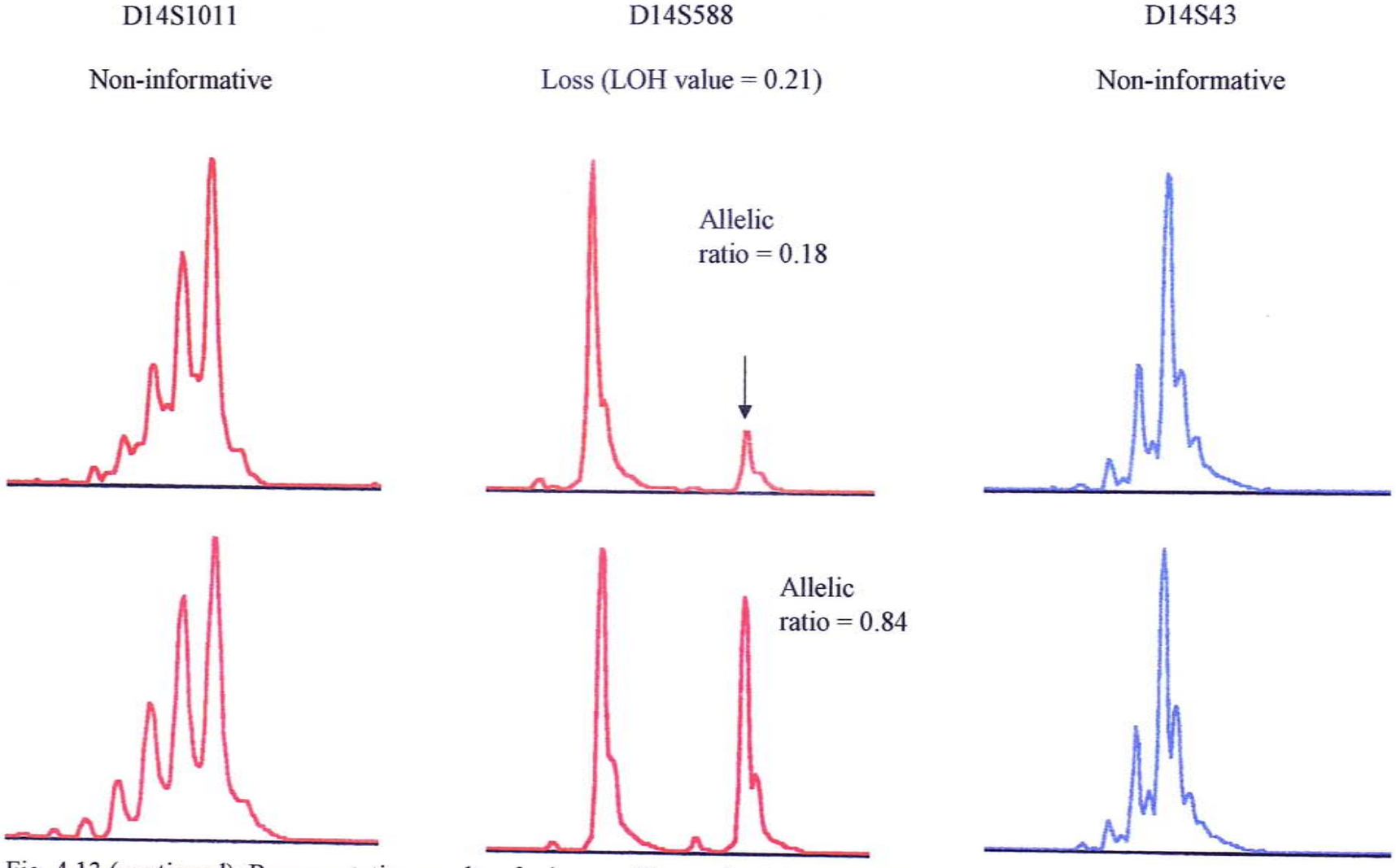

Fig. 4.13 (continued). Representative results of microsatellite analysis in the diffuse astrocytoma case WN66.

Upper panel, tumor, lower panel, matched blood; arrows indicate LOH (continued on page 136).

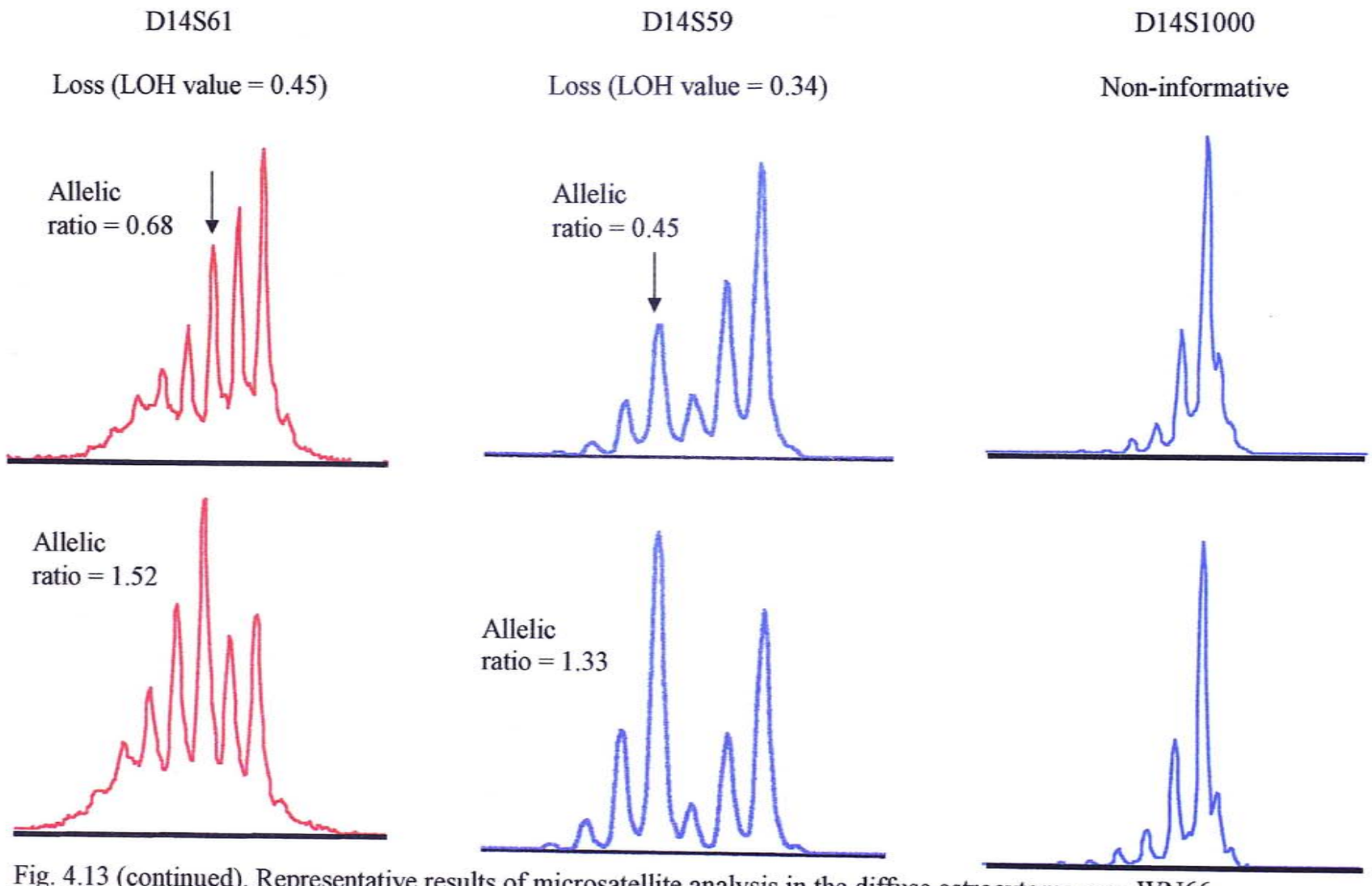

Fig. 4.13 (continued). Representative results of microsatellite analysis in the diffuse astrocytoma case WN66.

Upper panel, tumor, lower panel, matched blood; arrows indicate LOH (continued on page 137).

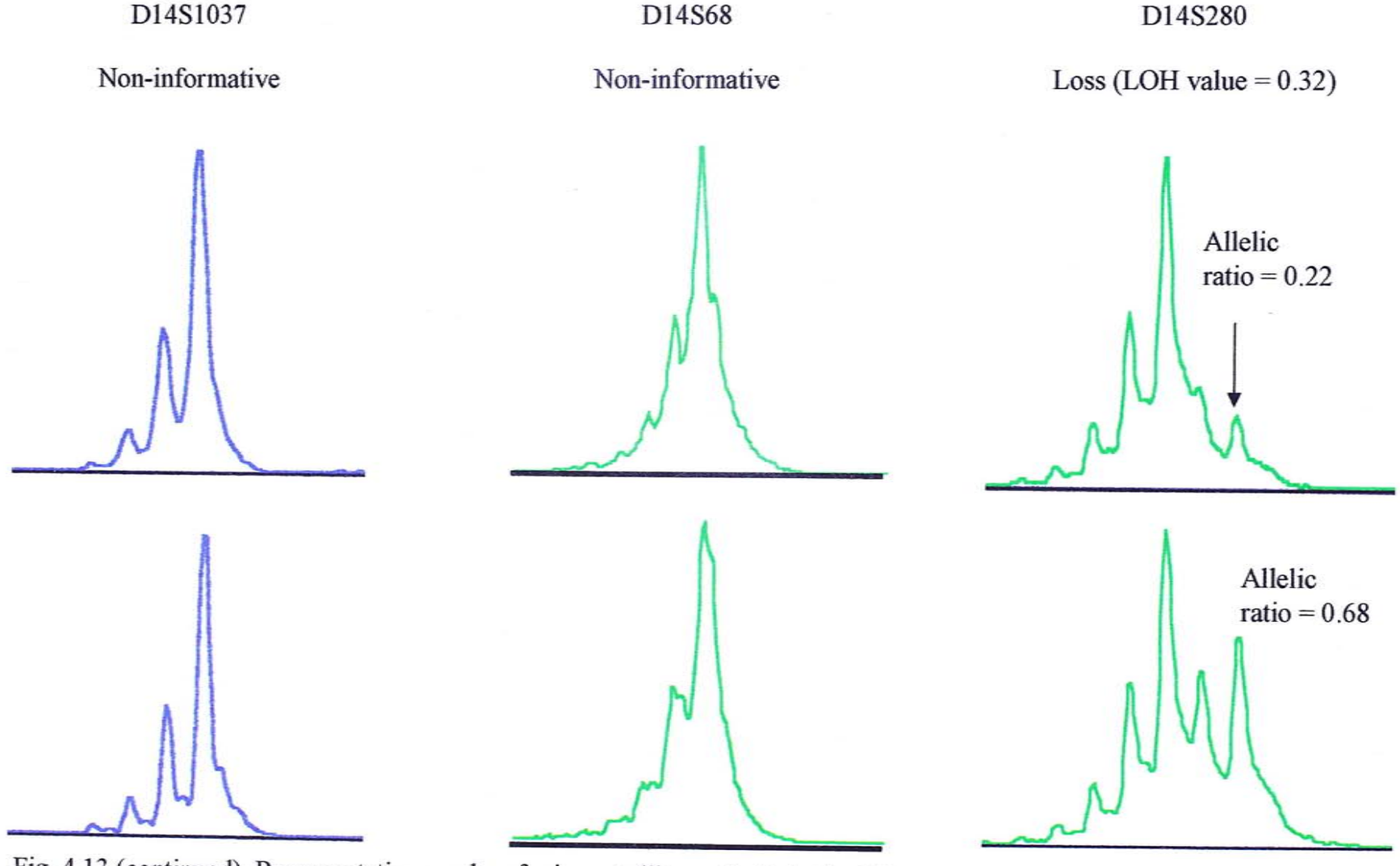

Fig. 4.13 (continued). Representative results of microsatellite analysis in the diffuse astrocytoma case WN66.

Upper panel, tumor, lower panel, matched blood; arrows indicate LOH.

The remaining two diffuse astrocytoma cases showed interstitial LOH pattern. In WN12 (Figure 4.14), LOH was found in D14S588, the marker next to D14S77 in this study, and in D14S1037. In NJ125 (Figure 4.15), LOH was detected only in D14S61 (confirmed by triplicate trials). The flanking markers of all three single locus with LOH (D14S588 in WN12; D14S61 in NJ125; D14S1037 in WN12) showed ROH.

In the AA case NJ5, all informative alleles centromeric from and including D14S61 showed LOH, while the 4 most distal loci (D14S1000, D14S1037, D14S68 and D14S280) showed ROH. The marker D14S59, telomeric from D14S61 and centromeric from D14S1000, was non-informative. The AA case WC114 also showed LOH at the centromeric end and had retention of both alleles at the 5 most distal loci, including D14S59. D14S61 and D14S43, the markers centromeric from and next to D14S59 in this study, were non-informative.

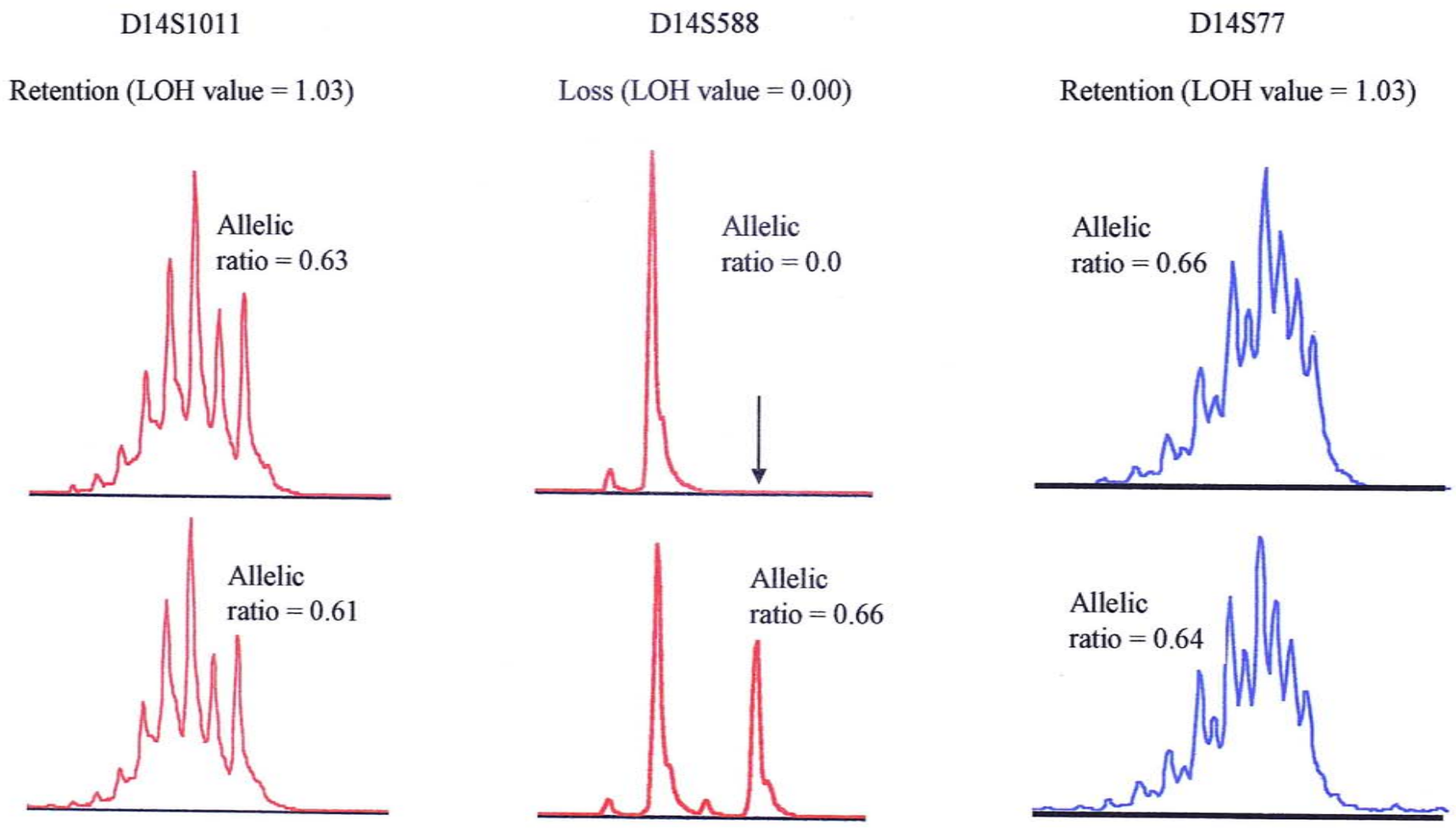

Fig. 4.14. Representative results of microsatellite analysis in the diffuse astrocytoma case WN12.

Upper panel, tumor; lower panel, matched blood; arrows indicate LOH (continued on page 140)

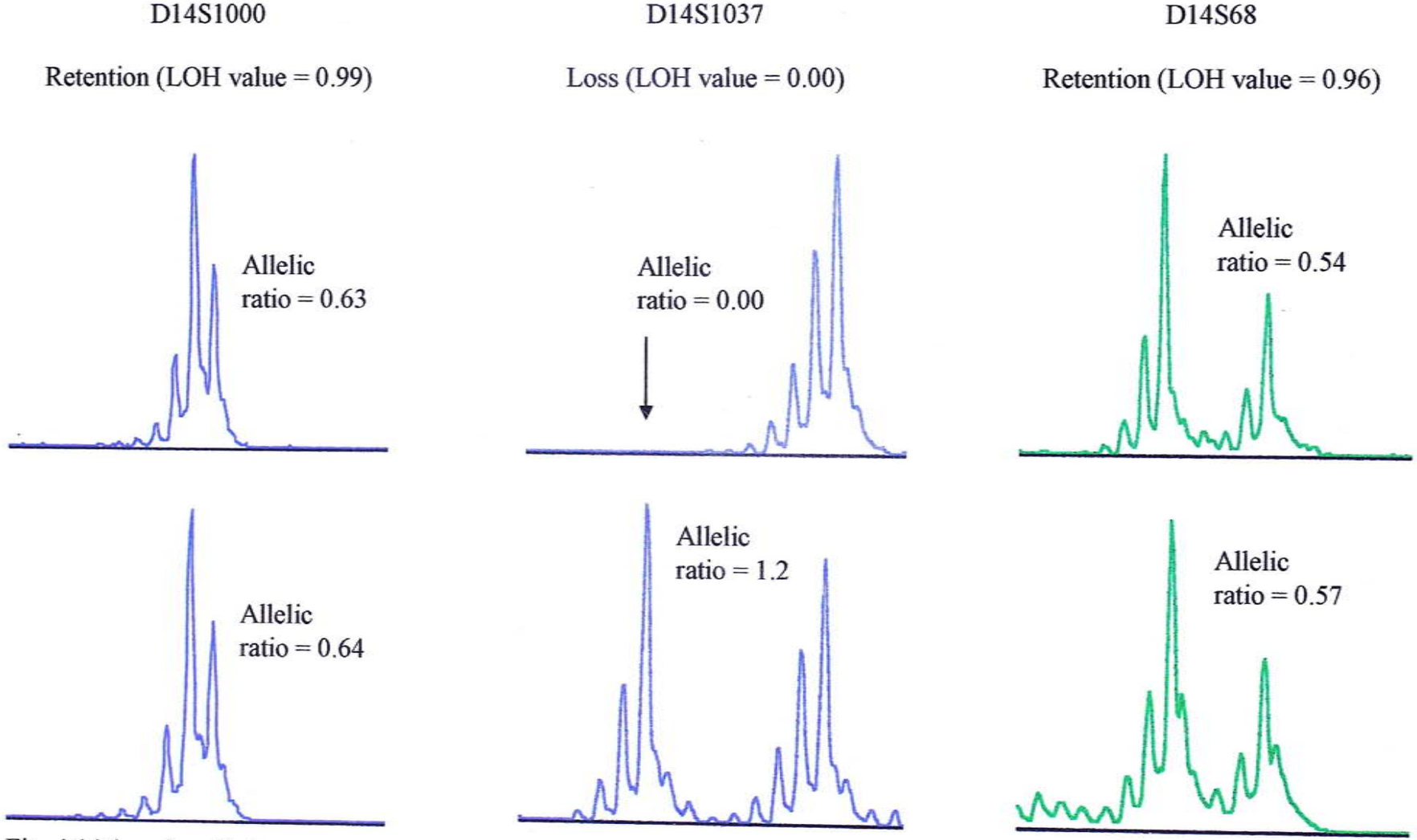

Fig. 4.14 (continued). Representative results of microsatellite analysis in the diffuse astrocytoma case WN12.

Upper panel, tumor; lower panel, matched blood; arrows indicate LOH.

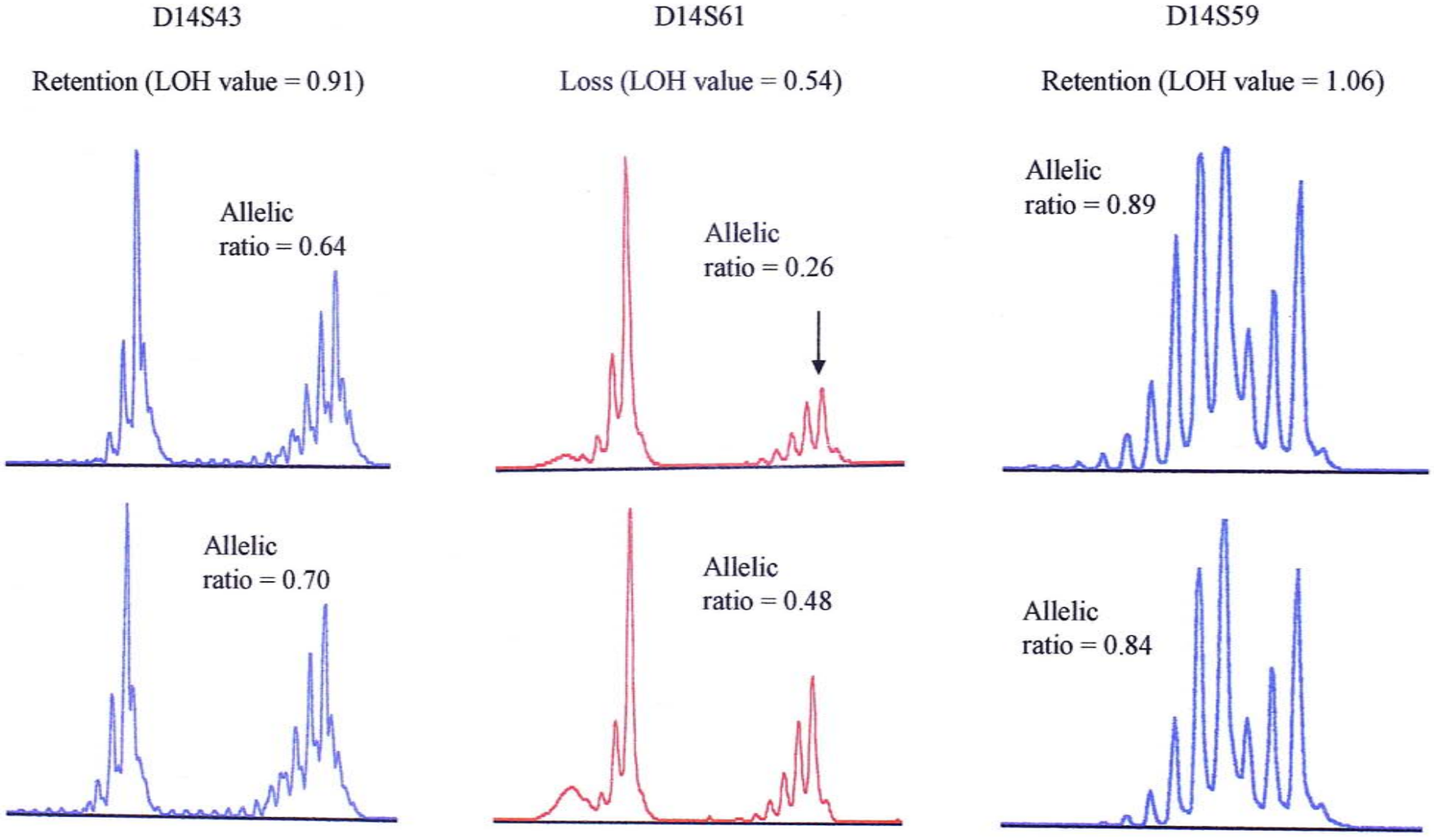

Fig. 4.15. Representative results of microsatellite analysis in the diffuse astrocytoma case NJ125.

Upper panel, tumor; lower panel, matched blood; arrows indicate LOH.

All 3 GBM cases, including the GS variant, showed interstitial LOH. WC121 harbored LOH in the centromeric region of the long arm of chromosome 14, starting from D14S997, and in the telemetric region starting from D14S1037. Within the central ROH region of WC121, LOH was also detected in a single locus, D14S588. Single loss in this locus was seen also in the diffuse astrocytoma case WN12. D14S1000, the marker next to D14S1037, formed the LOH boundary in both WC121 and WN12. Similarly, the marker D14S1026 next to D14S997 in WC121 acted as a flanking marker in both WC121 and NJ111. D14S997 was the only locus showed LOH in NJ111, confirmed by triplicate trials (Figure 4.16). The other flanking marker of LOH locus in NJ111 was D14S592.

Because of limited amount of available DNA in the GS case WC111, not all loci were investigated for LOH between D14S288 and D14S280. LOH was detected in D14S1026, with flanking ROH markers being D14S1057 and D14S1011. The LOH region in WC111 contained the LOH locus D14S997 in NJ111.

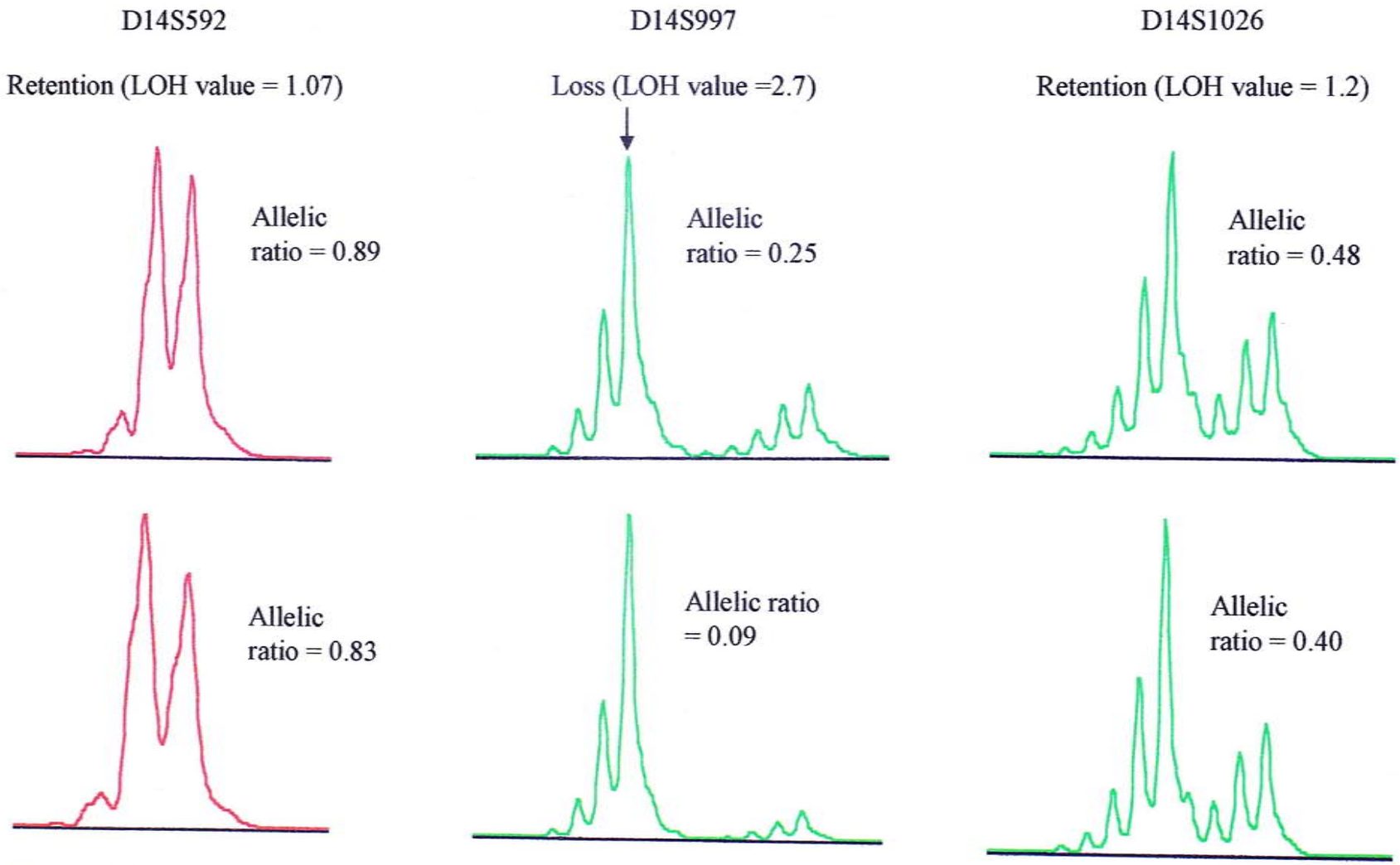

Fig. 4.16. Representative results of microsatellite analysis in the GBM case NJ111.

Upper panel, tumor; lower panel, matched blood; arrows indicate LOH.

Based on the LOH pattern in tumors with interstitial LOH loci or with LOH region in partial arm of chromosomal 14q, four CRDs could be defined (Figure 4.17). CRD 1 was mapped between D14S592 and D14S1026. In NJ111, ROH was detected in consecutive loci centromeric from D14S997 starting from D14S592 and in consecutive loci telomeric from D14S997 starting from D14S1026. ROH in D14S1026 and the more telomeric marker D14S1011 was also detected in WC121. D14S997 gave the highest percentage of LOH (21.7 %) among all markers except D14S1068, for which informative rate was only 38 % (Figure 4.18).

CRD2 was defined between D14S1011 and D14S77. The marker D14S588 showed LOH singly in WN12 and WC121, with ROH in at least two consecutive loci in each flanking boundary, starting centromeric from D14S1011 or telemetric form D14S77. Frequency of LOH in D14S588 (19.2 %) was just a bit lower then that in D14S997.

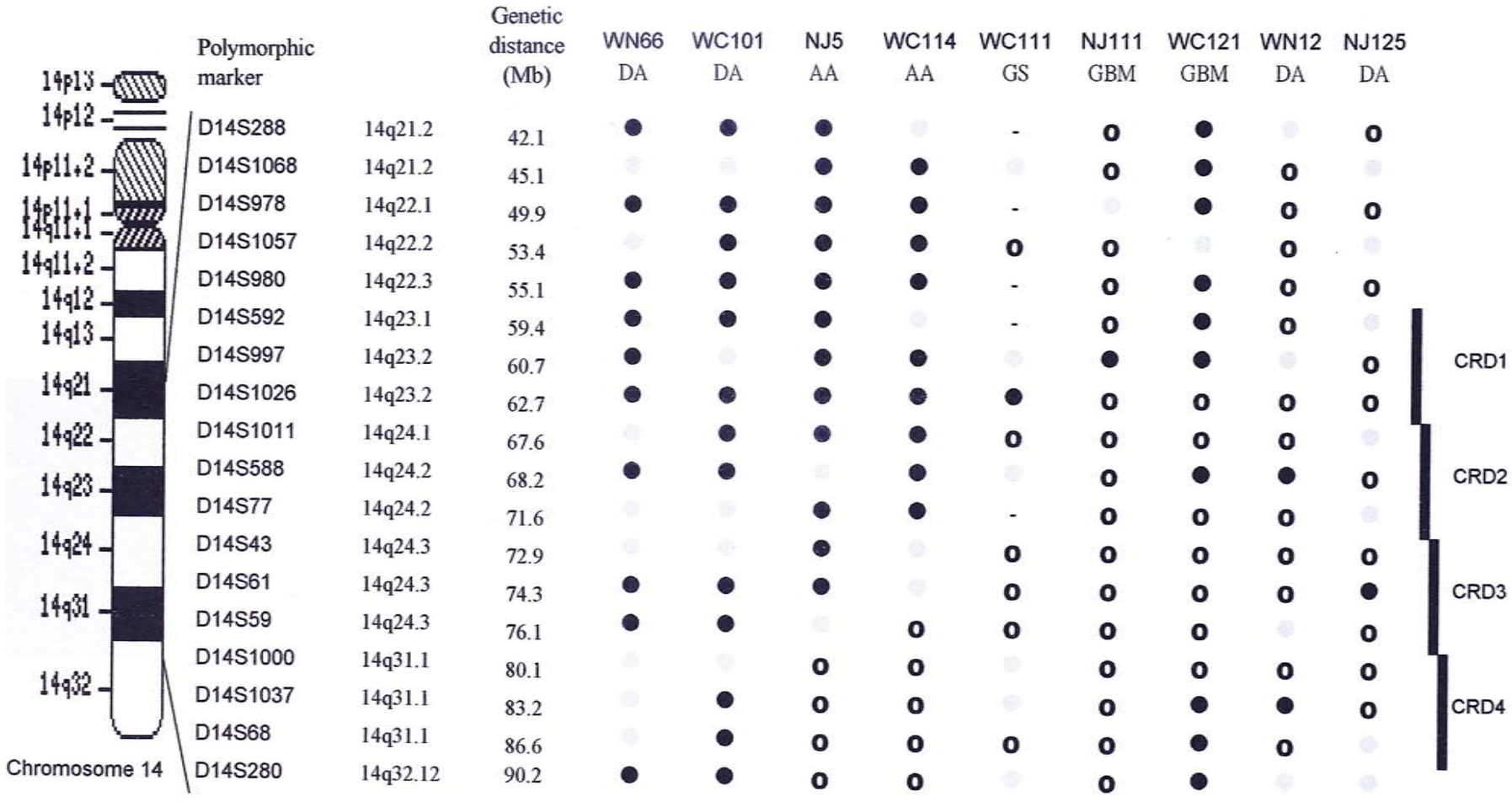

Fig 4.17 Delineation of four common regions of deletions on chromosome arm 14q in astrocytic tumors.

O, retention of heterozygosity; ●, loss of heterozygosity; ●, non-informative; -, not done. CRD, common region of deletions.

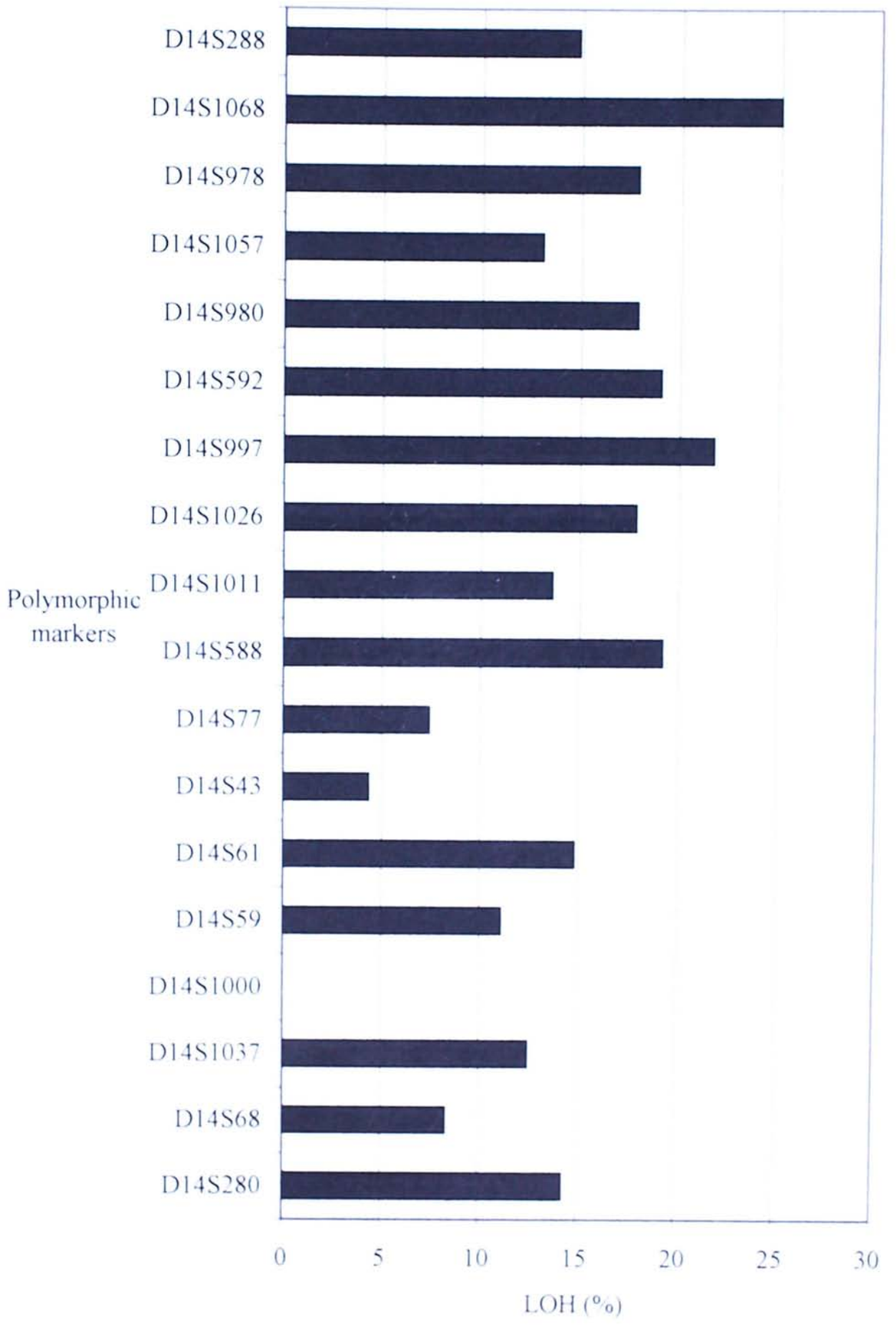

Fig 4.18 LOH frequency of individual polymorphic marker

CRD3 was defined by markers D14S43 and D14S59. The marker between the two flanking boundary showed LOH singly in D14S61 of NJ125. ROH in markers telomeric from D14S61 was also noted in the two AA cases showing partial deletion of the 14q in all informative markers centromeric from D14S59.

CRD4 was defined by LOH at D14S1037 and ROH at D14S1000 in WN12 and WC121, and ROH at D14S68 in WN12. D14S280 as flanking locus is further supported by a previous GBM case (case 3) in Hu *et al.*, 2002.

5. Discussions

5.1. BRAF mutations as common events in human cancers

BRAF mutations in human cancers were discovered only recently. Except in gliomas, *BRAF* mutations in all other cell lines being examined in Davies *et al.*'s study were confirmed in tumor specimen of the same type in the same or in later studies. Dysplastic tissues and cancers with high *BRAF* mutation frequencies (Table 1.3) included melanocytic nevi and melanoma (more than 60%; Brose *et al.*, 2002; Davies *et al.*, 2002; Pollock *et al.*, 2003), papillary thyroid cancer (46%; Cohen *et al.*, 2003; Soares *et al.*, 2003; Kimura *et al.*, 2003), cholangiocarcinoma (21.7%; Tannapfel *et al.*, 2003), hyperplastic polpy (33.3%; Yuen *et al.*, 2002) and colorectal carcinoma (12.1%; Davies *et al.*, 2002). Less frequent (below 5%) mutations were also found in non-papillary thyroid cancer (Cohen *et al.*, 2003; Kimura *et al.*, 2003; Soares *et al.*, 2003), colorectal adenoma (Yuen *et al.*, 2002), ovarian cancer (Davies *et al.*, 2002; Gemignani *et al.*, 2003), head and neck squamous cell carcinoma (Cohen *et al.*, 2003; Davies *et al.*, 2002), lung cancer (Brose *et al.*, 2002; Cohen *et al.*, 2003; Naoki *et al.*, 2002) and sarcoma (Davies *et al.*, 2002).

5.2. BRAF mutations in CNS tumor specimens

Although 10.5% glioma cell lines were found to harbor *BRAF* mutation, no mutation was detected among 15 glioma specimens. Compared with specimens of other tumor types, the number of glioma cases examined was relatively low. Therefore, frequency of *BRAF* mutation resulted from these glioma samples might not be representative (Davies *et al.*, 2002).

Glioma comprises of 3 major types of tumors. Histologically, they are classified into astrocytic tumors, oligodendroglial tumors and ependymal tumors. Each of these tumor groups contains several histological variants. It would be more useful to analyze the frequency of *BRAF* mutation in separate glioma types. Considering the presence of *BRAF* mutation in a wide variety of cancers, it is attractive to expand the glioma series to include a larger number and variety of CNS tumor samples.

To investigate the pattern of *BRAF* mutation status in CNS tumors, 195 CNS tumor samples and 10 cell lines were recruited in the current study. Astrocytic tumors represent approximately 25% of all primary intracranial neoplasms. However, they constituted half of the samples examined in this study, including GBM in half of them. Astrocytic tumors were the focus of the current study because treatment of GBMs is difficult and patient survivals rarely go beyond two years. Therefore, any

role of *BRAF* alterations in tumorigenesis of astrocytic tumors might provide additional therapeutic targets.

In Davies *et al.*'s study (2002), a total of 545 tumor cell lines, comprising of 18 human cancer types, were included for *BRAF* mutation screening. Interestingly, all mutations found, including those in glioma cell lines, were located within exon 15 and exon 11, with a single mutation, the T1796A substitution in exon 15 constituting 80% of total mutations. Hence, mutations of *BRAF* in exons 11 and 15 were regarded as the regions with highest mutation frequencies in human tumors. In this study, I used the direct sequencing approach to screen for *BRAF* mutations on exons 11 and 15 in CNS tumors.

My results showed *BRAF* mutations in 1 of 53 GBM cases and 2 (GBM2603 and GBM6840) of 6 GBM cell lines. Mutations in all three cases were heterozygous T1796A base substitution. Pattern of heterozygous mutations were commonly observed in other studies. For example, 30 of 32 colorectal tumors harboring *BRAF* mutations were heterozygous (Rajagopalan *et al.*, 2002). Of note were the imbalance peak heights of wild-type and mutant alleles in the two GBM cell lines. Karyotypes of both cell lines showed more than one copy of chromosome 7. Combining karyotyping and sequencing results, the number of mutant alleles was higher than that

of normal alleles. Increase in mutant copies of *BRAF* in our cell lines suggested that gain in mutant copies may provide growth advantage to tumorigenesis.

An increase in copy number of the *BRAF* gene had not been proposed in other tumors. However, increased copy of chromosome 7 is common in melanoma. Application of FISH to 7 primary malignant melanomas revealed trisomy in all 7 cases in D'Alessandro *et al.*'s study (1997). Another FISH study revealed gain of chromosome 7 in 40.9% of malignant melanomas cases which included 14 primary and 8 metastatic ones (Matsuta *et al.*, 1997). More recently, the number of chromosome 7 copies was determined in short-term primary cell cultures of nevi, primary melanomas, and metastases. The highest fraction of cell nuclei with more than 2 copies of chromosome 7 was detected in the group of metastases (Udart *et al.*, 2001). Gain of chromosome 7 was also suggested to be a significant aberration in the tumorigenesis of colonic carcinomas in which no endoreduplication has occurred (Herbergs *et al.*, 1996). Nevertheless, B-Raf expression had not been reported in these tumors. We do not know whether they also harbor increased mutant copies of the *BRAF* gene.

Mutation in astrocytic tumors is less frequent than in tumors like melanoma, papillary thyroid cancer, cholangiocarcinoma and colorectal cancer. This suggests the relation of mutation in the *BRAF* gene to tumorigenesis in a minor astrocytic tumor subset. It is hard to tell whether mutation was exclusive in the most malignant end-point due to the scarcity of mutations in the astrocytic tumor type and the inclusion of fewer lower-grade astrocytic tumor samples.

BRAF mutation was not detected in all other CNS tumors, including 31 oliogodendroglial tumors, 23 ependymal tumors, 21 MBs, 25 meningeal tumors, 3 cell lines from MB and 1 cell line from PNET. Thus, mutation in the *BRAF* gene is not a major genetic abnormality in non-astrocytic CNS tumors.

5.2.1. Tumorigenic effect of the V599E substitution

The V599 amino acid residue at B-Raf is conserved among the three Raf proteins (Figure 1.4). Two functional assays of B-Raf mutants were reported in Davies *et al.*'s study. Firstly, Myc-epitope-tagged expressions of cDNAs containing different mutations were transiently expressed in COS cells, immunoprecipitated using the Myc-tag and examined in kinase cascade assay. Compared with cells harboring wild-type *BRAF*, $BRAF^{V599E}$ mutant cells had elevated basal kinase activity of 10.7 folds.

Similar to cells with wild-type *BRAF*, $BRAF^{V599E}$ mutant cells were also able to activate endogenous Erk (Davies *et al.*, 2002).

Secondly, epitope-tagged cDNA constructs of *BRAF* mutants was transfected into NIH3T3 cells to assay their focus-forming ability. $BRAF^{V599E}$ was then found to be 70 – 138 times more efficiently than wild-type *BRAF* in transforming activity. Treatment of V599E mutant tumor cell lines with the Mek1/2 inhibitor, which inhibited DNA synthesis, resulted in at least 80% blockage of Erk1/2 phosphorylation (Davies *et al.*, 2002). In another study, knock down of $BRAF^{V599E}$ expression completely abrogated transformation as assessed by colony formation in agar (Hingorani *et al.*, 2003). Therefore, activating signals from B-Raf, at least in part, acts through the classical Raf/Mek/Erk cascade to promote proliferation.

A role in tumor initiation by *BRAF* mutant had been proposed in melanoma studies. *BRAF* mutation was a frequent event in atypical and malignant melanocytic lesions of the skin (Uribe *et al.*, 2003). Detection of high *BRAF* mutation frequency in benign lesions suggested the inadequacy of B-Raf in tumor initiation. Either abnormalities in addition to *BRAF* mutation were required for tumor initiation or the *BRAF* mutation was related to other tumorigenic events. Later, the detection of *BRAF* mutation in only 10% of the earliest stage or rapid-growth-phase melanoma by

Dong *et al.* (2003) further supported a role of B-Raf mutant in tumor progression rather than initiation.

5.2.2. V599E B-Raf mutant activation independent of Ras activation

Both Ras and B-Raf are members of the Ras/Raf/Mek/Erk signaling pathway. Mutation of either gene may produce similar effects. In Davies *et al.*'s study, Ras-neutralizing monoclonal antibody did not block cell proliferation of $BRAF^{V599E}$ mutant cell lines. This indicates the uncoupling of $BRAF^{V599E}$ mutants from their proliferation requirement of Ras.

Mutation pattern of the *RAS* and *BRAF* genes in the same tumor samples had been studied in many tumors, but no simultaneous mutations of the *RAS* genes and V599E mutation in *BRAF* in tumors have been detected so far. Mutually exclusive mutation patterns of *RAS* mutations and *BRAF* mutation of T1796A in the same tumors were present in colorectal cancers (Rajagopalan *et al.*, 2002; Yuen *et al.*, 2002), melanoma (Pollock *et al.*, 2003), non-small cell lung carcinoma (Brose *et al.*, 2002), micropapillary ovarian serous carcinomas and serous borderline tumors (Singer *et al.*, 2003) and papillary thyroid carcinoma (Kimura *et al.*, 2003; Soares *et al.*, 2003).

In astrocytic tumors, mutation of the *RAS* gene is rare (Bos 1989; Bredel and Pollack, 1999; Gomori *et al.*, 1999; Guha 1997). Evaluation of mutation status of

both the *RAS* and *BRAF* genes may not yield significant results. In considering mutually exclusive mutation pattern in the tumors mentioned above, $BRAF^{V599E}$ mutant in astrocytic tumors is likely to be capable of activating downstream members independent of Ras stimulation and plays a role in tumorigenesis.

5.2.3. Autocrine stimulation of Ras signaling in V599E B-Raf mutant

Despite the higher kinase activity of V599E B-Raf mutant compared with wild-type B-Raf being activated by H-Ras^{G12V}, V599E B-Raf mutant possesses 50-fold lower transforming activity in NIH3T3 cells than H-Ras^{G12V} (Davies *et al.*, 2002). This may reflect Ras signalling to a number of effector molecules. Three cell lines derived from human choroidal melanoma with $BRAF^{V599E}$ which showed 10-fold increase in endogeneous B-Raf activity activated Mek/Erk pathway constitutively and independent of Ras. However, inhibition of endogenous Ras significantly decreases cell proliferation rate, without affecting Mek/Erk activity (Calipel *et al.*, 2003). Accordingly, cell proliferation resulted from *BRAF* mutation was only partially elevated, which could be further enhanced by parallel signaling pathway from Ras activation.

In melanoma, cell surface signaling by growth factor receptors through autocrine mechanisms is well established. Aggressive melanoma cells express both FGF and FGF receptor, forming an autocrine loop (Rodeck *et al.*, 1991). Inhibition of this loop inhibited Erk1/2 phosphorylation (Kinkl *et al.*, 2001). Melanoma cells also express c-Met and secrete its ligand HGF. HGF also induces Erk1/2 phosphorylation through activation of its receptor, which can be inhibited by neutralizing antibody against HGF (Li *et al.*, 2001).

Activating mutations in the kinase domain of B-Raf were detected in the majority of the melanoma cell lines with constitutively activated Ras without underlying mutations. Dramatic inhibition of Erk1/2 activation was observed when effects of FGF or HGF were neutralized. From these results, Satyamoorthy *et al.* (2003) proposed that melanoma growth, invasion, and metastasis are attributable to constitutively activated Erk apparently mediated by B-Raf kinase activation and also excessive growth factors through autocrine mechanisms.

Autocrine or paracrine loops are also present in astrocytic tumors. The heparin binding epidermal growth factor-like growth factor (HB-EGF) is abundantly expressed in GBMs and is co-expressed with EGFR in 52% of GBMs. Anti-HB-EGF blocking antibodies reduced glioma cell growth by 30 – 40%. HB-EGF stimulation

efficiently induced glioma cell proliferation *in vitro*. Also, HB-EGF, FGF, or TGF stimulation rapidly induced HB-EGF expression (Mishima *et al.*, 1998).

TGF expression was found in 88% of GBMs (Maruno *et al.*, 1991). Increased tumor growth *in vivo* caused by autocrine TGF stimulation was later shown to be mediated via EGFR activation, which was accessible to an EGFR specific tyrosine kinase inhibitor (El-Obeid *et al.*, 2002). Hence, in the cases where EGFR expression is normal, overexpression of wild-type B-Raf could also be stimulated by autocrine signaling to induce proliferation.

5.3. BRAF expression in astrocytic tumors

Other than activating mutation, abnormal expression of an oncogene might also provide advantages to tumorigenesis. The possibility of such an effect of *BRAF* was supported by the observation of an increased number of mutant copies of *BRAF* in the cell lines GBM2603 and GBM6840.

According to Dugan *et al.*, B-Raf expression was absent in normal astrocytes. Indeed, B-Raf protein was not detected in astrocytes of specimens examined in this study. However, the same paper showed negative B-Raf immunoreactivity in human glioma U373 and rat glioma C6. Detection of *BRAF* mutation in the astrocytic tumor series brought up the necessity of clarifying B-Raf expression pattern in tumor specimens. My results not only showed positive B-Raf immunoreactivity in the $BRAF^{V599E}$ mutant, but also revealed positive results in astrocytic tumors harboring wild-type B-Raf. Expression of the *BRAF* gene was detected in all grades of astrocytic tumors. The number of aberrant B-Raf expressing tumor cases did not increase with astrocytic tumor grade.

Higher expression of B-Raf in astrocytic tumors than in normal astrocytes pointed to possible functional changes in favor of tumorigenesis. In neurons, activation of Erk by cAMP analogues in a Rap1/B-Raf-dependent manner rescued neurons from death (Dugan *et al.*, 1999; Vossler *et al.*, 1997). On the contrary, cAMP decreased

Erk activity in normal astrocytes lacking the B-Raf protein. However, ectopic expression of B-Raf in rat astrocytoma cells increased Erk activation and enhanced proliferation in the presence of serum (Dugan *et al.*, 1999). Accordingly, abnormal expression of B-Raf in astrocytes may restrain negative regulation of survival and proliferation, leading to tumorigenesis.

In melanocytes, B-Raf also mediates activation of Mek1 by cAMP. However, it is Ras but not Rap1 which mediates the cAMP-dependent activation of Erk. The effect is also independent on Sos1 and suggests the existence of a melanocyte-specific Ras exchange factor directly regulated by cAMP (Busca *et al.*, 2000). Currently, it is not known whether a similar Ras exchange factor exist in astrocytes.

B-Raf expression may play a tumorigenic role similar to *BRAF* mutation. Although wild-type B-Raf is dependent of Ras activation, an autocrine system could activate various effectors from Ras, including B-Raf. Furthermore, the effect of B-Raf expression may not only as an additive to C-Raf activation. B-Raf and C-Raf can act co-operatively to produce synergistic effects in response to growth signals. Upon Ras activation, the COOH-terminus of C-Raf was exposed from 14-3-3 binding sites and constitutively associated with B-Raf (Weber *et al.*, 2001).

5.4. *Mutually exclusive pattern between EGFR amplification and BRAF expression*

As discussed in Section 5.2.2, Ras mutation is rare among astrocytic tumors. However, *EGFR* amplification in primary GBM could reach 50% (Figure 1.1) and the Ras protein has been considered as the downstream effector of EGFR, which relays signals to the MAPK cascade. Considering the mutually exclusive pattern of Ras and B-Raf in other tumor, it is interesting to investigate the correlation between *EGFR* amplification and *BRAF* mutation and the correlation between *EGFR* amplification and B-Raf immunoreactivity in astrocytic tumors.

The investigation began with the determination of *EGFR* amplification in the astrocytic tumor samples involved in *BRAF* mutation screening. In the current series, *EGFR* gain was detected in 1 of 14 AAs (7.1%) and 2 of 24 GBMs (8.3%), whereas *EGFR* amplification was found in 1 of 14 AAs (7.1%) and 6 of 24 GBMs (25%). Frequency of *EGFR* amplification in the current study was found to be lower than in literature.

In a previous study in our group, only a small proportion (17%, $n = 29$) of primary GBM exhibited *EGFR* amplification while a high proportion (62%) showed either *TP53* mutations or allelic loss of 17p13.1 (Cheng *et al.*, 1999). In this study,

frequencies of *EGFR* and *TP53*abnormalities did not conform to the currently accepted models of GBM development which sub-classified GBM into primary and secondary ones. In Das *et al.*'s study (2002), 7 of the 39 primary GBM samples (18%) available for DNA sequencing (7/39) had *TP53* mutations, including three mutations previously undocumented in GBM. Therefore, frequencies of *EGFR* amplification in primary GBM of Asian population may be lower than that in Western countries. Tumor progress of primary GBM in Asians may be more dependent on *TP53* mutations and other alterations other than *EGFR* amplifications.

To increase sample size of tumors harboring *EGFR* amplification, 6 samples from another study were recruited in B-Raf immunohistochemistry and included in statistical correlations. As a result, three subtypes of astrocytic tumors were defined. They are tumors with *EGFR* amplification but negative B-Raf immunoreactivity, tumors with positive B-Raf immunoreactivity but no *EGFR* amplification and tumors harboring alterations in neither. Not considering the 6 addition samples which were included due to the presence of known *EGFR* amplification, the tumor group with *EGFR* amplification but negative B-Raf immunoreactivity constituted 25.0% (6/24) of the current series of astrocytic tumors. The second group, comprising of tumors with positive B-Raf immunoreactivity but no *EGFR* amplification, constituted 29.2%

(7/24) of the series. The remaining tumors harbor alterations in neither and comprised 45.8% (11/24).

5.4.1. Similar effect of EGFR activation and B-Raf activation

Both EGFR activation and B-Raf activation are related to vascular proliferation and dysregulation of apoptosis. On one hand, EGF activation of EGFR expressed on glioma cells resulted in enhanced secretion of VEGF by glioma cells (Goldman *et al.*, 1993). Both C-Raf activation and subsequent Mek1-dependent protection from extrinsic-mediated apoptosis are activated by VEGF, which are pivotal for endothelial cell survival during angiogenesis (Alavi *et al.*, 2003). A role of *EGFR* amplification in dysregulation of apoptosis was given by monoclonal anti-EGFR antibody which promoted apoptosis while decreasing proliferation and VEGF expression. On the other hand, B-Raf was demonstrated as a critical signalling factor in the formation of the vascular system during development. *BRAF* knock-out mice possessed increased number of endothelial precursor cells, dramatically enlarged blood vessels and apoptotic death of differentiated endothelial cells (Wojnowski *et al.*, 1997). Indispensable of B-Raf in survival was demonstrated in explanted embryonic motor neurons and sensory neurons using knock-out mice (Wiese *et al.*, 2001).

Overexpression of B-Raf confered resistance to apoptosis induced by growth factor withdrawal or PI3K inhibition (Erhardt *et al.*, 1999). Suppression of $BRAF^{V599E}$ in human melanoma by siRNA caused growth arrest and promoted apoptosis.

Possibly, blockage of apoptosis by B-Raf was through the Raf/Mek/Erk pathway because phosphorylation of caspase-9 by Erk was sufficient to block caspase-9 processing and subsequent caspase-3 activation (Allan *et al.*, 2003). This was also supported by a previous study in which the addition of cytochrome C to cytosols of cells overexpressing B-Raf failed to induce caspase activation (Erhardt *et al.*, 1999). Therefore, B-Raf plays a role in dysregulation of apoptosis and a partial role in proliferation similar to *EGFR* amplification.

5.4.2. Mutual effects between Ras/Raf/Mek/Erk and Akt signaling

Activation of both the Raf/Mek/Erk and the Akt pathways are considered tumorigenic. Erk phosphorylates and activates several targets in growth control (Mandell *et al.*, 1998). It may contribute to tumorigenesis by inhibition of apoptosis (Allan *et al.*, 2003). It is highly activated in both low-grade and malignant gliomas (Besson and Yong, 2001; Shapiro, 2002). On the other hand, GBM cells expressing mutant PTEN contain high endogenous Akt activity and high levels of PtdIns-3,4,5-

P_3 and PtdIns-3,4-P_2. Deletion and/or mutation of *PTEN* are common in primary GBM (Section 1.2.3). Mutation of *PTEN*, which leads to high Akt activity, induces cell proliferation (Staal *et al.*, 2002). Akt also inhibits apoptosis by leading to proteolysis of cyclin D and restraining $p21^{WAF1}$ in the cytoplasm. LOH around *PTEN* is closely associated with a reduced overall survival of GBM patients (Fan *et al.*, 2002).

Spontaneously activation of EGFR resulted in constitutive phosphorylation of Erk but not members of the Akt pathway in the astrocytic tumor cell line SKMG3 (Thomas *et al.*, 2003). Nevertheless, the Raf/Mek/Erk and Akt pathways can be co-operative. Inhibition of PI3K signaling with pharmacologic inhibitor or by the reconstitution of physiological levels of PTEN to dephosphorylate the lipid products of PI3K negated the growth advantage imparted by EGFRvIII (Klingler-Hoffmann *et al.*, 2003). In human GBM cells, both introduction of wild-type PTEN and inhibition of EGFR decreased VEGF mRNA levels (Pore *et al.*, 2003).

Unexpectedly, phosphorylation of C-Raf by Akt inhibited the Raf/Mek/Erk pathway in breast cancer cell line (Zimmermann and Moelling, 1999). Expression of Akt inhibited EGFR-induced B-Raf activity and inhibition of Akt up-regulated B-Raf in HEK293 cells (Guan *et al.*, 2000). Although the contradictory role of Akt could not be explained presently, cross-talk between the Akt and the Ras/Raf/Mek/Erk

pathways at B-Raf suggested important role of *BRAF* alterations in tumorigenesis. Activation of the B-Raf protein by mutation and/or increased expression of B-Raf could disrupt the modulation of cell proliferation and the regulation of apoptosis.

5.5. Microsatellite analysis of chromosome 14q in human cancers

LOH of chromosome 14q is common in a wide variety of tumors. These include lung adenocarcinoma, ovarian carcinoma, malignant mesothelioma, gastrointestinal stromal tumors, renal cell carcinoma, astrocytic tumors, neuroblastoma, meningiomas, nasopharyngeal carcinoma, colorectal carcinoma and head and neck squamous cell carcinoma (Figure 5.1). Four CRDs have been identified suggesting the presence of multiple TSGs. These regions are mapped, from the centromere to the telomere of the q arm, to 14q11.2 – q13.1 (R1), 14q23.2 – q24.2 (R2), 14q31.3 – q32.12 (R3) and 14q32.2 (R4).

R1 contains two consecutive regions with high LOH frequency. On one hand, CRDs of lung adenocarcinoma, malignant mesothelioma and gastrointestinal stromal tumors overlap in 14q11.2, a region centromeric form D14S80. LOH at the marker D14S283 in gastrointestinal stromal tumors reached 71% (El-Rifai *et al.*, 2000). On the other, ovarian carcinoma and nasopharyngeal carcinoma possess CRDs overlapping in 14q12, telomeric from D14S80. LOH at the marker D14S70 in ovarian carcinoma attained 45% (Bandera *et al.*, 1997).

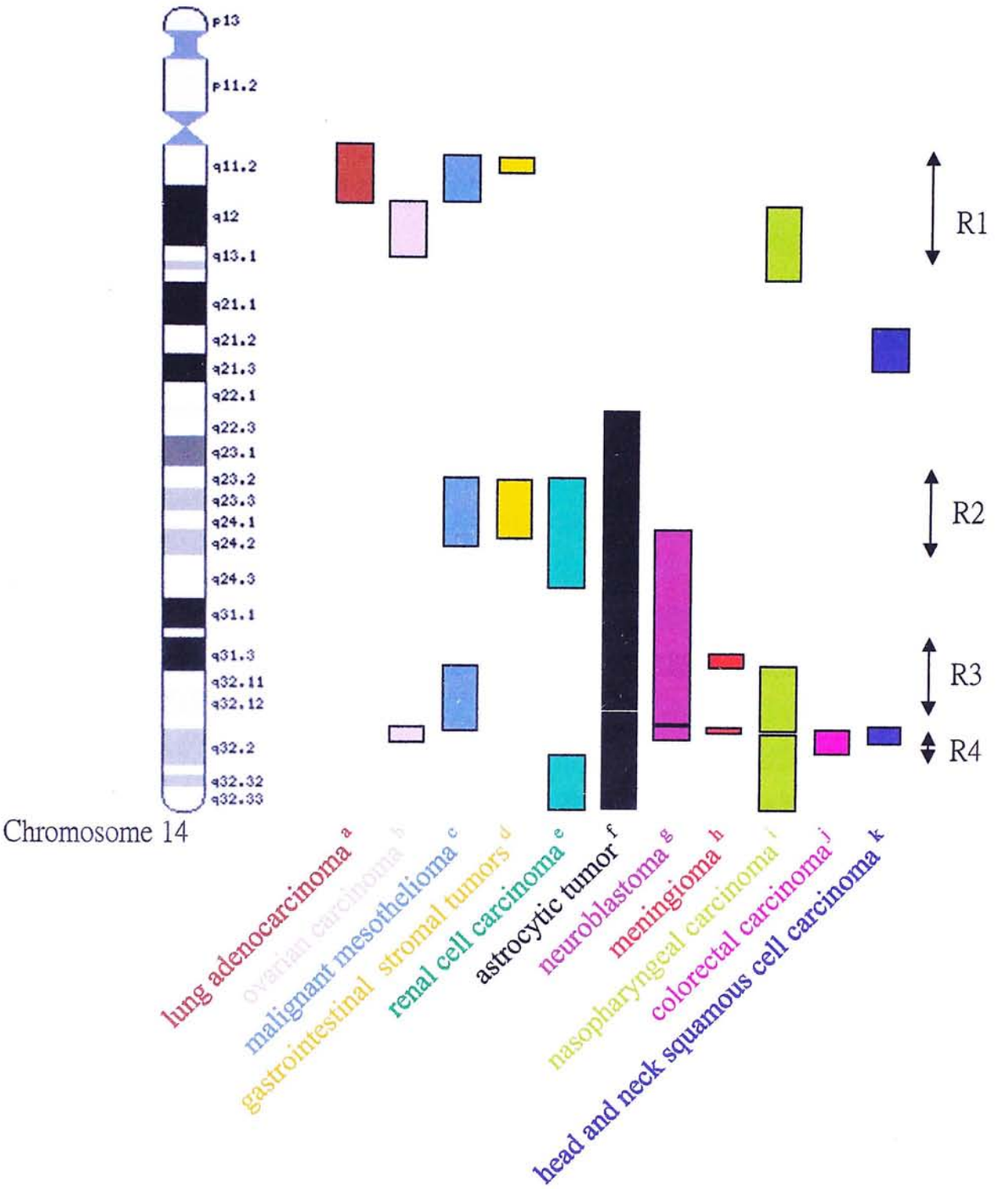

Figure 5.1. Chromosomal regions with high LOH frequency in human cancers.
Thick Bars, chromosomal regions with frequent LOH;
R, common region of deletions.
a, Abujiang *et al*., 1998; b, Bandera *et al*., 1997; c, Bjorkqvist *et al*., 1999 and de Rienzo *et al*., 2000; d, El-Rifai *et al*., 2000; e, Schwerdtle *et al*., 1997; f, Hu *et al*., 2001; g, Hoshi *et al*., 2000 and Thompson *et al*., 2001; h, Simon *et al*., 1995 and Tse *et al*., 1997; i, Cheng *et al*., 1997 and Mutirangura *et al*., 1998; j, Bando *et al*., 1999; k, Lee *et al*., 1997.

R2 locates on 14q24.1, which spans an interval of approximately 1.5 Mb. The tumors involved are malignant mesothelioma, gastrointestinal stromal tumors, renal cell carcinoma and astrocytic tumors. At D14S258, LOH was detected in 63% of gastrointestinal stromal tumors (El-Rifai *et al.*, 2000).

R3 is associated with malignant mesothelioma, astrocytic tumors, neuroblastoma, meningioma and nasopharyngeal carcinoma. While CRDs of astrocytic tumors and neuroblastoma span the whole region, meningioma showed LOH in markers centromeric from D14S68, malignant mesothelioma and nasopharyngeal carcinoma showed LOH in markers telomeric to D14S68. LOH was detected in 8 of 11 informative meningioma cases at D14S48 and in 7 of 7 informative cases at D14S81. CRDs of malignant mesothelioma, astrocytic tumors, neuroblastoma and nasopharyngeal carcinoma extended to R4.

R4 is the smallest among the four CRDs. Nevertheless, it contains CRDs of at least nine tumors. They include ovarian carcinoma, malignant mesothelioma, renal cell carcinoma, astrocytic tumors, neuroblastoma, meningioma, nasopharyngeal carcinoma, colorectal carcinoma and head and neck squamous cell carcinoma.

Other than the above four regions, a CRD in 14q12.2 – q21.3 is singly discovered in head and neck squamous cell carcinoma. Thus, as many as 7 separate regions on 14q are in potential of containing TSG.

5.6. Microsatellite analysis of chromosome 14q in astrocytic tumors

In literature, two CRDs have been defined in astrocytic tumors. The first CRD, 14q21.2 – q32.12, covers R2 and extends to R3 and the second region, 14q32.12 – qter, overlaps with R3 – R4. The more centromeric CRD in astrocytic tumor, 14q21.2 – q32.12 has undergone finer mapping in this study. This region overlaps with CRDs of renal oncocytoma (Schwerdtle *et al.*, 1997), gastrointestinal stromal tumors (El-Rifai *et al.*, 2000), malignant mesothelioma (Bjorkqvist *et al.*, 1999; de Rienzo *et al.*, 2000), neuroblastoma (Hoshi *et al.*, 2000; Thompson *et al.*, 2001), meningioma (Simon *et al.*, 1995; Tse *et al.*, 1997), and nasopharyngeal carcinoma (Cheng *et al.*, 1997; Mutirangura *et al.*, 1998). It spans approximately 48.1 Mb, as revealed by a high-resolution genome-wide allelotype and CGH analyses (Hu *et al.*, 2001 and 2002). The region is defined between D14S288 and D14S280, which is derived from breakpoints of interstitial deletions detected in 2 diffuse astrocytomas and 3 GBMs.

5.6.1. Finer mapping of common regions of deletion

Microsatellite analysis was performed using 18 polymorphic markers located between D14S288 and D14S280 on chromosome 14q. Allelic loss was defined at loci with LOH value smaller than 0.6 or greater than 1.67. Tomlinson *et al.* (2001)

advocated a critical allelic ratio of 0.5 for defining LOH. However, our samples were not microdissected. Endogenous endothelial cells were expected to be present among tumor cells. Also, in a number of studies, the critical allelic ratio for indication of LOH was defined to be 0.7 in non-microdissected sample. Therefore, a critical value of < 0.6 or >1.67 for LOH was considered appropriate in the present study.

LOH in at least one locus was detected in 4 of 12 diffuse astrocytomas (33%), 2 of 5 AAs (40%) and 3 of 13 GBMs (23%, including 1 of 2 GSs). These loci were considered to be the result of allelic loss rather than chromosomal gain, after consideration of CGH studies. Analysis of the 9 cases harboring LOH revealed interstitial deletion of chromosome 14q. Based on the overlapping deletion regions, four CRDs (Figure 5.2) were identified.

CRD1 spans a region of 3.3 Mb, flanked by D14S592 and D14S1026. CRD1 contained two markers with high LOH frequencies (21.7% LOH in D14S997; 19.0% LOH in D14S592). It overlaps with CRDs identified in malignant mesothelioma, gastrointestinal stromal tumors and renal cell carcinoma.

Polymorphic markers and putative tumor suppressor genes[a]	Starting genetic position (Mb)	Interstitual genetic distance (Mb) [b]
D14S592	59.39	2.44
PPP2R5E	61.83	0.64
D14S63	62.64	0.07
D14S1026	62.71	4.85
D14S1011	67.56	0.65
D14S588	68.21	1.34
D14S289	69.56	1.46
D14S277	71.02	0.54
D14S77	71.56	1.37
D14S43	72.93	0.54
MLH3	73.47	2.55
D14S59	76.06	0.59
D14S74	76.65	3.45
D14S1000	80.10	2.57
D14S55	82.67	0.41
D14S73	83.07	3.55
D14S68	86.62	

Figure 5.2. Four common regions of deletion (CRDs) in astrocytic tumors and CRDs in other tumors of the same chromosomal region.
a, Bold, putative tumor suppressor gene; Italic, polymorphic markers used in other studies but not the current study.
b, Interstitual genetic distance of marker or gene in the same and the next row.

CRD2 spans an interval of 4.0 Mb between D14S1011 and D14S77. It overlaps with CRDs identified in neuroblastoma and the three tumor types just mentioned above. CRD3 is the smallest region and spans approximately 3.2 Mb between D14S43 and D14S59. It overlaps with CRDs identified in renal cell carcinoma and neuroblastoma. CRD4 covers 6.5 Mb between D14S1000 and D14S68 and overlaps with CRDs identified in neuroblastoma and meningioma.

5.6.2. Genes within the common regions of deletion

To search for potential TSGs within the CRDs, all referenced sequence genes within the CRDs retrieved from Human Genome Reference Sequence (Build 34, http://www.genome.ucsc.edu/) were evaluated.

CRD1 contains 14 referenced genes (Table 5.1). All except one have been reported in PubMed (http://www.ncbi.nlm.nih.gov/). One of them with high possibility of being tumor suppressor was *protein phosphatase 2, regulatory subunit B (B56), epsilon isoform (PPP2R5E).*

CRD2 contains 20 referenced genes (Table 5.2). Eighteen of them have been reported in PubMed. However, none of the genes revealed their identity as tumor suppressors after evaluation from existing information.

Table 5.1. Reference Sequenced genes in CRD1 (between D14S592 and D14S1026).

Gene	Product	Known	Predicted
MNAT1	menage a trois 1 (CAK assembly factor)	✔	
SLC38A6	solute carrier family 38, member 6	✔	
PRKCH	protein kinase C, eta	✔	
HIF1A	hypoxia-inducible factor 1, alpha subunit (basic helix-loop-helix)	✔	
SNAPC1	small nuclear RNA activating complex, polypeptide 1, 43kDa	✔	
SYT14R	synaptotagmin XIV-related	✔	
KCNH5	potassium voltage-gated channel, subfamily H (eag-related), member 5	✔	
ARHJ	ras homolog gene family, member J	✔	
GPB5	glycoprotein beta 5	✔	
PPP2R5E	protein phosphatase 2, regulatory subunit B (B56), epsilon isoform	✔	
LOC112840	similar to RIKEN cDNA 2600001A11 gene		✔
SGPP1	sphingosine-1-phosphatase phosphatsae 1	✔	
SYNE2	spectrin repeat containing, nuclear envelope 2	✔	
ESR2	estrogen receptor 2 (ER beta)	✔	
	Total	*13*	*1*

Table 5.2. Reference Sequenced genes in CRD2 (between D14S1011 and D14S77).

Gene	Product	Known	Predicted
C14orf114	chromosome 14 open reading frame 114	✔	
ERH	enhancer of rudimentary homolog (Drosophila)	✔	
FLJ11274	hypothetical protein FLJ11274		✔
PLPL	myelin proteolipid protein-like protein		✔
KIAA0247	KIAA0247 gene product	✔	
SFRS5	splicing factor, arginine/serine-rich 5	✔	
SLC10A1	solute carrier family 10 (sodium/bile acid cotransporter familiy), member 1	✔	
SMOC1	SPARC related modular calcium binding 1	✔	
SLC8A3	solute carrier family 8 (sodium-calcium exchanger), member 3	✔	
C14orf112	chromosome 14 open reading frame 112	✔	
SYNJ2BP	synaptojanin 2 binding protein	✔	
ADAM21	a disintegrin and metalloproteinase domain 21	✔	
ADAM20	a disintegrin and metalloproteinase domain 20	✔	
MED6	mediator of RNA polymerase II transcription, subunit 6 homolog (yeast)	✔	
PCNX	pecanex homolog (Drosophila)	✔	
KIAA0440	signal-induced proliferation-associated 1-like 1	✔	
RGS6	regulator of G-protein signalling 6	✔	
DPF3	D4, zinc and double PHD fingers, family 3	✔	
WDR21	WD repeat domain 21	✔	
ZFYVE1	zinc finger, FYVE domain containing 1	✔	
	Total	*18*	*2*

Despite being the smallest CRD in the current study, CRD3 (Table 5.3) contains 64 referenced genes. Thirty-three of them have been reported in PubMed. Of note is the *MLH3* gene which has been suggested to be a tumor suppressor.

CRD4 contains three referenced genes (Table 5.4). Similar to CRD2, there is no information revealing their identity as tumor suppressors.

Based on existing information, *PPP2R5E* and *MLH3* harbor the potential of being tumor suppressors. Functions and evidences in support of being TSGs of the two genes were given below:

PPP2R5E

PPP2R5E encodes one of the protein subunits of protein phosphatase 2A (PP2A) which is a major serine/threonine phosphatase for reversible protein phosphorylation in all eukaryotic cells and thereby, implicated in a variety of cellular function. PP2A is related to the regulation of cellular metabolism, transcription, RNA splicing, translation, cell cycle progression, cell morphology and development. It is a structurally complex protein in which a single catalytic (C) subunit associates with a wide array of regulatory subunits termed variable subunits through a structural subunit A (Millward *et al.*, 1999; Schonthal, 2001). Protein product of *PPP2R5E* belongs to one of the families of the variable subunits.

Table 5.3. Reference Sequenced genes in CRD3 (between D14S43 and D14S59).

Gene	Product	Known	Predicted
NPC2	Niemann-Pick disease, type C2 precursor	✔	
HBLD1	HESB like domain containing 1		✔
BX248252	human full-length cDNA clone CS0DF015YC15 of fetal brain		✔
BC032893	hypothetical protein		✔
C14orf141	chromosome 14 open reading frame 141		✔
LTBP2	latent transforming growth factor-beta-binding protein-2	✔	
BC032944	similar to ubiquitin-ligase		✔
KIAA0317	KIAA0317 gene product		✔
BX248747	human full-length cDNA 5-prime end of clone CS0CAP004YO05		✔
C14orf111	chromosome 14 open reading frame 111	✔	
BC044636	similar to ZAP3 protein		✔
AK090435	FLJ00353 protein		✔
AK091050	hypothetical protein FLJ33731		✔
ZAP3	ZAP3 protein	✔	
BC007792	hypothetical protein		✔
AK094068	hypothetical protein FLJ36749		✔
BX248276	human full-length cDNA clone CS0DI006YM01 of placenta		✔
DLST	dihydrolipoamide S-succinyltransferase (E2 component of 2-oxo-glutarate complex)	✔	
BX248764	human full-length cDNA 5-prime end of clone CS0DB006YE12 of neuroblastoma		✔
BX248774	human full-length cDNA 5-prime end of clone CS0DJ009YL13 of T cells		✔
RPS6KL1	ribosomal protein S6 kinase-like 1	✔	
PGF	placental growth factor, vascular endothelial growth factor-related protein	✔	

(Continued on page 177)

Table 5.3 (Continued). Reference Sequenced genes in CRD3 (between D14S43 and D14S59).

Gene	Product	Known	Predicted
BT007182	hypothetical protein		✔
BX248289	hypothetical protein		✔
EIF2B2	eukaryotic translation initiation factor 2B, subunit 2 beta, 39kDa	✔	
MLH3	mutL homolog 3 (E. coli)	✔	
AL833875	hypothetical protein		✔
ACYP1	acylphosphatase 1, erythrocyte (common) type	✔	
C14orf140	chromosome 14 open reading frame 140		✔
NEK9	NIMA (never in mitosis gene a)- related kinase 9	✔	
TMP21	transmembrane trafficking protein	✔	
FOS	v-fos FBJ murine osteosarcoma viral oncogene homolog	✔	
JDP2	jun dimerization protein 2	✔	
BATF	basic leucine zipper transcription factor, ATF-like	✔	
C14orf58	chromosome 14 open reading frame 58	✔	
AK027804	hypothetical protein		✔
C14orf1	chromosome 14 open reading frame 1	✔	
BX248022	human full-length cDNA clone CS0DC006YI13 of neuroblastoma		✔
KIAA0998	KIAA0998 protein	✔	
TGFB3	transforming growth factor, beta 3	✔	
MGC16026	similar to RIKEN cDNA 1700019E19 gene		✔
C14orf118	chromosome 14 open reading frame 118	✔	
ESRRB	estrogen-related receptor beta	✔	
KIAA1036	KIAA1036 protein	✔	

(Continued on page 178)

Table 5.3 (Continued). Reference Sequenced genes in CRD3 (between D14S43 and D14S59).

Gene	Product	Known	Predicted
KIAA0759	KIAA0759 protein	✔	
C14orf4	chromosome 14 open reading frame 4	✔	
KIAA1737	KIAA1737 protein	✔	
C14orf59	chromosome 14 open reading frame 59		✔
BX248756	human full-length cDNA 3-prime end of clone CS0DF025YA24 of fetal brain		✔
BX248759	human full-length cDNA 5-prime end of clone CS0DF035YD13 of fetal brain		✔
DKFZP434P0111	hypothetical protein DKFZp434P0111		✔
NGB	neuroglobin	✔	
POMT2	protein-O-mannosyltransferase 2	✔	
GSTZ1	glutathione transferase zeta 1 (maleylacetoacetate isomerase)	✔	
BX248262	human full-length cDNA clone CS0DN001YD20 of adult brain		✔
LOC122945	hypothetical protein FLJ32809		✔
C14orf133	chromosome 14 open reading frame 133		✔
AHSA1	AHA1, activator of heat shock 90kDa protein ATPase homolog 1 (yeast)	✔	
LOC145501	hypothetical protein LOC145501	✔	
BX248280	human full-length cDNA clone CS0DI024YA19 of placenta		✔
BX248277	human full-length cDNA clone CS0DI014YN05 of placenta		✔
BX248770	human full-length cDNA 5-prime end of clone CS0DI033YJ09 of placenta		✔
BX248771	human full-length cDNA 5-prime end of clone CS0DI052YD12 of placenta		✔
SPTLC2	serine palmitoyltransferase, long chain base subunit 2	✔	
	Total	*31*	*33*

Table 5.4. Reference Sequenced genes in CRD4 (between D14S1000 and D14S68).

Gene	Product	Known	Predicted
FLRT2	fibronectin leucine rich transmembrane protein 1	✔	
GALC	galactosylceramidase (Krabbe disease)	✔	
GPR65	G protein-coupled receptor 65	✔	
	Total	*3*	*0*

Subunits A and C of PP2A are ubiquitously expressed as alpha and beta isoforms with highly conserved sequence. Subunit A acts as a scaffold protein for recruitment of variable subunits or other regulatory proteins. The variable subunits are classified into four families of unrelated proteins, the B, B', B'' and B''' family. Each family consists of a number of isoforms given by alternative splicing from one or more genes.

In mammalia, the B subunit is encoded by four genes. Bα and Bδ are widely distributed and Bβ and Bγ are highly enriched in brain. The B' family contains at least five distinct gene products in human. B'α and B'γ are widely expressed, and are extremely abundant in heart and skeletal muscle. B'β and B'δ are expressed predominantly in brain. *PPP2R5E* in 14q23.1 encodes the B'ε subunit of PP2A, which is a cytoplasmic phosphoprotein highly expressed in the brain (McCright *et al.*, 1996). The B'' family is consisted of PR48, PR59, PR72, PR130, which may be involved in the regulation of the G1/S transition. Based on conserved epitope shared with the B' subunits, stratin and S/G2 nuclear autoantigen were identified as new members of a potential B''' subunit family. These variable subunits determine the substrate specificity, cellular and sub-cellular localization and catalytic activity of the holoenzyme (Janssens and Goris, 2001; Lechward *et al.*, 2001).

It has been suggested that the A subunit of PP2A is a tumor suppressor because gene encoding the Aβ subunit was mutated in 15% of primary lung tumors and in

15% of colorectal carcinomas (Wang *et al.*, 1998). Later, alterations in both Aα and Aβ subunits were detected in a variety of primary human cancers such as breast carcinomas, lung carcinomas, melanoma (Calin *et al.*, 2000), chronic lymphocytic leukemias (Zhu *et al.*, 2001) and parathyroid adenomas (Hemmer *et al.*, 2002). Recently, reduced expression of the Aα subunit of PP2A in human gliomas was detected by Western blot. However, only silent mutations in the Aα gene were detected (Colella *et al.*, 2001). Site-directed mutagenesis studies revealed that N-terminal mutants of Aα discovered in breast carcinoma are defective in binding B' but not B and B'' (Ruediger *et al.*, 2001).

According to Ruediger *et al.*, the Aα and Aβ subunit of PP2A are different in binding affinity toward subunit B and C (Ruediger *et al.*, 2001). Notably, APC interacted with all assayed members of the B' family, whereas there was no detectable interaction with Bα, B'', A, or C subunits. Also, β-catenin was specifically down-regulated by PP2A of the B' family (Seeling *et al.*, 1999). PP2A subunit B' may, therefore, direct PP2A to dephosphorylate specific components of the APC-dependent signaling complex and inhibit Wnt signaling.

Alteration of the tumor suppressor *TP53* is common in malignancy. Cyclin G, whose mRNA expression does not change significantly during cell cycle, was demonstrated to be a transcriptional target of *TP53* (Okamoto and Beach, 1994).

More recently, cyclin G1 and G2 were found to associate with a variety of B' subunits and even interact directly with the catalytic C subunit without the A subunit. G2-PP2A complexes induced nuclear aberrations and hence G1/S cell cycle arrest (Bennin *et al.*, 2002).

Negative role of PP2A is also linked to mitogenic signaling (Anderson *et al.*, 1990; Ugi *et al.*, 2002; Zhou *et al.*, 2002) and other aspects of cell cycle progression (Schonthal and Feramisco, 1993; Yan and Mumby, 1999;). However, the specific subunit was not clearly stated in those studies.

PPP2R5E maps at chromosome 14q23.1 lay between D14S997, the locus with frequent LOH, and the flanking locus D14S1026 of the CRD1. Whether loss of *PPP2R5E* provides advantage to tumorigenesis awaits further refinement of CRD1 and functional studies specific to the gene.

MutL homolog 3 (MLH3)

DNA mismatch-repair is one of multiple replication, repair, and recombination processes that are required to maintain genomic stability in prokaryotes and eukaryotes. The isolation of *E. coli* strains with elevated frequencies of spontaneous mutations, contributed to the identification of four mutator genes that play central roles in mismatch-repair. They are *MutS*, *MutL*, *MutH* and *MutU* (Buermeyer *et al.*,

1999). In human, expressed product of the homologs of bacterial *MutL (MLH)* forms various heterodimeric complexes with product of homologs of bacterial *MutS (MSH)* to mediate mismatch-repair (Jiricny, 1998).

Muller A and Fishel R (2002) searched extensively for mutations in mismatch-repair genes in HNPCC families and revealed that the majority of the alterations in *MSH2* (40%) and *MLH1* (40%) genes constitute the majority of alterations among mismatch-repair genes, while mutation of other mismatch-repair genes are less common (5%). However, LOH in the chromosomal region containing *MLH3* was detected in 30% of human colorectal cancers (Weber *et al.*, 1999). Lipkin *et al.* (2001) defined *MLH3* mutation in 6 tumors in screening of 36 colon tumors with high MSI. Four of the mutations were biallelic inactivation of *MLH3*, suggesting that *MLH3* is a putative TSG.

For gliomas, reports on MSI are conflicting. Zhu *et al.* (1996) found MSI in only 3% of astrocytic tumors (n = 33) using di-, tri- and tetranucleotide repeat microsatellite markers localized on chromosome 4 and 9, X, 13 and 22. Dams *et al.* (1995) showed MSI in 5 of 10 GBMs but not in 1 AA and 4 DAs using 17 different microsatellite loci over 7 different chromosomes. Four allelic shifts were defined in 4 different GBM cases. The remaining showed an extra allele at two different loci.

The author concluded that MSI was a rather common phenomenon in gliomas, but the frequency of MSI in glioma was lower than that in HNPCC.

In Leung *et al.*'s study (1998), MSI were detected in 3 of 17 (17.6%) GBMs and 1 of 3 AAs. One of the GBMs with high MSI harbors germline and somatic mutation in the two alleles of the *MLH1* gene. The other two showed *MSH2* mutation and somatic allele loss in tumor by sequencing. Since all patient donors of the tumors recruited in this study were aged 45 years or less, the author suggested that a proportion of primary GBMs in young patients could be caused by germline mutations of mismatch-repair genes. From this study, MSI might be more common among young patients and lead to contradictory results from different studies. Further study is required to investigate whether alterations in *MLH3* was associated with subset of astrocytic tumors, especially within young patients.

Due to the mismatch-repair function of MLH and MSH, MSI could be an indicator of alterations in these genes. However, MSI was detectable in less than 1% of nine markers (mononucleotide, dinucleotide and tetranuclotide) in a *MLH3*$^{-/-}$ mice, indistinguishable from wild-type fibroblasts (Lipkin *et al.*, 2002). To test whether mutations in DNA mismatch-repair genes cause an inherited risk of colorectal cancer, Liu *et al.* (2003) screened 70 patients suggestive of genetic predisposition for germ-line mutations in *MLH3*. One frame-shift mutation and 11 missense mutations were

identified in 16 patients (23%). In one family, *MLH3* mutation segregated with disease together with a missense mutation in *MSH2*. Interestingly, none of the tumors with *MLH3* mutations showed MSI. This suggested function other than mismatch-repair of *MLH3*. In fact, *MLH3* is involved in at least one other cellular function. Meiotic arrest and aneuploidy was detected in *MLH3*$^{-/-}$ mice of Lipkin *et al.* (2002). Therefore, studies on *MLH3* should not be limited to tumors with high MSI. Further studies are needed to investigate the functional role of *MLH3* in tumor suppression, which may not be related to MSI. Further fine-mapping of CRD3 is also required to evaluate whether *MLH3* is related to astrocytic tumors.

5.6.3. Overlapping deletion regions in astrocytic and non-CNS tumors

Only two genes were discussed above despite four CRDs were defined because functional studies of the reference sequenced genes are far from completion. Some publications describe gene cloning without any functional work. Thus, little information is available for evaluation of functions in tumor suppression. Although no genes within CRD2 were regarded as a candidate in the mean time, this region overlaps with four other human cancers (Figure 5.2) which are included in R2, the region with the second highest frequency of LOH (Figure 5.1).

Studies on R2 are rather limited to renal cell carcinoma. In earlier FISH and microsatellite analysis of non-papillary renal cell carcinoma, a positive correlation between the frequency of 14q LOH and increasing grade ($P < 0.001$) and stage ($P < 0.001$) of tumors were found (Herbers *et al.*, 1997, and Wu *et al.*, 1996). Herbers *et al.* demonstrated recombination at chromosome 14q, which may lead to loss of one allele and duplication of the other. Combining data from Hu *et al.*'s study (2002) and the current studies, 34.5% of ($n = 29$) diffuse astrocytoma, 40% ($n = 5$) of AA and 38.9% of GBM (34 GBM and two GS) showed LOH in at least one polymorphic locus on 14q. An increasing LOH frequency in increasing tumor grade was not found.

More recently, chromosome 14q LOH was analyzed in clear cell renal cell carcinomas using three microsatellite markers (Mitsumori *et al.*, 2002). One of them was D14S588 and the other two lay on 14q32.12 and q32.2 (both telomeric from D14S280). LOH was present in 35.4% of informative cases out of 130 cases at D14S588 and 39.5% for any one of the three markers. The proportion of cells with 14q LOH was found to associate with tumor aggressiveness, implying the 14q LOH as a marker of latent metastatic potential in clear cell renal cell carcinoma (Mitsumori *et al.*, 2002). Loss in D14S588 constituted 19.2% of astrocytic tumors in the current study, which is the marker with second highest imbalance frequency among the 14q markers used (except D14S1068). Whether these tumors, including three diffuse

astrocytomas, one AA and one GBM, with LOH in D14S588 possessed poorer prognosis or worse survival remained unknown due to limited clinical data. In Debiec-Rychter *et al.*'s cytogenetic study, loss in 14q was also detected in two diffuse astrocytomas, both related to poor prognosis.

Another study was on gastrointestinal stromal tumors (Gunawan *et al.*, 2002). All tumors employed displayed clonal chromosomal aberrations; 15 were hypo- to near diploid, and four were near-triploid and hypotetraploid. The most common abnormalities detected were loss of chromosomes 14 and/or 22. It this study, loss of chromosome 14 and/or 22 was found to be early changes in gastrointestinal stromal tumorigenesis irrespective of site or differentiation. It cannot be predicted on whether the same tumor suppressor is shared by these stromal tumors and astrocytic tumors. However, the presence of 14q loss in diffuse astrocytoma revealed the abnormality is an early event. It is worth noting that Debiec-Rychter *et al.* detected total or partial losses of chromosome 14 in 11 GBMs, all of which were abnormal clones.

CRD4, which is relatively large and also with no TSG candidates included, overlapped with CRDs in two other CNS tumors, neuroblastoma and meningioma in R3. In contrary to other tumors, abnormalities of chromosome 14 in meningioma contribute to a better prognostic stratification of patients at diagnosis. Multivariate analysis showed that tumor grade together with chromosome 14 status and age were

the best combination of independent variables for predicting relapse-free survival. Therefore, an oncogenic gene rather than a tumor suppressor may be present in R3. No hints on the position of the abnormalities on chromosome 14q were given in this study. In another study of meningioma, only 14q13 and 14q32 were included. Benign non-recurring meningiomas were less likely to harbor 14q deletions than recurring cases (17% versus 50%, $P = 0.013$; Cai *et al.*, 2001). Considering results from both studies, better prognosis may be limited to 14q LOH in R3.

In summary, identification of tumor suppressors in the four CRDs awaits further positional mapping and functional studies of genes within CRDs. More clinical data are also required to relate the CRDs with specific astrocytic tumor subtype.

6. Further studies

6.1. Role of BRAF alterations in astrocytic tumors

BRAF mutations have been detected in tumor specimens of various human cancers. However, *BRAF* mutation had only been revealed in glioma cell lines. In the current study, mutation and immunohistochemistry demonstrated *BRAF* alterations in astrocytic tumor specimens. These included a T1796A substitution in one GBM sample among a series of 24 diffuse astrocytomas, 17 AAs and 53 GBMs, and B-Raf immunoreactivity in 31.9% of an astrocytic tumor series consisting of 25 GBMs, 13 AAs and 9 diffuse astrocytomas. Although mutation of the *BRAF* gene is rare among astrocytic tumors, sequencing and karyotyping analyses indicated increased copies of $BRAF^{V599E}$ in two additional GBM cell lines. These results suggest that B-Raf plays a role in the tumorigenesis of astrocytic tumors. The exact tumorigenic role of B-Raf in astrocytic tumor remains to be clarified. Therefore, an investigation on the biological effect of wild-type and V599E B-Raf expression was proposed.

To investigate the functional effects of $BRAF^{V599E}$ on astrocytic tumors, full length *BRAF* cDNA containing the V599E mutation can be obtained by reverse transcription-PCR of our cell lines, for example, GBM2603. The PCR products can then be digested with restriction enzymes and cloned into mammalian expression

vector. Next, *BRAF*^{V599E}-harboring vectors and vectors without gene insert can be used to transfect GBM cell lines without B-Raf expression. Functional assays of V599E transfected cells could then be compared with control cells with respect of proliferation and apoptosis.

In contrast to other tumors derived from B-Raf-expressing normal tissue, expression of wild-type B-Raf was seen in astrocytic tumors but not in normal astrocytes. To determine the functional effect of wild-type B-Raf on astrocytic tumors, transfection of the same GBM cell line with full-length wild-type *BRAF* cDNA is also to be performed. This also enables the comparison of the functions of wild-type B-Raf with those of V599E B-Raf mutant.

To further investigate the functional effects of wild-type and mutant *BRAF* on tumorigenesis, the transfection experiments described above could be complemented by loss-of-function experiments in cell lines. Functional inactivation of *BRAF* gene by siRNA is regarded as an efficient and specific method in reducing B-Raf protein in tumor cell lines. Any reduction in proliferation or increase in apoptosis resulted from stable suppression of B-Raf expression can provide strong evidence for the roles being played by wild-type and V599E mutant *BRAF* in astrocytic tumors.

Moreover, wild-type *BRAF*- and mutant *BRAF*-transfected tumor cells and/or suppressed GBM cells could be transplanted into nude mice so as to examine the *in vivo* tumorigenecity of wild-type and mutant *BRAF* in astrocytic tumors.

6.2. B-Raf expression in astrocytic tumors and correlation with EGFR over-expression

As stated before, immunohistochemistry revealed B-Raf expression in astrocytic tumor specimens but not in normal astrocytes. Positive B-Raf immunoreactivity was detected in about one-third of astrocytic tumors. This suggests a selective growth advantage provided by the B-Raf protein. However, immunoreactivity has not revealed the level of B-Raf expression in tumor cells examined. A precise quantification of B-Raf expression from diffuse astrocytoma to GBM is recommended for evaluation of the significance of *BRAF* in tumor development. For accurate quantification of B-Raf expression, a reverse transcription real-time PCR is suggested. Correlation analysis between B-Raf expression level and tumor grade can be performed.

Moreover, about 20% of primary GBM without *EGFR* amplification also overexpress EGFR (Kleihues and Cavennee, 2000). The B-Raf expression status in EGFR-overexpressing tumors which do not harbor *EGFR* amplification has not been studied. For correlation analysis between EGFR expression and B-Raf expression, quantification of EGFR expression by reverse transcription real-time PCR in the same series of tumor samples is proposed.

6.3. Microsatellite analysis of 14q in astrocytic tumors

Microsatellite analysis in 14q21.2 – q32.12 defined 4 CRDs. Each of the CRDs overlaps with CRDs in other tumors. However, none of them is small enough to propose a putative TSG. Therefore, more polymorphic markers within the CRDs are required for finer mapping of tumor suppressor loci.

Moreover, since more than one CRD is present on 14q, more samples are to be recruited in future for finer mapping of CRDs. Also, a larger sample size is more representative in reflecting the actual frequency of LOH on 14q. In this study, overall allelic loss was detected in 9 of 32 astrocytic tumors (28%), a frequency lower than in the previous whole-genome allelotype study of Hu *et al.*, 2002 (GBM, 50%, $n = 21$; diffuse astrocytoma, 35%, $n = 17$). Discrepancy in LOH frequencies is likely attributed to the use of small sample size in both of our studies. Furthermore, the use of adequate samples with clinical data may reveal the pattern of CRDs in 14q of astrocytic tumors in relation to survival and prognostic parameters.

Furthermore, the study of Hu *et al.* (2002) defined 2 CRDs in 14q of astrocytic tumors. The present study only included fine-mapping of the more centromeric region. Fine mapping is also to be done for the more telomeric one.

7. Conclusions

BRAF^{V599E} mutation was detected in one of 53 GBMs but not in 24 diffuse astrocytomas, 17 AAs, 31 oligodendroglial tumors, 23 ependymal tumors, 21 MBs and 25 meningeal tumors. These results indicate that *BRAF* mutation is a rare event in CNS tumors and is limited to GBM in the series examined.

BRAF^{V599E} mutation was also detected in GBM2603 and GBM6840 of 10 CNS cell lines (6 from astrocytic tumors, 3 from MBs and 1 from PNET) examined. Both of which are derived from GBM. Karyotype analysis showed increased copies of chromosome 7 and sequence electropherograms displayed stronger signal of mutant *BRAF* allele than wild-type allele in both GBM2603 and GBM6840. Therefore, a preferential increase in copy number of *BRAF*^{V599E} exists in the GBM cell lines. Elevation of *BRAF*^{V599E} copies in cancer cells is a novel finding. Together, these results suggest that both sequence alteration and enhanced copy number of mutant *BRAF* allele are involved in the development of GBM.

B-Raf expression in normal astrocytes was undetectable by immunohistochemistry. However, B-Raf expression was detectable in about 30% of astrocytic tumors. Elevated B-Raf expression was found in WHO grade II to grade IV astrocytic tumors. The abnormal expression of wild-type B-Raf protein in the

low-grade diffuse astrocytoma suggests that *BRAF* alteration occurs early in the tumorigenesis of astrocytic tumors. My results are in line with those observed in melanoma (Pollock *et al.*, 2003), supporting the notion that B-Raf is involved in early stages of tumorigenesis.

Because B-Raf is a downstream effector of the EGFR pathway and *EGFR* amplification is a common genetic alteration seen in GBM. I therefore examined the relationship between *BRAF* mutation and *EGFR* amplification in a GBM series. My data showed that the $BRAF^{V599E}$-containing GBM, BJ10, did not harbor *EGFR* amplification. This result suggests that *BRAF* mutation and *EGFR* amplification are mutually exclusive events. However, such relationship should be verified in a larger series. Furthermore, I also investigated the relationship between B-Raf expression and *EGFR* amplification. Of the 30 astrocytic tumor specimens tested, *EGFR* amplification and B-Raf expression were mutually exclusive. Tumorigenic effect of wild-type B-Raf which is incapable in self-activation was thought to be sustained by autocrine or paracrine stimulation.

Taking together, my data demonstrated that *BRAF* can be altered both in the gene level and in the transcription level, and such alterations play an important role in the tumorigenesis of astrocytic tumors.

Other than examining *BRAF* alterations among CNS tumors, the current study also included fine mapping of a CRD located in the long arm of chromosome 14 of astrocytic tumors. In a previous allelotype analysis on diffuse astrocytoma (fibrillary) and GBM, two CRDs were located to 14q. The second aim of the current study is to fine map the more centromeric CRD, which is located in 14q21.2 – q32.12. Using 18 polymorphic markers, this region of 48.1Mb was found to contain four separate CRDs. The new four CRDs within 14q21.2 – q32.12 span approximately 3.3Mb, 4.0Mb, 3.2Mb and 6.5Mb, respectively. All of them overlap with those of other cancer types. This indicates that functional inactivation of one or more shared TSG contributes to their etiology. Based on current knowledge on the candidate genes annotated in the CRDs, *PPP2R5E* and *MLH3* may be putative TSGs within two of the four regions and worth further characterization. However, these regions are still considerably too large for positional cloning of candidate genes. Further refinement of the CRDs followed by characterization of the target TSGs will enhance our understanding of tumorigenesis of astrocytic tumors.

8. References

Abraham D, Podar K, Pacher M, Kubicek M, Welzel N, Hemmings BA, Dilworth SM, Mischak H, Kolch W and Baccarini M (2000). Raf-1-associated protein phosphatase 2A as a positive regulator of kinase activation. J Biol Chem. 275:22300-22304

Abujiang P, Mori TJ, Takahashi T, Tanaka F, Kasyu I, Hitomi S and Hiai H (1998). Loss of heterozygosity (LOH) at 17q and 14q in human lung cancers. Oncogene. 17:3029-3033

Actor B, Cobbers JM, Buschges R, Wolter M, Knobbe CB, Reifenberger G and Weber RG (2002). Comprehensive analysis of genomic alterations in gliosarcoma and its two tissue components. Genes Chromosomes Cancer. 34:416-427

Agarwal ML, Agarwal A, Taylor WR and Stark GR (1995). p53 controls both the G2/M and the G1 cell cycle checkpoints and mediates reversible growth arrest in human fibroblasts. Proc Natl Acad Sci U S A. 92:8493-8497

Alavi A, Hood JD, Frausto R, Stupack DG and Cheresh DA (2003). Role of Raf in vascular protection from distinct apoptotic stimuli. Science. 301:94-96

Albrecht S, von Deimling A, Pietsch T, Giangaspero F, Brandner S, Kleihues P and Wiestler OD (1994). Microsatellite analysis of loss of heterozygosity on chromosomes 9q, 11p and 17p in medulloblastomas. Neuropathol Appl Neurobiol. 20:74-81

Allan LA, Morrice N, Brady S, Magee G, Pathak S and Clarke PR (2003). Inhibition of caspase-9 through phosphorylation at Thr 125 by ERK MAPK. Nat Cell Biol. 5:647-654

Alonso ME, Bello MJ, Arjona D, Gonzalez-Gomez P, Lomas J, de Campos JM, Kusak ME, Isla A and Rey JA (2002). Analysis of the NF2 gene in oligodendrogliomas and ependymomas. Cancer Genet Cytogenet. 134:1-5

Anderson NG, Maller JL, Tonks NK and Sturgill TW (1990). Requirement for integration of signals from two distinct phosphorylation pathways for activation of MAP kinase. Nature. 343:651-653

Avruch J, Zhang XF and Kyriakis JM (1994). Raf meets Ras: completing the framework of a signal transduction pathway. Trends Biochem Sci. 19:279-283

Bandera CA, Takahashi H, Behbakht K, Liu PC, LiVolsi VA, Benjamin I, Morgan MA, King SA, Rubin SC and Boyd J (1997). Deletion mapping of two potential chromosome 14 tumor suppressor gene loci in ovarian carcinoma. Cancer Res. 57:513-515

Bando T, Kato Y, Ihara Y, Yamagishi F, Tsukada K and Isobe M (1999). Loss of heterozygosity of 14q32 in colorectal carcinoma. Cancer Genet Cytogenet. 111:161-165

Barnier JV, Papin C, Eychene A, Lecoq O and Calothy G (1995). The mouse B-raf gene encodes multiple protein isoforms with tissue-specific expression. J Biol Chem. 270:23381-23389

Bennin DA, Don AS, Brake T, McKenzie JL, Rosenbaum H, Ortiz L, DePaoli-Roach AA and Horne MC (2002). Cyclin G2 associates with protein phosphatase 2A catalytic and regulatory B' subunits in active complexes and induces nuclear aberrations and a G1/S phase cell cycle arrest. J Biol Chem. 277:27449-27467

Besson A and Yong VW (2001). Mitogenic signaling and the relationship to cell cycle regulation in astrocytomas. J Neurooncol. 51:245-264

Biernat W, Kleihues P, Yonekawa Y and Ohgaki H (1997). Amplification and overexpression of MDM2 in primary (de novo) glioblastomas. J Neuropathol Exp Neurol. 56:180-185

Bjorkqvist AM, Wolf M, Nordling S, Tammilehto L, Knuuttila A, Kere J, Mattson K and Knuutila S (1999). Deletions at 14q in malignant mesothelioma detected by microsatellite marker analysis. Br J Cancer. 81:1111-1115

Bos JL (1989). ras oncogenes in human cancer: a review. Cancer Res. 49:4682-4689

Boveri T (1914). Zur Frage der Entstehung maligner Tumoren. Fischer, Jena.

Bredel M and Pollack IF (1999). The p21-Ras signal transduction pathway and growth regulation in human high-grade gliomas. Brain Res Brain Res Rev. 29:232-249

Brose MS, Volpe P, Feldman M, Kumar M, Rishi I, Gerrero R, Einhorn E, Herlyn M, Minna J, Nicholson A, Roth JA, Albelda SM, Davies H, Cox C, Brignell G, Stephens P, Futreal PA, Wooster R, Stratton MR and Weber BL (2002). BRAF and RAS mutations in human lung cancer and melanoma. Cancer Res. 62:6997-7000

Brunner C, Jung V, Henn W, Zang KD and Urbschat S (2000). Comparative genomic hybridization reveals recurrent enhancements on chromosome 20 and in one case combined amplification sites on 15q24q26 and 20p11p12 in glioblastomas. Cancer Genet Cytogenet. 121:124-127

Buchkovich K, Duffy LA and Harlow E (1989). The retinoblastoma protein is phosphorylated during specific phases of the cell cycle. Cell. 58:1097-1105

Buermeyer AB, Deschenes SM, Baker SM and Liskay RM (1999). Buermeyer AB, Mammalian DNA mismatch repair. Annu Rev Genet. 33:533-564

Burton EC, Lamborn KR, Feuerstein BG, Prados M, Scott J, Forsyth P, Passe S, Jenkins RB and Aldape KD (2002). Genetic aberrations defined by comparative genomic hybridization distinguish long-term from typical survivors of glioblastoma. Cancer Res. 62:6205-6210

Busca R, Abbe P, Mantoux F, Aberdam E, Peyssonnaux C, Eychene A, Ortonne JP and Ballotti R (2000). Ras mediates the cAMP-dependent activation of extracellular signal-regulated kinasess (ERKs) in melanocytes. EMBO J. 19:2900-2910

Cai DX, Banerjee R, Scheithauer BW, Lohse CM, Kleinschmidt-Demasters BK and Perry A (2001). Chromosome 1p and 14q FISH analysis in clinicopathologic subsets of meningioma: diagnostic and prognostic implications. J Neuropathol Exp Neurol.60:628-636

Calin GA, di Iasio MG, Caprini E, Vorechovsky I, Natali PG, Sozzi G, Croce CM, Barbanti-Brodano G, Russo G and Negrini M (2000). Low frequency of alterations of the alpha (PPP2R1A) and beta (PPP2R1B) isoforms of the subunit A of the serine-threonine phosphatase 2A in human neoplasms. Oncogene. 19:1191-1195

Calipel A, Lefevre G, Pouponnot C, Mouriaux F, Eychene A and Mascarelli F (2003). Mutation of B-Raf in human choroidal melanoma cells mediates cell proliferation and transformation through the MEK/ERK pathway. J Biol Chem. Epub ahead of print

Cantley LC and Neel BG (1999). New insights into tumor suppression: PTEN suppresses tumor formation by restraining the phosphoinositide 3-kinase/AKT pathway. Proc Natl Acad Sci U S A. 96:4240-4245

Central Brain Tumor Registry of the United States (2000)

Chamberlain MC (2001). Meningiomas. Curr Treat Options Neurol. 3:67-76

Chen L, Lu W, Agrawal S, Zhou W, Zhang R and Chen J (1999). Ubiquitous induction of p53 in tumor cells by antisense inhibition of MDM2 expression. Mol Med. 5:21-34

Cheng RYS, Lo KW, Huang DP and Tsao SW (1997). Loss of heterozygosity on chromosome 14 in primary nasopharyngeal carcinoma. Int J Oncol. 10:1047-1050

Cheng Y, Ng HK, Ding M, Zhang SF, Pang JC and Lo KW (1999). Molecular analysis of microdissected de novo glioblastomas and paired astrocytic tumors. J Neuropathol Exp Neurol. 58:120-128

Cohen Y, Xing M, Mambo E, Guo Z, Wu G, Trink B, Beller U, Westra WH, Ladenson PW and Sidransky D (2003). BRAF mutation in papillary thyroid carcinoma. J Natl Cancer Inst. 95:625-627

Colella S, Ohgaki H, Ruediger R, Yang F, Nakamura M, Fujisawa H, Kleihues P and Walter G (2001). Reduced expression of the Aalpha subunit of protein phosphatase 2A in human gliomas in the absence of mutations in the Aalpha and Abeta subunit genes. Int J Cancer. 93:798-804

Costello JF, Berger MS, Huang HS and Cavenee WK (1996). Silencing of p16/CDKN2 expression in human gliomas by methylation and chromatin condensation. Cancer Res. 56:2405-2410

D'Alessandro I, Zitzelsberger H, Hutzler P, Lehmann L, Braselmann H, Chimenti S and Hofler H (1997). Numerical aberrations of chromosome 7 detected in 15 microns paraffin-embedded tissue sections of primary cutaneous melanomas by fluorescence in situ hybridization and confocal laser scanning microscopy. J Cutan Pathol. 24:70-75

Dams E, Van de Kelft EJ, Martin JJ, Verlooy J and Willems PJ (1995). Instability of microsatellites in human gliomas. Cancer Res. 55:1547-1549

Das A, Tan WL, Teo J and Smith DR (2002). Glioblastoma multiforme in an Asian population: evidence for a distinct genetic pathway. J Neurooncol. 60:117-125

Davies H, Bignell GR, Cox C, Stephens P, Edkins S, Clegg S, Teague J, Woffendin H, Garnett MJ, Bottomley W, Davis N, Dicks E, Ewing R, Floyd Y, Gray K, Hall S, Hawes R, Hughes J, Kosmidou V, Menzies A, Mould C, Parker A, Stevens C, Watt S, Hooper S, Wilson R, Jayatilake H, Gusterson BA, Cooper C, Shipley J, Hargrave D, Pritchard-Jones K, Maitland N, Chenevix-Trench G, Riggins GJ, Bigner DD, Palmieri G, Cossu A, Flanagan A, Nicholson A, Ho JW, Leung SY, Yuen ST, Weber BL, Seigler HF, Darrow TL, Paterson H, Marais R, Marshall CJ, Wooster R, Stratton MR and Futreal PA (2002). Mutations of the BRAF gene in human cancer. Nature. 417:949-954

De Rienzo A, Jhanwar SC and Testa JR (2000). Loss of heterozygosity analysis of 13q and 14q in human malignant mesothelioma. Genes Chromosomes Cancer. 28:337-341

Debiec-Rychter M, Alwasiak J, Liberski PP, Nedoszytko B, Babinska M, Mrozek K, Imielinski B, Borowska-Lehman J and Limon J (1995). Accumulation of chromosomal changes in human glioma progression. A cytogenetic study of 50 cases. Cancer Genet Cytogenet. 85:61-67

Dhillon AS, Meikle S, Yazici Z, Eulitz M and Kolch W (2002). Regulation of Raf-1 activation and signalling by dephosphorylation. EMBO J. 21:64-71

Di Cristofano A and Pandolfi PP (2000). The multiple roles of PTEN in tumor suppression. Cell. 100:387-390

Di Tomaso E, Pang JC, Lam HK, Tian XX, Suen KW, Hui AB and Hjelm NM (2000). Establishment and characterization of a human cell line from paediatric cerebellar glioblastoma multiforme. Neuropathol Appl Neurobiol. 26:22-30

Dietzmann K, von Bossanyi P, Sallaba J, Kirches E, Synowitz HJ and Warich-Kirches M (1996). Immunohistochemically detectable p53 and mdm-2 oncoprotein expression in astrocytic gliomas and their correlation to cell proliferation. Gen Diagn Pathol. 141:339-344

Ding H, Roncari L, Shannon P, Wu X, Lau N, Karaskova J, Gutmann DH, Squire JA, Nagy A and Guha A (2001). Astrocyte-specific expression of activated p21-ras results in malignant astrocytoma formation in a transgenic mouse model of human gliomas. Cancer Res. 61:3826-3836

Dong J, Phelps RG, Qiao R, Yao S, Benard O, Ronai Z and Aaronson SA (2003). BRAF Oncogenic Mutations Correlate with Progression rather than Initiation of Human Melanoma. Cancer Res. 63:3883-3885

Dong SM, Pang JC, Hu J, Zhou LF and Ng HK (2002a). Transcriptional inactivation of TP73 expression in oligodendroglial tumors. Int J Cancer. 98:370-375

Dong SM, Pang JC, Poon WS, Hu J, To KF, Chang AR and Ng HK (2001). Concurrent hypermethylation of multiple genes is associated with grade of oligodendroglial tumors. J Neuropathol Exp Neurol. 60:808-816

Dong ZQ, Pang JC, Tong CY, Zhou LF and Ng HK (2002b). Clonality of oligoastrocytomas. Hum Pathol. 33:528-535

Dugan LL, Kim JS, Zhang Y, Bart RD, Sun Y, Holtzman DM and Gutmann DH (1999). Differential effects of cAMP in neurons and astrocytes. Role of B-raf. J Biol Chem. 274:25842-25848

Ebert C, von Haken M, Meyer-Puttlitz B, Wiestler OD, Reifenberger G, Pietsch T and von Deimling A (1999). Molecular genetic analysis of ependymal tumors. NF2 mutations and chromosome 22q loss occur preferentially in intramedullary spinal ependymomas. Am J Pathol. 155:627-632

Ekstrand AJ, James CD, Cavenee WK, Seliger B, Pettersson RF and Collins VP (1991). Genes for epidermal growth factor receptor, transforming growth factor alpha, and epidermal growth factor and their expression in human gliomas in vivo. Cancer Res. 51:2164-2172

Ellison D (2002). Classifying the medulloblastoma: insights from morphology and molecular genetics. Neuropathol Appl Neurobiol. 28:257-282

El-Obeid A, Hesselager G, Westermark B and Nister M (2002). TGF-alpha-driven tumor growth is inhibited by an EGF receptor tyrosine kinase inhibitor. Biochem Biophys Res Commun. 290:349-358

El-Rifai W, Sarlomo-Rikala M, Andersson LC, Miettinen M and Knuutila S (2000). High-resolution deletion mapping of chromosome 14 in stromal tumors of the gastrointestinal tract suggests two distinct tumor suppressor loci. Genes Chromosomes Cancer. 27:387-391

Erhardt P, Schremser EJ and Cooper GM (1999). B-Raf inhibits programmed cell death downstream of cytochrome c release from mitochondria by activating the MEK/Erk pathway. Mol Cell Biol. 19:5308-5315

Evans DG, Farndon PA, Burnell LD, Gattamaneni HR and Birch JM (1991). The incidence of Gorlin syndrome in 173 consecutive cases of medulloblastoma. Br J Cancer. 64:959-961

Eychene A, Dusanter-Fourt I, Barnier JV, Papin C, Charon M, Gisselbrecht S and Calothy G (1995). Expression and activation of B-Raf kinase isoforms in human and murine leukemia cell lines. Oncogene. 10:1159-1165

Fan X, Munoz J, Sanko SG and Castresana JS (2002). PTEN, DMBT1, and p16 alterations in diffusely infiltrating astrocytomas. Int J Oncol. 21:667-674

Fenstermaker RA and Ciesielski MJ (2000). Deletion and tandem duplication of exons 2 - 7 in the epidermal growth factor receptor gene of a human malignant glioma. Oncogene. 19:4542-4548

Freeman WM, Walker SJ and Vrana KE (1999). Quantitative RT-PCR: pitfalls and potential. Biotechniques. 26:112-125

Fueyo J, Gomez-Manzano C, Yung WK, Liu TJ, Alemany R, Bruner JM, Chintala SK, Rao JS, Levin VA and Kyritsis AP (1998). Suppression of human glioma growth by adenovirus-mediated Rb gene transfer. Neurology. 50:1307-1315

Fujisawa H, Kurrer M, Reis RM, Yonekawa Y, Kleihues P and Ohgaki H (1999). Acquisition of the glioblastoma phenotype during astrocytoma progression is associated with loss of heterozygosity on 10q25-qter. Am J Pathol. 155:387-394

Fujisawa H, Reis RM, Nakamura M, Colella S, Yonekawa Y, Kleihues P and Ohgaki H (2000). Loss of heterozygosity on chromosome 10 is more extensive in primary (de novo) than in secondary glioblastomas. Lab Invest. 80:65-72

Fulci G, Labuhn M, Maier D, Lachat Y, Hausmann O, Hegi ME, Janzer RC, Merlo A and Van Meir EG (2000). p53 gene mutation and ink4a-arf deletion appear to be two mutually exclusive events in human glioblastoma. Oncogene. 19:3816-3822

Fults D, Brockmeyer D, Tullous MW, Pedone CA and Cawthon RM (1992). p53 mutation and loss of heterozygosity on chromosomes 17 and 10 during human astrocytoma progression. Cancer Res. 52:674-679

Fults D, Pedone CA, Thomas GA and White R (1990). Allelotype of human malignant astrocytoma. Cancer Res. 50:5784-5789

Gemignani ML, Schlaerth AC, Bogomolniy F, Barakat RR, Lin O, Soslow R, Venkatraman E and Boyd J (2003). Role of KRAS and BRAF gene mutations in mucinous ovarian carcinoma. Gynecol Oncol. 90:378-381

Giulietti A, Overbergh L, Valckx D, Decallonne B, Bouillon R and Mathieu C (2001). An overview of real-time quantitative PCR: applications to quantify cytokine gene expression. Methods. 25:386-401

Goldman CK, Kim J, Wong WL, King V, Brock T and Gillespie GY (1993). Epidermal growth factor stimulates vascular endothelial growth factor production by human malignant glioma cells: a model of glioblastoma multiforme pathophysiology. Mol Biol Cell. 4:121-133

Gomez-Manzano C, Fueyo J, Kyritsis AP, McDonnell TJ, Steck PA, Levin VA and Yung WK (1997). Characterization of p53 and p21 functional interactions in glioma cells en route to apoptosis. J Natl Cancer Inst. 89:1036-1044

Gomori E, Doczi T, Pajor L and Matolcsy A (1999). Sporadic p53 mutations and absence of ras mutations in glioblastomas. Acta Neurochir (Wien). 141:593-599

Gonzalez-Gomez P, Bello MJ, Alonso ME, Arjona D, Lomas J, de Campos JM, Isla A and Rey JA (2003). CpG island methylation status and mutation analysis of the RB1 gene essential promoter region and protein-binding pocket domain in nervous system tumours. Br J Cancer. 88:109-114

Goussia AC, Kyritsis AP, Mitlianga P and Bruner JM (2001). Genetic abnormalities in oligodendroglial and ependymal tumours. J Neurol. 248:1030-1035

Guan KL, Figueroa C, Brtva TR, Zhu T, Taylor J, Barber TD and Vojtek AB (2000). Negative regulation of the serine/threonine kinase B-Raf by Akt. J Biol Chem. 275:27354-27359

Guha A, Feldkamp MM, Lau N, Boss G and Pawson A (1997). Proliferation of human malignant astrocytomas is dependent on Ras activation. Oncogene. 15:2755-2765

Gunawan B, Bergmann F, Hoer J, Langer C, Schumpelick V, Becker H and Fuzesi L (2002). Biological and clinical significance of cytogenetic abnormalities in low-risk and high-risk gastrointestinal stromal tumors. Hum Pathol. 33:316-321

Haas-Kogan D, Shalev N, Wong M, Mills G, Yount G and Stokoe D (1998). Protein kinase B (PKB/Akt) activity is elevated in glioblastoma cells due to mutation of the tumor suppressor PTEN/MMAC. Curr Biol. 8:1195-1198

Hagemann C and Rapp UR (1999). Isotype-specific functions of Raf kinases. Exp Cell Res. 253:34-46

Hahn H, Christiansen J, Wicking C, Zaphiropoulos PG, Chidambaram A, Gerrard B, Vorechovsky I, Bale AE, Toftgard R, Dean M and Wainwright B (1996). A mammalian patched homolog is expressed in target tissues of sonic hedgehog and maps to a region associated with developmental abnormalities. J Biol Chem. 271:12125-12128

Haley JD, Hsuan JJ and Waterfield MD (1989). Analysis of mammalian fibroblast transformation by normal and mutated human EGF receptors. Oncogene. 4:273-283

Harada K, Kurisu K, Tahara H, Tahara E, Ide T and Tahara E (2000). Telomerase activity in primary and secondary glioblastomas multiforme as a novel molecular tumor marker. J Neurosurg. 93:618-625

Heid CA, Stevens J, Livak KJ and Williams PM (1996). Real time quantitative PCR. Genome Res. 6:986-994

Heinrich B, Hartmann C, Stemmer-Rachamimov AO, Louis DN and MacCollin M (2003). Multiple meningiomas: Investigating the molecular basis of sporadic and familial forms. Int J Cancer. 103:483-488

Hemmer S, Wasenius VM, Haglund C, Zhu Y, Knuutila S, Franssila K and Joensuu H (2002). Alterations in the suppressor gene PPP2R1B in parathyroid hyperplasias and adenomas. Cancer Genet Cytogenet. 134:13-17

Henson JW, Schnitker BL, Correa KM, von Deimling A, Fassbender F, Xu HJ, Benedict WF, Yandell DW and Louis DN (1994). The retinoblastoma gene is involved in malignant progression of astrocytomas. Ann Neurol. 36:714-721

Herbergs J, Hopman AH, De Bruine AP, Ramaekers FC and Arends JW (1996). In situ hybridization and flow cytometric analysis of colorectal tumours suggests two routes of tumourigenesis characterized by gain of chromosome 7 or loss of chromosomes 17 and 18. J Pathol. 179:243-247

Herbers J, Schullerus D, Muller H, Kenck C, Chudek J, Weimer J, Bugert P and Kovacs G (1997). Significance of chromosome arm 14q loss in nonpapillary renal cell carcinomas. Genes Chromosomes Cancer. 19:29-35

Herman JG, Jen J, Merlo A and Baylin SB (1996). Hypermethylation-associated inactivation indicates a tumor suppressor role for p15INK4B. Cancer Res. 56:722-727

Herman JG, Umar A, Polyak K, Graff JR, Ahuja N, Issa JP, Markowitz S, Willson JK, Hamilton SR, Kinzler KW, Kane MF, Kolodner RD, Vogelstein B, Kunkel TA and Baylin SB (1998). Incidence and functional consequences of hMLH1 promoter hypermethylation in colorectal carcinoma. Proc Natl Acad Sci U S A. 95:6870-6875

Hilger RA, Scheulen ME and Strumberg D (2002). The Ras-Raf-MEK-ERK pathway in the treatment of cancer. Onkologie. 25:511-518

Hingorani SR, Jacobetz MA, Robertson GP, Herlyn M and Tuveson DA (2003). Suppression of BRAF(V599E) in human melanoma abrogates transformation. Cancer Res. 63:5198-5202

Hoshi M, Shiwaku HO, Hayashi Y, Kaneko Y and Horii A (2000). Deletion mapping of 14q32 in human neuroblastoma defines an 1,100-kb region of common allelic loss. Med Pediatr Oncol. 35:522-525

Hu J, Jiang C, Ng HK, Pang JC, Tong CY. (2001). A preliminary study of loss of heterozygosity on chromosome 14 in glioblastoma. Zhonghua Yi Xue Yi Chuan Xue Za Zhi.18:347-350

Hu J, Pang JC, Tong CY, Lau B, Yin XL, Poon WS, Jiang CC, Zhou LF and Ng HK (2002). High-resolution genome-wide allelotype analysis identifies loss of chromosome 14q as a recurrent genetic alteration in astrocytic tumours. Br J Cancer. 87:218-224

Huang B, Starostik P, Kuhl J, Tonn JC and Roggendorf W (2002). Loss of heterozygosity on chromosome 22 in human ependymomas. Acta Neuropathol (Berl). 103:415-420

Huang H, Mahler-Araujo BM, Sankila A, Chimelli L, Yonekawa Y, Kleihues P and Ohgaki H (2000). APC mutations in sporadic medulloblastomas. Am J Pathol. 156:433-437

Humphrey PA, Wong AJ, Vogelstein B, Friedman HS, Werner MH, Bigner DD and Bigner SH (1988). Amplification and expression of the epidermal growth factor receptor gene in human glioma xenografts. Cancer Res. 48:2231-2238

Hung KS, Hong CY, Lee J, Lin SK, Huang SC, Wang TM, Tse V, Sliverberg GD, Weng SC and Hsiao M (2000). Expression of p16(INK4A) induces dominant suppression of glioblastoma growth in situ through necrosis and cell cycle arrest. Biochem Biophys Res Commun. 269:718-725

Hurtt MR, Moossy J, Donovan-Peluso M and Locker J (1992). Amplification of epidermal growth factor receptor gene in gliomas: histopathology and prognosis. J Neuropathol Exp Neurol. 51:84-90

Husemann K, Wolter M, Buschges R, Bostrom J, Sabel M and Reifenberger G (1999). Identification of two distinct deleted regions on the short arm of chromosome 1 and rare mutation of the CDKN2C gene from 1p32 in oligodendroglial tumors. J Neuropathol Exp Neurol. 58:1041-1050

Ichimura K, Schmidt EE, Goike HM and Collins VP (1996). Human glioblastomas with no alterations of the CDKN2A (p16INK4A, MTS1) and CDK4 genes have frequent mutations of the retinoblastoma gene. Oncogene. 13:1065-1072

Ichimura K, Schmidt EE, Miyakawa A, Goike HM and Collins VP (1998). Distinct patterns of deletion on 10p and 10q suggest involvement of multiple tumor suppressor genes in the development of astrocytic gliomas of different malignancy grades. Genes Chromosomes Cancer. 22:9-15

Janssens V and Goris J (2001). Protein phosphatase 2A: a highly regulated family of serine/threonine phosphatases implicated in cell growth and signalling. Biochem J. 353:417-439

Jiricny J (1998). Replication errors: cha(lle)nging the genome. EMBO J. 17:6427-2636

Johnson RL, Rothman AL, Xie J, Goodrich LV, Bare JW, Bonifas JM, Quinn AG, Myers RM, Cox DR, Epstein EH Jr and Scott MP (1996). Human homolog of patched, a candidate gene for the basal cell nevus syndrome. Science. 272:1668-1671

Jorissen RN, Walker F, Pouliot N, Garrett TP, Ward CW and Burgess AW (2003). Epidermal growth factor receptor: mechanisms of activation and signalling. Exp Cell Res. 284:31-53

Joseph JT, Lisle DK, Jacoby LB, Paulus W, Barone R, Cohen ML, Roggendorf WH, Bruner JM, Gusella JF and Louis DN (1995). NF2 gene analysis distinguishes hemangiopericytoma from meningioma. Am J Pathol. 147:1450-1455

Kallioniemi A, Kallioniemi OP, Sudar D, Rutovitz D, Gray JW, Waldman F and Pinkel D (1992). Comparative genomic hybridization for molecular cytogenetic analysis of solid tumors. Science. 258:818-821

Kimura ET, Nikiforova MN, Zhu Z, Knauf JA, Nikiforov YE and Fagin JA (2003). High prevalence of BRAF mutations in thyroid cancer: genetic evidence for constitutive activation of the RET/PTC-RAS-BRAF signaling pathway in papillary thyroid carcinoma. Cancer Res. 63:1454-1457

Kinkl N, Sahel J and Hicks D (2001). Alternate FGF2-ERK1/2 signaling pathways in retinal photoreceptor and glial cells in vitro. J Biol Chem. 276:43871-43878

Kleihues P and Cavennee WK (2000). World Health Organization Classification of Tumours of the Nervous System. 1sted. IARC: Lyon

Kleihues P and Ohgaki H (1999). Primary and secondary glioblastomas: from concept to clinical diagnosis. Neuro-oncol. 1:44-51

Klingler-Hoffmann M, Bukczynska P and Tiganis T (2003). Inhibition of phosphatidylinositol 3-kinase signaling negates the growth advantage imparted by a mutant epidermal growth factor receptor on human glioblastoma cells. Int J Cancer. 105:331-339

Knudson AG (2001). Two genetic hits (more or less) to cancer. Nat Rev Cancer. 1:157-162

Kogerman P, Grimm T, Kogerman L, Krause D, Unden AB, Sandstedt B, Toftgard R and Zaphiropoulos PG (1999). Mammalian suppressor-of-fused modulates nuclear-cytoplasmic shuttling of Gli-1. Nat Cell Biol. 1:312-319

Kolch W (2000). Meaningful relationships: the regulation of the Ras/Raf/MEK/ERK pathway by protein interactions. Biochem J. 351:289-305

Kondo S, Morimura T, Barnett GH, Kondo Y, Peterson JW, Kaakaji R, Takeuchi J, Toms SA, Liu J, Werbel B and Barna BP (1996). The transforming activities of MDM2 in cultured neonatal rat astrocytes. Oncogene. 13:1773-1779

Koschny R, Koschny T, Froster UG, Krupp W and Zuber MA (2002). Comparative genomic hybridization in glioma: a meta-analysis of 509 cases. Cancer Genet Cytogenet. 135:147-159

Labuhn M, Jones G, Speel EJ, Maier D, Zweifel C, Gratzl O, Van Meir EG, Hegi ME and Merlo A (2001). Quantitative real-time PCR does not show selective targeting of p14(ARF) but concomitant inactivation of both p16(INK4A) and p14(ARF) in 105 human primary gliomas. Oncogene. 20:1103-1109

Lacombe D, Chateil JF, Fontan D and Battin J (1990). Medulloblastoma in the nevoid basal-cell carcinoma syndrome: case reports and review of the literature. Genet Couns. 1:273-277

Lamszus K, Lachenmayer L, Heinemann U, Kluwe L, Finckh U, Hoppner W, Stavrou D, Fillbrandt R and Westphal M (2001). Molecular genetic alterations on chromosomes 11 and 22 in ependymomas. Int J Cancer. 91:803-808

Lechward K, Awotunde OS, Swiatek W and Muszynska G (2001). Protein phosphatase 2A: variety of forms and diversity of functions. Acta Biochim Pol. 48:921-933

Lee DJ, Koch WM, Yoo G, Lango M, Reed A, Califano J, Brennan JA, Westra WH, Zahurak M and Sidransky D (1997). Impact of chromosome 14q loss on survival in primary head and neck squamous cell carcinoma. Clin Cancer Res. 3:501-505

Lemmon MA and Schlessinger J (1994). Regulation of signal transduction and signal diversity by receptor oligomerization. Trends Biochem Sci. 19:459-463

Leng RP, Lin Y, Ma W, Wu H, Lemmers B, Chung S, Parant JM, Lozano G, Hakem R and Benchimol S (2003). Pirh2, a p53-induced ubiquitin-protein ligase, promotes p53 degradation. Cell. 112:779-791

Leung SY, Chan TL, Chung LP, Chan AS, Fan YW, Hung KN, Kwong WK, Ho JW and Yuen ST (1998). Microsatellite instability and mutation of DNA mismatch repair genes in gliomas. Am J Pathol. 153:1181-1188

Li G, Schaider H, Satyamoorthy K, Hanakawa Y, Hashimoto K and Herlyn M (2001). Downregulation of E-cadherin and Desmoglein 1 by autocrine hepatocyte growth factor during melanoma development. Oncogene. 20:8125-8135

Li Y, Millikan RC, Carozza S, Newman B, Liu E, Davis R, Miike R and Wrensch M (1998). p53 mutations in malignant gliomas. Cancer Epidemiol Biomarkers Prev. 7:303-308

Liang J and Slingerland JM (2003). Multiple Roles of the PI3K/PKB (Akt) Pathway in Cell Cycle Progression. Cell Cycle. 2:339-345

Libermann TA, Nusbaum HR, Razon N, Kris R, Lax I, Soreq H, Whittle N, Waterfield MD, Ullrich A and Schlessinger J (1985). Amplification, enhanced expression and possible rearrangement of EGF receptor gene in primary human brain tumours of glial origin. Nature. 313:144-147

Lipkin SM, Moens PB, Wang V, Lenzi M, Shanmugarajah D, Gilgeous A, Thomas J, Cheng J, Touchman JW, Green ED, Schwartzberg P, Collins FS and Cohen PE (2002). Meiotic arrest and aneuploidy in MLH3-deficient mice. Nat Genet. 31:385-390

Lipkin SM, Wang V, Stoler DL, Anderson GR, Kirsch I, Hadley D, Lynch HT and Collins FS (2001). Germline and somatic mutation analyses in the DNA mismatch repair gene MLH3: Evidence for somatic mutation in colorectal cancers. Hum Mutat. 17:389-396

Liu HX, Zhou XL, Liu T, Werelius B, Lindmark G, Dahl N and Lindblom A (2003). The role of hMLH3 in familial colorectal cancer. Cancer Res. 63:1894-1899

Liu L, Ichimura K, Pettersson EH and Collins VP (1998). Chromosome 7 rearrangements in glioblastomas; loci adjacent to EGFR are independently amplified. J Neuropathol Exp Neurol. 57:1138-1145

Longo MC, Berninger MS and Hartley JL (1990). Use of uracil DNA glycosylase to control carry-over contamination in polymerase chain reactions. Gene. 93:125-128

Louis DN, Holland EC and Cairncross JG (2001). Glioma classification: a molecular reappraisal. Am J Pathol. 159:779-786

Lundberg AS and Weinberg RA (1999). Control of the cell cycle and apoptosis. Eur J Cancer. 35:1886-1894

Lutterbach J, Guttenberger R and Pagenstecher A (2001). Gliosarcoma: a clinical study. Radiother Oncol. 61:57-64

MacNicol MC, Muslin AJ and MacNicol AM (2000). Disruption of the 14-3-3 binding site within the B-Raf kinase domain uncouples catalytic activity from PC12 cell differentiation. J Biol Chem. 275:3803-3809

Maher EA, Furnari FB, Bachoo RM, Rowitch DH, Louis DN, Cavenee WK and DePinho RA (2001). Malignant glioma: genetics and biology of a grave matter. Genes Dev. 15:1311-1333

Mandell JW, Hussaini IM, Zecevic M, Weber MJ and VandenBerg SR (1998). In situ visualization of intratumor growth factor signaling: immunohistochemical localization of activated ERK/MAP kinase in glial neoplasms. Am J Pathol. 153:1411-1423

Marais R, Light Y, Paterson HF, Mason CS and Marshall CJ (1997). Differential regulation of Raf-1, A-Raf, and B-Raf by oncogenic ras and tyrosine kinases. J Biol Chem. 272:4378-4383

Marigo V, Davey RA, Zuo Y, Cunningham JM and Tabin CJ (1996). Biochemical evidence that patched is the Hedgehog receptor. Nature. 384:176-179

Maruno M, Kovach JS, Kelly PJ and Yanagihara T (1991). Transforming growth factor-alpha, epidermal growth factor receptor, and proliferating potential in benign and malignant gliomas. J Neurosurg. 75:97-102

Mason CS, Springer CJ, Cooper RG, Superti-Furga G, Marshall CJ and Marais R (1999). Serine and tyrosine phosphorylations cooperate in Raf-1, but not B-Raf activation. EMBO J. 18:2137-2148

Matsumoto R, Tada M, Nozaki M, Zhang CL, Sawamura Y and Abe H (1998). Short alternative splice transcripts of the mdm2 oncogene correlate to malignancy in human astrocytic neoplasms. Cancer Res. 58:609-613

Matsuta M, Imamura Y, Matsuta M, Sasaki K and Kon S (1997). Detection of numerical chromosomal aberrations in malignant melanomas using fluorescence in situ hybridization. J Cutan Pathol. 24:201-205

Mazzola CA and Pollack IF (2003). Medulloblastoma. Curr Treat Options Neurol. 5:189-198

McCright B, Rivers AM, Audlin S and Virshup DM (1996). The B56 family of protein phosphatase 2A (PP2A) regulatory subunits encodes differentiation-induced phosphoproteins that target PP2A to both nucleus and cytoplasm. J Biol Chem. 271:22081-22089

Meis JM, Martz KL and Nelson JS (1991). Mixed glioblastoma multiforme and sarcoma. A clinicopathologic study of 26 radiation therapy oncology group cases. Cancer. 67:2342-2349

Mercer KE and Pritchard CA (2003). Raf proteins and cancer: B-Raf is identified as a mutational target. Biochim Biophys Acta. 1653:25-40

Millward TA, Zolnierowicz S and Hemmings BA (1999). Regulation of protein kinase cascades by protein phosphatase 2A. Trends Biochem Sci. 24:186-191

Mishima K, Higashiyama S, Asai A, Yamaoka K, Nagashima Y, Taniguchi N, Kitanaka C, Kirino T and Kuchino Y (1998). Heparin-binding epidermal growth factor-like growth factor stimulates mitogenic signaling and is highly expressed in human malignant gliomas. Acta Neuropathol (Berl). 96:322-328

Mitsumori K, Kittleson JM, Itoh N, Delahunt B, Heathcott RW, Stewart JH, McCredie MR and Reeve AE (2002). Chromosome 14q LOH in localized clear cell renal cell carcinoma. J Pathol. 198:110-114

Mohapatra G, Bollen AW, Kim DH, Lamborn K, Moore DH, Prados MD and Feuerstein BG (1998). Genetic analysis of glioblastoma multiforme provides evidence for subgroups within the grade. Genes Chromosomes Cancer. 21:195-206

Morantz RA, Feigin I and Ransohoff J 3rd (1976). Clinical and pathological study of 24 cases of gliosarcoma. J Neurosurg. 45:398-408

Mueller W, Hartmann C, Hoffmann A, Lanksch W, Kiwit J, Tonn J, Veelken J, Schramm J, Weller M, Wiestler OD, Louis DN and von Deimling A (2002). Genetic signature of oligoastrocytomas correlates with tumor location and denotes distinct molecular subsets. Am J Pathol. 161:313-319

Muller A and Fishel R (2002). Mismatch repair and the hereditary non-polyposis colorectal cancer syndrome (HNPCC). Cancer Invest. 20:102-109

Mutirangura A, Pornthanakasem W, Sriuranpong V, Supiyaphun P and Voravud N (1998). Loss of heterozygosity on chromosome 14 in nasopharyngeal carcinoma. Int J Cancer. 78:153-156

Nakamura M, Watanabe T, Klangby U, Asker C, Wiman K, Yonekawa Y, Kleihues P and Ohgaki H (2001b). p14ARF deletion and methylation in genetic pathways to glioblastomas. Brain Pathol. 11:159-168

Nakamura M, Yang F, Fujisawa H, Yonekawa Y, Kleihues P and Ohgaki H (2000). Loss of heterozygosity on chromosome 19 in secondary glioblastomas. J Neuropathol Exp Neurol. 59:539-543

Nakamura M, Yonekawa Y, Kleihues P and Ohgaki H (2001a). Promoter hypermethylation of the RB1 gene in glioblastomas. Lab Invest. 81:77-82

Naoki K, Chen TH, Richards WG, Sugarbaker DJ and Meyerson M (2002). Missense mutations of the BRAF gene in human lung adenocarcinoma. Cancer Res. 62:7001-7003

Naumann U, Hoffmeyer A, Flory E and Rapp UR (1996). Protein Phosphorylation. VCH, Weinheim

Ng HK, Poon WS, South JR and Lee JC (1988). Tumours of the central nervous system in Chinese in Hong Kong: a histological review. Aust N Z J Surg. 58:573-578

Nishikawa R, Ji XD, Harmon RC, Lazar CS, Gill GN, Cavenee WK and Huang HJ (1994). A mutant epidermal growth factor receptor common in human glioma confers enhanced tumorigenicity. Proc Natl Acad Sci U S A. 91:7727-7731

Nishizaki T, Ozaki S, Harada K, Ito H, Arai H, Beppu T and Sasaki K (1998). Investigation of genetic alterations associated with the grade of astrocytic tumor by comparative genomic hybridization. Genes Chromosomes Cancer. 21:340-346

Nozaki M, Tada M, Kobayashi H, Zhang CL, Sawamura Y, Abe H, Ishii N and Van Meir EG (1999). Roles of the functional loss of p53 and other genes in astrocytoma tumorigenesis and progression. Neuro-oncol. 1:124-137

Okada Y, Hurwitz EE, Esposito JM, Brower MA, Nutt CL and Louis DN (2003). Selection pressures of TP53 mutation and microenvironmental location influence epidermal growth factor receptor gene amplification in human glioblastomas. Cancer Res. 63:413-416

Okamoto K and Beach D (1994). Cyclin G is a transcriptional target of the p53 tumor suppressor protein. EMBO J. 13:4816-4822

Ono Y, Ueki K, Joseph JT and Louis DN (1996). Homozygous deletions of the CDKN2/p16 gene in dural hemangiopericytomas. Acta Neuropathol (Berl). 91:221-225

Papin C, Denouel-Galy A, Laugier D, Calothy G and Eychene A (1998). Modulation of kinase activity and oncogenic properties by alternative splicing reveals a novel regulatory mechanism for B-Raf. J Biol Chem. 273:24939-24947

Park SH, Jung KC, Ro JY, Kang GH and Khang SK (2000). 5' CpG island methylation of p16 is associated with absence of p16 expression in glioblastomas. J Korean Med Sci. 15:555-559

Pietenpol JA and Stewart ZA (2002). Cell cycle checkpoint signaling: cell cycle arrest versus apoptosis. Toxicology. 181-182:475-481

Pietsch T, Waha A, Koch A, Kraus J, Albrecht S, Tonn J, Sorensen N, Berthold F, Henk B, Schmandt N, Wolf HK, von Deimling A, Wainwright B, Chenevix-Trench G, Wiestler OD and Wicking C (1997). Medulloblastomas of the desmoplastic variant carry mutations of the human homologue of Drosophila patched. Cancer Res. 57:2085-2088

Pollock PM, Harper UL, Hansen KS, Yudt LM, Stark M, Robbins CM, Moses TY, Hostetter G, Wagner U, Kakareka J, Salem G, Pohida T, Heenan P, Duray P, Kallioniemi O, Hayward NK, Trent JM and Meltzer PS (2003). High frequency of BRAF mutations in nevi. Nat Genet. 33:19-20

Polyak K, Xia Y, Zweier JL, Kinzler KW and Vogelstein B (1997). A model for p53-induced apoptosis. Nature. 389:300-305

Poon WS and Ng HK (1992). Brain tumors: the local experience 1984-1992. J Hong Kong Med Assoc. 44:235-240

Pore N, Liu S, Haas-Kogan DA, O'Rourke DM and Maity A (2003). PTEN mutation and epidermal growth factor receptor activation regulate vascular endothelial growth factor (VEGF) mRNA expression in human glioblastoma cells by transactivating the proximal VEGF promoter. Cancer Res. 63:236-241

Powell B, Soong R, Iacopetta B, Seshadri R and Smith DR (2000). Prognostic significance of mutations to different structural and functional regions of the p53 gene in breast cancer. Clin Cancer Res. 6:443-451

Pramanik P, Sharma MC, Mukhopadhyay P, Singh VP and Sarkar C (2003). A comparative study of classical vs. desmoplastic medulloblastomas. Neurol India. 51:27-34

Prayson RA and Suh JH (1999). Subependymomas: clinicopathologic study of 14 tumors, including comparative MIB-1 immunohistochemical analysis with other ependymal neoplasms. Arch Pathol Lab Med. 123:306-309

Raffel C, Jenkins RB, Frederick L, Hebrink D, Alderete B, Fults DW and James CD (1997). Sporadic medulloblastomas contain PTCH mutations. Cancer Res. 57:842-845

Rajagopalan H, Bardelli A, Lengauer C, Kinzler KW, Vogelstein B and Velculescu VE (2002). Tumorigenesis: RAF/RAS oncogenes and mismatch-repair status. Nature. 418:934

Reifenberger G and Louis DN (2003). Oligodendroglioma: toward molecular definitions in diagnostic neuro-oncology. J Neuropathol Exp Neurol. 62:111-126

Reifenberger G, Liu L, Ichimura K, Schmidt EE and Collins VP (1993). Amplification and overexpression of the MDM2 gene in a subset of human malignant gliomas without p53 mutations. Cancer Res. 53:2736-2739

Reifenberger G, Reifenberger J, Ichimura K, Meltzer PS and Collins VP (1994). Amplification of multiple genes from chromosomal region 12q13-14 in human malignant gliomas: preliminary mapping of the amplicons shows preferential involvement of CDK4, SAS, and MDM2. Cancer Res. 54:4299-4303

Reis RM, Konu-Leblebliciogłu D, Lopes JM, Kleihues P and Ohgaki H (2000). Genetic profile of gliosarcomas. Am J Pathol. 156:425-432

Rodeck U (1993). Growth factor independence and growth regulatory pathways in human melanoma development. Cancer Metastasis Rev. 12:219-226

Rodeck U, Bvecker D and Herlyn M (1991). Basic fibroblast growth factor in human melanoma. Cancer cells. 3:308-311

Rosenberg JE, Lisle DK, Burwick JA, Ueki K, von Deimling A, Mohrenweiser HW and Louis DN (1996). Refined deletion mapping of the chromosome 19q glioma tumor suppressor gene to the D19S412-STD interval. Oncogene. 13:2483-2485

Rubio MP, Correa KM, Ramesh V, MacCollin MM, Jacoby LB, von Deimling A, Gusella JF and Louis DN (1994). Analysis of the neurofibromatosis 2 gene in human ependymomas and astrocytomas. Cancer Res. 54:45-47

Ruediger R, Pham HT and Walter G. (2001). Disruption of protein phosphatase 2A subunit interaction in human cancers with mutations in the A alpha subunit gene. Oncogene. 20:10-15

Sallinen SL, Sallinen P, Haapasalo H, Kononen J, Karhu R, Helen P and Isola J (1997). Accumulation of genetic changes is associated with poor prognosis in grade II astrocytomas. Am J Pathol. 151:1799-1807

Sarkar C, Pramanik P, Karak AK, Mukhopadhyay P, Sharma MC, Singh VP and Mehta VS (2002). Are childhood and adult medulloblastomas different? A comparative study of clinicopathological features, proliferation index and apoptotic index. J Neurooncol. 59:49-61

Satyamoorthy K, Li G, Gerrero MR, Brose MS, Volpe P, Weber BL, Van Belle P, Elder DE and Herlyn M (2003). Constitutive mitogen-activated protein kinase activation in melanoma is mediated by both BRAF mutations and autocrine growth factor stimulation. Cancer Res. 63:756-759

Sauter G, Maeda T, Waldman FM, Davis RL and Feuerstein BG (1996). Patterns of epidermal growth factor receptor amplification in malignant gliomas. Am J Pathol. 148:1047-1053

Schiebe M, Ohneseit P, Hoffmann W, Meyermann R, Rodemann HP and Bamberg M (2000). Analysis of mdm2 and p53 gene alterations in glioblastomas and its correlation with clinical factors. J Neurooncol. 49:197-203

Schlegel J, Piontek G, Budde B, Neff F and Kraus A (2000). The Akt/protein kinase B-dependent anti-apoptotic pathway and the mitogen-activated protein kinase cascade are alternatively activated in human glioblastoma multiforme. Cancer Lett. 158:103-108

Schofield D, West DC, Anthony DC, Marshal R and Sklar J (1995). Correlation of loss of heterozygosity at chromosome 9q with histological subtype in medulloblastomas. Am J Pathol. 146:472-480

Schonthal A and Feramisco JR (1993). Inhibition of histone H1 kinase expression, retinoblastoma protein phosphorylation, and cell proliferation by the phosphatase inhibitor okadaic acid. Oncogene. 8:433-441

Schonthal AH (2001). Role of serine/threonine protein phosphatase 2A in cancer. Cancer Lett. 170:1-13

Schrock E, Thiel G, Lozanova T, du Manoir S, Meffert MC, Jauch A, Speicher MR, Nurnberg P, Vogel S, Janisch W, Donis-Keller H, Red T, Witkowski R and Cremer T (1994). Comparative genomic hybridization of human malignant gliomas reveals multiple amplification sites and nonrandom chromosomal gains and losses. Am J Pathol. 144:1203-1218

Schuler M and Green DR (2001). Mechanisms of p53-dependent apoptosis. Biochem Soc Trans. 29:684-687

Schwerdtle RF, Winterpacht A, Storkel S, Brenner W, Hohenfellner R, Zabel B, Huber C and Decker HJ (1997). Loss of heterozygosity studies and deletion mapping identify two putative chromosome 14q tumor suppressor loci in renal oncocytomas. Cancer Res. 57:5009-5012

Seeling JM, Miller JR, Gil R, Moon RT, White R and Virshup DM (1999). Regulation of beta-catenin signaling by the B56 subunit of protein phosphatase 2A. Science. 283:2089-2091

Shapiro P (2002). Ras-MAP kinase signaling pathways and control of cell proliferation: relevance to cancer therapy. Crit Rev Clin Lab Sci. 39:285-330

Shibamoto Y, Kitakabu Y, Takahashi M, Yamashita J, Oda Y, Kikuchi H and Abe M (1993). Supratentorial low-grade astrocytoma. Correlation of computed tomography findings with effect of radiation therapy and prognostic variables. Cancer. 72:190-195

Shiraishi S, Tada K, Nakamura H, Makino K, Kochi M, Saya H, Kuratsu J and Ushio Y (2002). Influence of p53 mutations on prognosis of patients with glioblastoma. Cancer. 95:249-257

Simmons ML, Lamborn KR, Takahashi M, Chen P, Israel MA, Berger MS, Godfrey T, Nigro J, Prados M, Chang S, Barker FG 2nd and Aldape K (2001). Analysis of complex relationships between age, p53, epidermal growth factor receptor, and survival in glioblastoma patients. Cancer Res. 61:1122-1128

Simon M, Koster G, Menon AG and Schramm J (1999). Functional evidence for a role of combined CDKN2A (p16-p14(ARF))/CDKN2B (p15) gene inactivation in malignant gliomas. Acta Neuropathol (Berl). 98:444-452

Simon M, von Deimling A, Larson JJ, Wellenreuther R, Kaskel P, Waha A, Warnick RE, Tew JM Jr and Menon AG (1995). Allelic losses on chromosomes 14, 10, and 1 in atypical and malignant meningiomas: a genetic model of meningioma progression. Cancer Res. 55:4696-4701

Simpson L and Parsons R (2001). PTEN: life as a tumor suppressor. Exp Cell Res. 264:29-41

Singer G, Oldt R 3rd, Cohen Y, Wang BG, Sidransky D, Kurman RJ and Shih IeM (2003). Mutations in BRAF and KRAS characterize the development of low-grade ovarian serous carcinoma. J Natl Cancer Inst. 95:484-486

Slavc I, MacCollin MM, Dunn M, Jones S, Sutton L, Gusella JF and Biegel JA (1995). Exon scanning for mutations of the NF2 gene in pediatric ependymomas, rhabdoid tumors and meningiomas. Int J Cancer. 64:243-247

Smith JS, Perry A, Borell TJ, Lee HK, O'Fallon J, Hosek SM, Kimmel D, Yates A, Burger PC, Scheithauer BW and Jenkins RB (2000). Alterations of chromosome arms 1p and 19q as predictors of survival in oligodendrogliomas, astrocytomas, and mixed oligoastrocytomas. J Clin Oncol. 18:636-645

Smith JS, Tachibana I, Passe SM, Huntley BK, Borell TJ, Iturria N, O'Fallon JR, Schaefer PL, Scheithauer BW, James CD, Buckner JC and Jenkins RB (2001). PTEN mutation, EGFR amplification, and outcome in patients with anaplastic astrocytoma and glioblastoma multiforme. J Natl Cancer Inst. 93:1246-1256

Soares P, Trovisco V, Rocha AS, Lima J, Castro P, Preto A, Maximo V, Botelho T, Seruca R and Sobrinho-Simoes M (2003). BRAF mutations and RET/PTC rearrangements are alternative events in the etiopathogenesis of PTC. Oncogene. 22:4578-580

Staal FJ, van der Luijt RB, Baert MR, van Drunen J, van Bakel H, Peters E, de Valk I, van Amstel HK, Taphoorn MJ, Jansen GH, van Veelen CW, Burgering B and Staal GE (2002). A novel germline mutation of PTEN associated with brain tumours of multiple lineages. Br J Cancer. 86:1586-1591

Steck PA, Lin H, Langford LA, Jasser SA, Koul D, Yung WK and Pershouse MA (1999). Functional and molecular analyses of 10q deletions in human gliomas. Genes Chromosomes Cancer. 24:135-143

Stevens B and Fields RD (2002). Regulation of the cell cycle in normal and pathological glia. Neuroscientist. 8:93-97

Stone DM, Hynes M, Armanini M, Swanson TA, Gu Q, Johnson RL, Scott MP, Pennica D, Goddard A, Phillips H, Noll M, Hooper JE, de Sauvage F and Rosenthal A (1996). The tumour-suppressor gene patched encodes a candidate receptor for Sonic hedgehog. Nature. 384:129-134

Tamura M, Gu J, Tran H and Yamada KM (1999). PTEN gene and integrin signaling in cancer. J Natl Cancer Inst. 91:1820-1828

Tannapfel A, Sommerer F, Benicke M, Katalinic A, Uhlmann D, Witzigmann H, Hauss J and Wittekind C (2003). Mutations of the BRAF gene in cholangiocarcinoma but not in hepatocellular carcinoma. Gut. 52:706-712

Taylor MD, Liu L, Raffel C, Hui CC, Mainprize TG, Zhang X, Agatep R, Chiappa S, Gao L, Lowrance A, Hao A, Goldstein AM, Stavrou T, Scherer SW, Dura WT, Wainwright B, Squire JA, Rutka JT and Hogg D (2002). Mutations in SUFU predispose to medulloblastoma. Nat Genet. 31:306-310

Testa JR and Bellacosa A (2001). AKT plays a central role in tumorigenesis. Proc Natl Acad Sci U S A. 98:10983-10985

Teyssier JR (1987). Nonrandom chromosomal changes in human solid tumors: application of an improved culture method. J Natl Cancer Inst. 79:1189-1198

Teyssier JR (1989). The chromosomal analysis of human solid tumors. A triple challenge. Cancer Genet Cytogenet. 37:103-125

Thomas CY, Chouinard M, Cox M, Parsons S, Stallings-Mann M, Garcia R, Jove R and Wharen R (2003). Spontaneous activation and signaling by overexpressed epidermal growth factor receptors in glioblastoma cells. Int J Cancer. 104:19-27

Thompson PM, Seifried BA, Kyemba SK, Jensen SJ, Guo C, Maris JM, Brodeur GM, Stram DO, Seeger RC, Gerbing R, Matthay KK, Matise TC and White PS (2001). Loss of heterozygosity for chromosome 14q in neuroblastoma.Loss of heterozygosity for chromosome 14q in neuroblastoma. Med Pediatr Oncol. 36:28-31

Tian XX, Lam PY, Chen J, Pang JC, To SS, Di-Tomaso E and Ng HK (1998). Antisense epidermal growth factor receptor RNA transfection in human malignant glioma cells leads to inhibition of proliferation and induction of differentiation. Neuropathol Appl Neurobiol. 24:389-396

Tomlinson IP, Roylance R and Houlston RS (2001). Two hits revisited again. J Med Genet. 38:81-85

Tong CY, Ng HK, Pang JC, Hui AB, Ko HC and Lee JC (1999). Molecular genetic analysis of non-astrocytic gliomas. Histopathology. 34:331-341

Tong CY, Zheng PP, Pang JC, Poon WS, Chang AR and Ng HK (2001). Identification of novel regions of allelic loss in ependymomas by high-resolution allelotyping with 384 microsatellite markers. J Neurosurg. 95:9-14

Torp SH, Helseth E, Ryan L, Stolan S, Dalen A and Unsgaard G (1991). Amplification of the epidermal growth factor receptor gene in human gliomas. Anticancer Res. 11:2095-2098

Tse JY, Ng HK, Lau KM, Lo KW, Poon WS and Huang DP (1997). Loss of heterozygosity of chromosome 14q in low- and high-grade meningiomas. Hum Pathol. 28:779-785

Tucker T and Friedman JM (2002). Pathogenesis of hereditary tumors: beyond the "two-hit" hypothesis. Clin Genet. 62:345-357

Udart M, Utikal J, Krahn GM and Peter RU (2001). Chromosome 7 aneusomy. A marker for metastatic melanoma? Expression of the epidermal growth factor receptor gene and chromosome 7 aneusomy in nevi, primary malignant melanomas and metastases. Neoplasia. 3:245-254

Ueki K, Nishikawa R, Nakazato Y, Hirose T, Hirato J, Funada N, Fujimaki T, Hojo S, Kubo O, Ide T, Usui M, Ochiai C, Ito S, Takahashi H, Mukasa A, Asai A and Kirino T (2002). Correlation of histology and molecular genetic analysis of 1p, 19q, 10q, TP53, EGFR, CDK4, and CDKN2A in 91 astrocytic and oligodendroglial tumors. Clin Cancer Res. 8:196-201

Ugi S, Imamura T, Ricketts W and Olefsky JM (2002). Protein phosphatase 2A forms a molecular complex with Shc and regulates Shc tyrosine phosphorylation and downstream mitogenic signaling. Mol Cell Biol. 22:2375-2387

Uhrbom L, Dai C, Celestino JC, Rosenblum MK, Fuller GN and Holland EC (2002). Ink4a-Arf loss cooperates with KRas activation in astrocytes and neural progenitors to generate glioblastomas of various morphologies depending on activated Akt. Cancer Res. 62:5551-5558

Uribe P, Wistuba II and Gonzalez S (2003). BRAF Mutation: A Frequent Event in Benign, Atypical, and Malignant Melanocytic Lesions of the Skin. Am J Dermatopathol. 25:365-370

Vagner-Capodano AM, Hairion D, Gambarelli D, Perez-Castillo AM and Grisoli F (1991). A new approach of brain tumors: the cytogenetic study. J Neuroradiol. 18:107-121

Vagner-Capodano AM, Zattara-Cannoni H, Gambarelli D, Figarella-Branger D, Lena G, Dufour H, Grisoli F and Choux M (1999). Cytogenetic study of 33 ependymomas. Cancer Genet Cytogenet. 115:96-99

Van Meir EG, Roemer K, Diserens AC, Kikuchi T, Rempel SA, Haas M, Huang HJ, Friedmann T, de Tribolet N and Cavenee WK (1995). Single cell monitoring of growth arrest and morphological changes induced by transfer of wild-type p53 alleles to glioblastoma cells. Proc Natl Acad Sci U S A. 92:1008-1012

Verheijen FM, Sprong M, Kloosterman JM, Blaauw G, Thijssen JH and Blankenstein MA (2002). TP53 mutations in human meningiomas. Int J Biol Markers. 17:42-48

Von Deimling A, Fimmers R, Schmidt MC, Bender B, Fassbender F, Nagel J, Jahnke R, Kaskel P, Duerr EM, Koopmann J, Maintz D, Steinbeck S, Wick W, Platten M, Muller DJ, Przkora R, Waha A, Blumcke B, Wellenreuther R, Meyer-Puttlitz B, Schmidt O, Mollenhauer J, Poustka A, Stangl AP, Lenartz D and von Ammon K (2000). Comprehensive allelotype and genetic anaysis of 466 human nervous system tumors. J Neuropathol Exp Neurol. 59:544-558

Vossler MR, Yao H, York RD, Pan MG, Rim CS and Stork PJ (1997). cAMP activates MAP kinase and Elk-1 through a B-Raf- and Rap1-dependent pathway. Cell. 89:73-82

Vousden KH and Lu X (2002). Live or let die: the cell's response to p53. Nat Rev Cancer. 2:594-604

Walker DG and Kaye AH (2001). Diagnosis and management of astrocytomas, oligodendrogliomas and mixed gliomas: a review. Australas Radiol. 45:472-482

Wang L, Cunningham JM, Winters JL, Guenther JC, French AJ, Boardman LA, Burgart LJ, McDonnell SK, Schaid DJ and Thibodeau SN (2003). BRAF mutations in colon cancer are not likely attributable to defective DNA mismatch repair. Cancer Res. 63:5209-5212

Wang SS, Esplin ED, Li JL, Huang L, Gazdar A, Minna J and Evans GA (1998). Alterations of the PPP2R1B gene in human lung and colon cancer. Science. 282:284-287

Weber CK, Slupsky JR, Herrmann C, Schuler M, Rapp UR and Block C (2000). Mitogenic signaling of Ras is regulated by differential interaction with Raf isozymes. Oncogene. 19:169-176

Weber CK, Slupsky JR, Kalmes HA and Rapp UR (2001). Active Ras induces heterodimerization of cRaf and Braf. Cancer Res. 61:3595-3598

Weber RG, Bostrom J, Wolter M, Baudis M, Collins VP, Reifenberger G and Lichter P (1997). Analysis of genomic alterations in benign, atypical, and anaplastic meningiomas: toward a genetic model of meningioma progression. Proc Natl Acad Sci U S A. 94:14719-14724

Weber TK, Conroy J, Keitz B, Rodriguez-Bigas M, Petrelli NJ, Stoler DL, Anderson GR, Shows TB and Nowak NJ (1999). Genome-wide allelotyping indicates increased loss of heterozygosity on 9p and 14q in early age of onset colorectal cancer. Cytogenet Cell Genet. 86:142-147

Wechsler-Reya R and Scott MP (2001). The developmental biology of brain tumors. Annu Rev Neurosci. 24:385-428

Weng LP, Brown JL and Eng C (2001). PTEN coordinates G(1) arrest by down-regulating cyclin D1 via its protein phosphatase activity and up-regulating p27 via its lipid phosphatase activity in a breast cancer model. Hum Mol Genet. 10:599-604

Wiese S, Pei G, Karch C, Troppmair J, Holtmann B, Rapp UR and Sendtner M (2001). Specific function of B-Raf in mediating survival of embryonic motoneurons and sensory neurons. Nat Neurosci. 4:137-142

Wojnowski L, Zimmer AM, Beck TW, Hahn H, Bernal R, Rapp UR and Zimmer A (1997). Endothelial apoptosis in Braf-deficient mice. Nat Genet. 16:293-297

Wu SQ, Hafez GR, Xing W, Newton M, Chen XR and Messing E (1996). The correlation between the loss of chromosome 14q with histologic tumor grade, pathologic stage, and outcome of patients with nonpapillary renal cell carcinoma. Cancer. 77:1154-1160

Yan Y and Mumby MC (1999). Distinct roles for PP1 and PP2A in phosphorylation of the retinoblastoma protein. PP2a regulates the activities of G(1) cyclin-dependent kinases. J Biol Chem. 274:31917-31924

Yap DB, Hsieh JK, Chan FS and Lu X (1999). mdm2: a bridge over the two tumour suppressors, p53 and Rb. Oncogene. 18:7681-7689

Yin XL, Pang JC and Ng HK (2002). Identification of a region of homozygous deletion on 8p22-23.1 in medulloblastoma. Oncogene. 21:1461-1468.

Yong WH, Chou D, Ueki K, Harsh GR 4th, von Deimling A, Gusella JF, Mohrenweiser HW and Louis DN (1995). Chromosome 19q deletions in human gliomas overlap telomeric to D19S219 and may target a 425 kb region centromeric to D19S112. J Neuropathol Exp Neurol. 54:622-626

Yuen ST, Davies H, Chan TL, Ho JW, Bignell GR, Cox C, Stephens P, Edkins S, Tsui WW, Chan AS, Futreal PA, Stratton MR, Wooster R and Leung SY (2002). Similarity of the phenotypic patterns associated with BRAF and KRAS mutations in colorectal neoplasia. Cancer Res. 62:6451-6455

Zheng PP, Pang JC, Hui AB and Ng HK (2000). Comparative genomic hybridization detects losses of chromosomes 22 and 16 as the most common recurrent genetic alterations in primary ependymomas. Cancer Genet Cytogenet. 122:18-25

Zhou B, Wang ZX, Zhao Y, Brautigan DL and Zhang ZY (2002). The specificity of extracellular signal-regulated kinase 2 dephosphorylation by protein phosphatases. J Biol Chem. 277:31818-31825

Zhu J, Guo SZ, Beggs AH, Maruyama T, Santarius T, Dashner K, Olsen N, Wu JK and Black P (1996). Microsatellite instability analysis of primary human brain tumors. Oncogene. 12:1417-1423

Zhu Y, Loukola A, Monni O, Kuokkanen K, Franssila K, Elonen E, Vilpo J, Joensuu H, Kere J, Aaltonen L and Knuutila S (2001). PPP2R1B gene in chronic lymphocytic leukemias and mantle cell lymphomas. Leuk Lymphoma. 41:177-183

Zimmermann S and Moelling K (1999). Phosphorylation and regulation of Raf by Akt (protein kinase B). Science. 286:1741-1744

Zulch KJ (1986). Brain Tumors, Their Biology And Pathology. 3rded. Springer-Verlag: Berlin Heideeberg

Zurawel RH, Chiappa SA, Allen C and Raffel C (1998). Sporadic medulloblastomas contain oncogenic beta-catenin mutations. Cancer Res. 58:896-899